Mechanisms of cone photoreceptor cell death in models for inherited retinal degeneration.

Dissertation

zur Erlangung des Grades eines
Doktors der Naturwissenschaften

der Mathematisch-Naturwissenschaftlichen Fakultät
und
der Medizinischen Fakultät
der Eberhard-Karls-Universität Tübingen

vorgelegt
von

Stine Mencl
aus Rostock, Deutschland

Februar - 2012

Tag der mündlichen Prüfung:	09.07.2012
Dekan der Math.-Nat. Fakultät:	Prof. Dr. W. Rosenstiel
Dekan der Medizinischen Fakultät:	Prof. Dr. I. B. Autenrieth
1. Berichterstatter:	Prof. Dr. E. Zrenner
2. Berichterstatter:	Prof. Dr. B. Wissinger
Prüfungskommission:	Prof. Dr. E. Zrenner
	Prof. Dr. B. Wissinger
	Prof. Dr. F. Schaeffel
	Prof. Dr. H. Mallot

I hereby declare that I have produced the work entitled: “Mechanisms of cone photoreceptor cell death in models for inherited retinal degeneration”,
submitted for the award of a doctorate, on my own (without external help), have used only the sources and aids indicated and have marked passages included from other works, whether verbatim or in content, as such. I swear upon oath that these statements are true and that I have not concealed anything. I am aware that making a false declaration under oath is punishable by a term of imprisonment of up to three years or by a fine.

Tübingen, _____ _____

Date Signature

Index

List of Figures

List of Tables

Abbreviations

Table 1: Explanation of abbreviations

Abbreviation	Name
%	percentage
§	signum sectionis
°C	degree Celsius
10x	10 times concentrated
µg	microgram
µl	micro liter
µm	micrometer
µM	micromolar
ADRP	autosomal dominant retinitis pigmentosa
AIF	apoptosis inducing factor
AMD	age-related macula degeneration
ARVO	The association for research in vision and ophthalmology
BAX	Bcl-2 associated X protein
bit	binary digit
BSA	bovine serum albumin
C3H-rd1	retinal degeneration 1
C3H-wt	wild type strain for retinal degeneration 1
Ca^{2+}	calcium
cAMP	cyclic adenosine monophosphate
CBP	CREB binding protein
CD-wt	wild type for *P23H* and *S334ter* rats
CFP	cyan fluorescent protein
cGMP	cyclic guanosine monophosphate
CNG channel	cyclic nucleotide-gated channel
CNGA3	cyclic nucleotide-gated-channel subtype A3
CO_2	carbon dioxide
cpfl1	cone photoreceptor function loss 1
***CRE* sequence**	DNA sequence 5'-TGACGTCA-3'; cAMP responsive element
CREB	cAMP response element-binding
CREM	cAMP responsive element modulator
$CuSO_4(H2O)_5$	copper(II) sulfate pentahydrate
Cy3	cyanine fluorescence dye 3
DABCO	1,4-Diazabicyclo(2,2,2)octane
DAPI	4',6-diamidino-2-phenylindole
DBM	double mutant
ddH_2O	bi-distilled water
DMEM	Dulbecco's modified Eagle's medium
DNA	deoxyribonucleic acid
DPBS	Dulbecco's phosphate buffered saline
DTT	dithiothreitol
E.coli	Escherichia coli
EDTA	ethylenediaminetetraacetic acid
EGFP	enhanced green fluorescent protein
FBS	fetal bovine serum
Fig.	figure

g	gram
GABA	gamma-aminobutyric acid
GCL	ganglia cell layer
GDP	guanosine diphosphate
GFAP	glial fibrillary acidic protein
GFP	green fluorescence protein
GP	glycogen phosphorylase
GTP	guanosine triphosphate
h	hours
HCl	hydrochloric acid
HEK293	human embryonic kidney cells strain 293
HeLa	cervical cancer cell line
HEPES	4-(2-hydroxyethyl)-1-piperazineethanesulfonic acid
HNE	4-hydroxynonenal
ICER	inducible cAMP early repressor
IFT	intraflagellar transport
IHC	immunohistochemistry
INL	inner nuclear layer
IPL	inner plexiform layer
IS	inner segment
K^+	potassium
KCl	potassium chloride
l	liter
JNK	c-Jun N-Terminal kinase
LB	Lysogeny broth
LCA	Leber congenital amaurosis
M	1 molar
mg	milligram
$MgCl_2$	magnesium chloride
min	minutes
ml	milliliter
mM	milimolar
$MnCl_2(H2O)_4$	manganese(II) chloride tetrahydrate
MNU	methylnitrosourea
Mowiol	polyvinyl alcohol
ms	milliseconds
mV	millivolt
Na^+	sodium
NaCl	sodium chloride
NaH2PO4	monosodium phosphate
NaH2PO4 x H2O	sodium phosphate monobasic monohydrate
$NaHCO_3$	sodium bicarbonate
$NaSeO_3(H2O)_5$	sodium selenite pentahydrate
nm	nanometer
NSE	neuron specific enolase
ONL	outer nuclear layer
OPL	outer plexiform layer
OS	outer segment
P	post natal
p	probability value
PARP	poly(ADP-ribose) polymerase
PB	phosphate buffer

PBS	phosphate buffered saline
PBST	phosphate buffered saline with Triton or Tween
PCD	programmed cell death
PCR	polymerase chain reaction
pCREB	active CREB phosphorylated at Serine 133
PDE6	phosphodiesterase 6
Pen/Strep	penicillin and streptomycin
PFA	paraformaldehyde
pH	pondus Hydrogenii
PI	propidiumiodide
PKA	cAMP-dependent protein kinase
PKG	cGMP-dependent protein kinase
PMSF	phenylmethanesulfonylfluoride
PNA	peanut agglutinin
PVDF transfer membranes	polyvinylidene fluoride transfer membranes
RCS rat	Royal College of Surgeons rat
rd	retinal degeneration
ROM	rod outer segment membrane protein
ROS	reactive oxygen species
rpm	rounds per minute
RP	Retinitis pigmentosa
RPE	retinal pigment epithelium
RPMI	Roswell Park Memorial Institute medium
RT	room temperature
SDS	sodium dodecyl sulfate
sec	seconds
SOC-medium	super Optimal broth with Catabolite repression
Tab.	table
TBS	Tris(hydroxymethyl)-aminomethan (Tris) buffered saline
TBST	Tris buffered saline containing Tween-20 or Triton-X100
TE	Tris/EDTA
Tris/ Trizma base	Tris(hydroxymethyl)aminomethane
TUNEL	terminal deoxynucleotidyl transferase-mediated biotinylated UTP nick end labeling
V	voltage
v/v	volume fraction or volume concentration
w/v	mass-volume percentage
WB	western blot
wt	wild type

Introduction

1.1 The Retina

The retina is localized at the back of the eye cup and is essential for vision. When light is entering the human eye, it is focused by the cornea and the lens towards the light-sensitive retina, where a sharp image is created (Fig.1 A). When light reaches the retina it travels through all layers of the retina, first the ganglion cell layer, then the inner nuclear layer, where the cell bodies of amacrine cells, Müller cells, bipolar and horizontal cells are located and finally the outer nuclear layer containing the light sensitive photoreceptor cells (Fig.1 B, C). After passing through the retina, the "left-over" light is absorbed by melanin-pigmented cells to prevent backward reflections from disturbing vision.

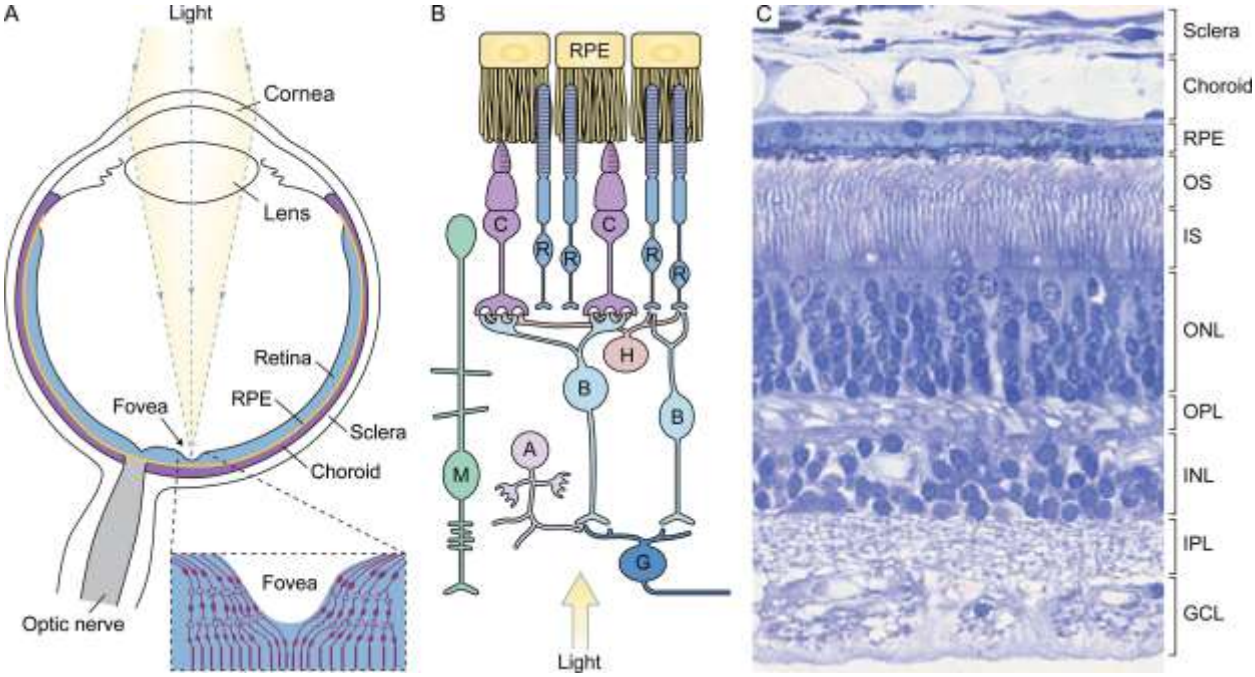

Figure 1: Human eye and retina: A) Diagram of the human eye with an enlarged scheme of the fovea. B) Scheme of retinal cell types and their connections C) Richardson's methylene blue/azure II stained transverse section of the human retina. Abbreviations: A=amacrine cell; B=bipolar cell; C=cone photoreceptor; G=ganglion cell; GCL=ganglion cell layer; H=horizontal cell; INL=inner nuclear layer; IPL=inner plexiform layer; IS=inner segments; M=Müller cell; ONL=outer nuclear layer; OPL=outer plexiform layer; OS=outer segments; R=rod photoreceptor; RPE=retinal pigment epithelial; (Figure was taken from Sung and Chuang 2010).

The human eye contains a special structure, called macula, which contains the fovea (Fig.1 A). Only humans and higher primates possess a fovea, allowing for sharp, high-resolution vision in the central parts of the visual field. Here, the cell bodies of all

cells except photoreceptors are shifted sideways, so the light can reach them more effectively. The fovea contains only cone photoreceptors, each of which transmits the light dependent signal towards a single so-called midget bipolar cell that in turn is contacted by a single ganglion cell. This direct, 1:1:1 connection increases the spatial resolution. However, since cones require bright light (photopic) conditions, high spatial resolution is only obtainable in daylight. This is opposed to the demands of dim light (scotopic) conditions, where the resolution is not as important as the amplification. Therefore, in all other parts of the retina the signal is pooled from several rod and/or cone photoreceptors (Fig.1 B). Apart from the fovea, there is the so-called “blind spot” of the retina, where the axons of all ganglion cells leave the eye and form the optic nerve.

1.1.1 Photoreceptor cells

The vertebrate retina consists of two types of photoreceptors, rods and cones, named after the cone or rod shaped morphology of the outer segments (Fig.2).

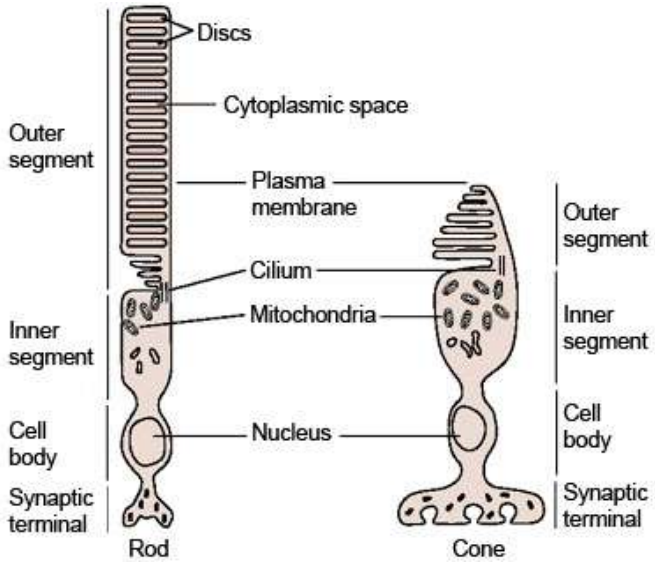

Figure 2: Morphology of rod and cone photoreceptor: Mammalian photoreceptor cells are roughly divided into four main parts. In the outer segment the membrane area is enlarged by sets of membrane stacks termed “discs” to increase the surface area for the phototransduction protein cascade. The outer and inner segments are connected only through a cilium, which controls the protein supply for the outer segment. In the inner segment mitochondria and in the cell body the nuclei are located. The synaptic terminal is connected to postsynaptic cells and transmits the light induced signals by releasing glutamate. (modified from Kandel *et al.* 2000)

The outer segments contain the light-transducing equipment in membranous compartments called discs. While new discs are synthesized at the bottom of the outer segment, old ones are phagocytosed at the distal part by retinal pigment epithelial cells. Almost all photoreceptor mitochondria are located in the inner segments and have to cover for the high-energy consumption of the outer segment and the whole cell. Additionally, most of the protein assembly machinery is inside the inner segments, which means all proteins required for the assembly of the discs and phototransduction need to be transferred to the outer segment. This is done via the so-called connecting cilium, which controls the protein supply of the outer segment with its intraflagellar transport machinery (Sedmak *et al.* 2009; Insinna and Besharse 2008). The cell body contains the nucleus and with the synaptic terminals, photoreceptors connect to bipolar and horizontal cells and transmit the light evoked signal using the neurotransmitter glutamate.

All rods contain the same light sensitive pigment called rhodopsin (Fig.3 Rh), while there are different cone opsins to allow for color discrimination. Rod and cone pigments are prototypical G protein-coupled receptors, embedded in the disc membrane of the outer segment and covalently linked to a chromophore, the 11-cis-retinal. Phototransduction, the process of transforming light into an electrical signal, was studied extensively in rod photoreceptors (for review see Luo *et al.* 2008; Yau and Hardie 2009). In dark, the cyclic-nucleotide-gated (CNG) channels are maintained in the open state by high levels of cyclic guanosine monophosphate (cGMP). When the unselective CNG channels are open, calcium (Ca^{2+}) and sodium (Na^{+}) ions are flowing in. A Na^{+}/Ca^{2+}, potassium (K^{+}) exchanger (NCKX) on the outer segment membrane couples Na^{+} influx to Ca^{2+} and K^{+}-efflux, to balance the CNG channel mediated Ca^{2+} influx. This so called dark current depolarizes the outer segment to a membrane potential of around minus 30mV (Altimimi and Schnetkamp 2007). When a photon hits the chromophore 11-cis-retinal, it undergoes a structural transformation to the active form, called all-trans-retinal, which in turn leads to the activation of rhodopsin. This active form is called metarhodopsin II, which is shown in Fig.3 as activated rhodopsin (Rh*). Rh* catalyzes an exchange of guanosine diphospate (GDP) to guanosine triphosphate (GTP) on the alpha subunit of the G protein transducin, thus activating it (Fig.3 $G_{t\alpha}$*). Subsequently, $G_{t\alpha}$* dissociates from the beta- and gamma-subunit and binds to the inhibitory γ-subunit of the rod phosphodiesterase 6 ($G_{t\alpha}$*·PDE*), which then dissociates as well. Now the activated PDE 6 hydrolyzes specifically cGMP and decreases cGMP levels. Decreased cGMP levels close the CNG channels and ion

influx stops, while the NCKX on the plasma membrane remains active, pumping net positive charge out of the cell. This imbalance leads to hyperpolarization of the photoreceptor, which is the signal to decrease the release of glutamate at the synapses. For vision, not only the light induced activation is important, but also the fast deactivation after light offset. This inactivation has to be done for each protein of the phototransduction cascade and can be regulated by intracellular Ca^{2+}, allowing for an adaptation to bright or dim light conditions (for review see Luo *et al.* 2008; Yau and Hardie 2009; Fain *et al.* 2001).

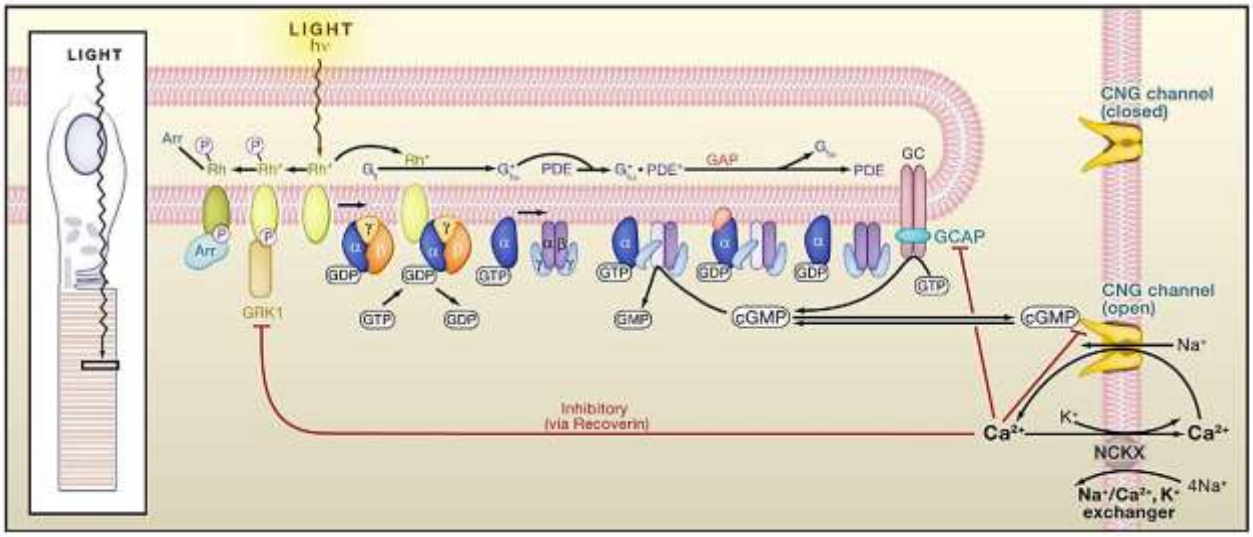

Figure 3: Phototransduction in a rod photoreceptor: When light hits a rhodopsin molecule, rhodopsin binds to the G-protein transducin. The activated transducin itself binds to the phosphodiesterase and activates it. cGMP is hydrolyzed and the CNG channels are closed. This closure hyperpolarizes the outer segment and this is forwarded to the synapses and the 2nd order neurons of the inner retina. Abbreviations: Arr = arrestin; cGMP= cyclic guanosine monophosphate; CNG channel= cyclic nucleotide gated channel; G=transducin; GDP= guanosine diphosphat; GMP= guanosine monophosphate; GTP= guanosine triphosphate; P= phosphate; PDE= phosphodiesterase; Rh= rhodopsin; (Figure was taken from Yau and Hardie 2009)

1.1.2 Other cell types

Based on the glutamate release at the synapses of photoreceptors the light signal is forwarded, amplified and/or inhibited in the inner retina. Bipolar cells, horizontal cells and amacrine cells are mediating this processing. This intense processing increases contrasts, allowes the detection of movement and filters out unnecessary information. Finally, ganglion cells transmit the light evoked signal to the visual areas of the brain.

1.1.3 Comparison between mouse and human retina

Although the eyes of vertebrates have the same general structure, there are some adaptations to certain modes of life, e.g. nocturnal or diurnal life. While diurnal vertebrate retinas are dominated by cones, retinas from nocturnal-animals contain more rods to gain an optimized vision (Peichl 2005). Mice and rats, animals typically used for laboratory research, are nocturnal animals. Therefore, they have rod-dominated retinas.

Vertebrates originally possessed four classes of cone opsins (without counting rhodopsin), but most mammalian species, among them mice and rats, have lost two types of opsin in the course of evolution. Hence, these animals have a dichromatic color vision. They can discriminate shorter wavelength (short-wavelength-sensitive opsin; S-cones) from middle wavelength light (middle-wavelength-sensitive opsin; M-cones) (Fu and Yau 2007). In the evolution of old world primates and humans, trichromatic vision appeared after a duplication event of the middle-wavelength-sensitive opsin, allowing for the discrimination between green and red. Not only the cone opsins differ between humans and mice, also the cone distribution is altered between different species. Humans (and some primates) show an extreme adaptation towards an improved visual acuity. This is more easily achievable for a diurnal species, because higher visual acuity requires less convergence and therefore needs brighter light (Peichl 2005).

Still, vertebrate visual systems share many features: for example analogue visual brain areas are innervated, the structure of eye cup and retina is similar, the processing mechanisms of visual signals in the inner retina are comparable, similar signal pathways are used and often the same genes are involved in vision of distinct species (Sanes and Zipursky 2010).

1.2 Inherited photoreceptor degeneration diseases

Inherited photoreceptor degenerations are a major cause of adult blindness in industrialized countries. While some of these diseases are exclusive genetically determined like Retinitis pigmentosa (RP), Leber congenital amaurosis (LCA) or cone dystrophies, others, such as age-related macular degeneration (AMD) are multifactorial. All mentioned diseases have one thing in common: hitherto no treatment is available.

1.2.1 Retinitis pigmentosa

RP is a group of inherited, usually monogenic photoreceptor diseases with a worldwide prevalence of about 1 in 4000 (Hartong *et al.* 2006). Caused by mutations in over 48 genes (http://www.sph.uth.tmc.edu/Retnet/sum-dis.htm#B-diseases; information retrieved May 23, 2011) RP can be inherited either in an autosomal recessive (41%), dominant (24%), x-linked (22%) or other (12%) fashion (Wright *et al.* 2010). Additionally, in about 20-30% of RP-patients, associations with more than 30 different syndromes were found (Hartong *et al.* 2006). Typically, mutations causing RP triggers similar symptoms like night blindness starting at youth or young adolescent age, followed by a gradual loss of peripheral vision and decreased visual acuity or blindness in older age (Hartong *et al.* 2006). Night blindness and the gradual loss of peripheral vision are due to loss of rods. Distinct mutations can influence the degree of the severity and the progression of disease. Unfortunately, for reasons unknown even the non-mutated cones degenerate secondarily following rod cell death (Wright *et al.* 2010).

1.2.2 Leber congenital amaurosis

Leber congenital amaurosis (LCA) is the most severe form of hereditary retinal dystrophies. The progression is much faster when compared with RP and causing blindness or severe impairment of vision before the age of one year (den Hollander *et al.* 2008). The prevalence in Northern America is one in 81,000 (Stone 2007) and as many as 15 genes lead to LCA, which is characterized by early visual loss, nystagmus, amaurotic pupils and the absence of ERG responses (Boldt *et al.* 2011). Several of the genes mutated in LCA-patients have been implicated in other retinal diseases such as RP (den Hollander *et al.* 2008).

1.2.3 Inherited cone dystrophies

Cone dystrophies are heterogeneous diseases, which can be inherited either in autosomal dominant, autosomal recessive, or in x-linked recessive fashion. They can be divided into stationary cone dystrophies, where the rods mostly remain functional (Michaelides *et al.* 2004) and progressive cone dystrophies, where cone degeneration often starts in childhood and progresses with age. The congenital stationary cone disorders include color vision deficiency, complete or incomplete achromatopsia, oligocone trichromacy, cone monochromatism, blue cone monochromatism and Bornholm eye disease (for review see Michaelides *et al.* 2004). Cone rod dystrophies

have a prevalence of one in 40,000 (Hamel 2007). Due to a mutation, the cone photoreceptors degenerate, sometimes accompanied or followed by rod photoreceptors. Therefore, progressive cone dystrophy is comparable with RP, but the other way round and generally more severe for the patients, because human vision depends much more on cone than on rod functionality. The first symptoms are decreased visual acuity, dyschromatopsia and photophobia, followed by progressive loss of peripheral vision and if the rods are involved, night blindness.

1.2.4 Age-related macular degeneration

Age-related macular degeneration (AMD) is the leading cause of blindness in the elderly, worldwide. It affects the central area of the retina, more precisely the macula. AMD is classified into an atrophic ("dry") form and a neovascular ("wet") form. Typically, the more severe vision loss is associated with the neovascular form. Although histological changes can already be measured in middle age, the clinical relevant changes are usually not apparent before the age of 55 (Klein *et al.* 2004). Symptoms of the atrophic form are pigment disruption and drusen, which are small yellowish deposits in the retina. While the "dry" form often proceeds asymptomatically, around 10-15% of AMD patients develop the "wet" form. In this form, a fibrotic scar is forming over several months under the macula, which is accompanied by a central scotoma. The term "wet" refers to some fluid (exudates or blood) in the extracellular space between the retina and the RPE. (for review see Hageman *et al.* 2008; http://webvision.med.utah.edu/; information retrieved February 27, 2012). The cause of AMD is not entirely genetic, but two high risk genes are already known. One is named complement factor H and the other age-related maculopathy susceptibility 2. Major non-hereditary risk factors are increasing age, smoking and a previous cataract surgery (Chakravarthy *et al.* 2010).

1.3 Retinal degeneration models

1.3.1 The Retinal degeneration 1(Pde6b$^{C3H\text{-}rd1}$) mouse

In 1924 C. E. Keeler realized, that some of his adult mice had no photoreceptors anymore and he named these mice rodless (*r*) (Keeler 1924). Later, in 1951 Brückner found up to 50% of all wild type (wt) mice around Basel showing a similar phenotype to Keeler´s rodless mouse and he named them retinal degeneration (*rd*) (Brückner 1951). In this time, other inbred mouse strains had been identified all showing the same phenotype inherited in an autosomal, recessive manner. The causing defect was shown to be a nonsense mutation in the β-subunit of the rod *Pde6* (Bowes *et al.* 1990; Pittler and Baehr 1991) and an insertion of the xenotropic murine leukemia virus (Xmv28) in the first intron of *Pde6* gene (Bowes *et al.* 1993). The degeneration phenotype could be rescued, when functional PDE6 was expressed in *rd* retinas (Lem *et al.* 1992). Polymerase chain reaction (PCR) analysis confirmed that the original rodless and *rd* mice are carrying the same genetic defect (Pittler *et al.* 1993). For many decades, the *rd* mouse was one of the main animal models for RP (Sidman and Green 1965; Dunn 1954; Karli 1952). Nowadays, the *rd* mouse is designated *rd1* and much more retinal degeneration models (*rd 2* – *rd10*) are available. In human patients, the mutation in the rod *PDE6β*-subunit gene is the second most common cause of RP after mutations in the rhodopsin gene (McLaughlin *et al.* 1993). The rod PDE6 function is reduced in *rd1*, (Farber and Lolley 1976) so that rod photoreceptors are not functional. The loss of PDE6 function is leading to an accumulation of cGMP (Farber and Lolley 1974) in rod photoreceptors, which somehow induces rod degeneration starting at P9. Rod cell death is most detectable at P13 (Paquet-Durand *et al.* 2011) and around P17, about 98% of the rods are already gone and only a single row of photoreceptor nuclei remains (Carter-Dawson *et al.* 1978). The cone photoreceptors, although unaffected by the mutation, start to degenerate around P21. After 18 months, only 1.5% of all cones remain (Carter-Dawson *et al.* 1978). The current knowledge on degeneration mechanisms in *rd1* rod photoreceptors will be explained in the next chapter "*Photoreceptor degeneration mechanisms".* In the results, *rd1* will be referred to as *C3H-rd1*, because the genetic background was the *C3H* mouse strain.

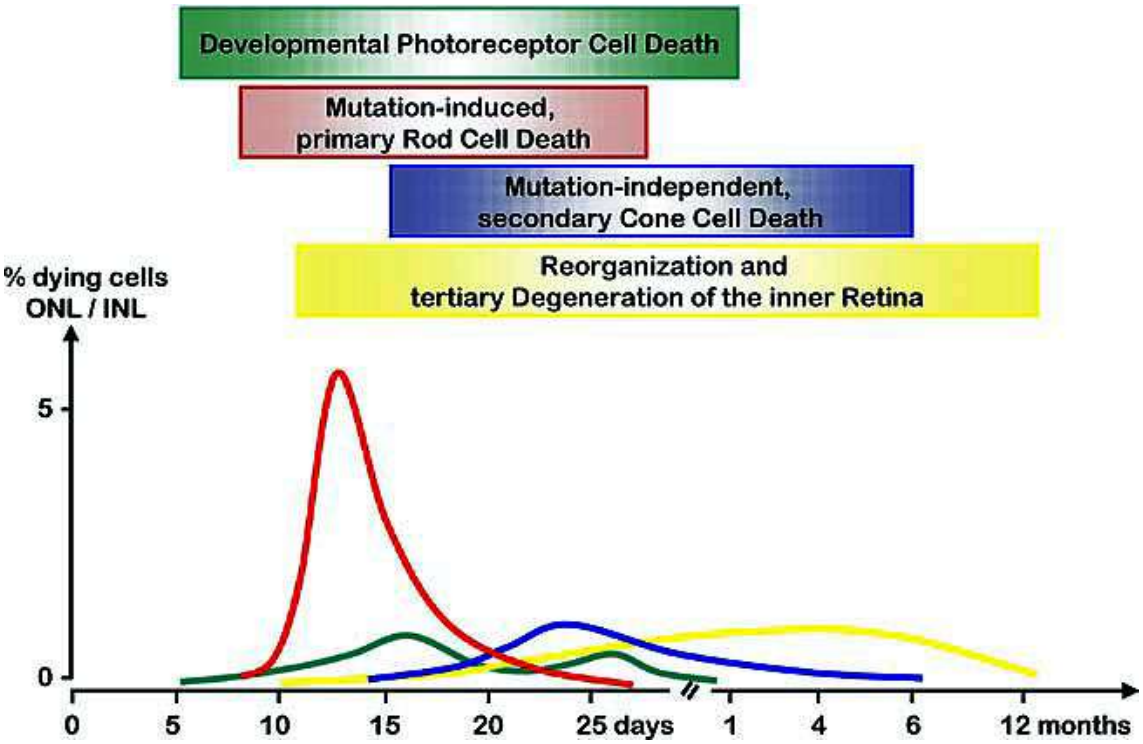

Figure 4: Cell death in *rd1* photoreceptor cells: A small amount of cell death is a normal event during post-natal development of wt retina (green line) and most likely driven by apoptosis. In *rd1,* the mutation dependent rod cell death (red line) begins around P7, shows a peak at P12 and nearly no rods are left after P25. Around P15 additionally cone photoreceptors start to degenerate (blue line), but in contrast to the rods this cell death is mutation independent and the trigger remains unknown. The missing input from photoreceptors is leading to a tertiary degeneration and reorganization of the remaining cells of the inner retina (yellow line). (Diagram from Sancho-Pelluz et al. 2008)

1.3.2 The cone photoreceptor function loss 1 (cpfl1) mouse

The *cpfl1* mouse carries a mutation in the catalytic subunit of the cone *Pde6* gene (*Pde6c*) (Chang *et al.* 2009). The mutation in the *Pde6* gene leads to a non-functional protein, which causes an accumulation of cGMP. This accumulation induces cone-degeneration, comparable with rod degeneration in *rd1* (Trifunović *et al.* 2010). The first changes in cone functionality are measurable three weeks after birth with ERG (Chang *et al.* 2002). The onset of cone cell death measured with TUNEL staining is detectable as early as P14; reaches a peak at P24 and at P60, nearly all cones are gone. Therefore, the *cpfl1* mouse is considered as a model for rapid and early cone loss (Trifunović *et al.* 2010), while retinal structure and rod functionality are not changed (Chang *et al.* 2002). In humans, analogue mutations cause autosomal recessive achromatopsia or early-onset progressive cone dystrophy (Thiadens *et al.* 2009; Chang *et al.* 2009). Therefore, the *cpfl1* mouse is used as model for achromatopsia (Chang *et al.* 2002).

1.3.3 The P23H line 1rat

In about 12% of autosomal dominant RP-patients in the US, a proline within the rhodopsin protein is substituted by a histidine (P23H) (Dryja *et al.* 1990a). To study this mutation a *P23H* mouse line was generated as well as a rat model, the *P23H* rats. The transgenic *P23H* rats contain the native rat opsin and additionally a mutated mouse opsin gene (Machida *et al.* 2000). There are different *P23H* lines available with different expression levels of transgenic protein and different degeneration rates. We showed with TUNEL staining, that rod degeneration showed a peak at P15 in *P23H* Line 1 (Kaur *et al.* 2011). At P30 approximately six rows of ONL cells are remaining, which was a 40% reduction compared to age-matched wt (Kaur *et al.* 2011). The mechanism of cell death is not entirely known, but rhodopsin misfolding and endoplasmatic reticulum stress has been proposed as possible causes of degeneration (Sung *et al.* 1991; Liu *et al.* 1996; Griciuc *et al.* 2010).

1.3.4 The S334ter line 3 rat

This rat model is referred as a model for autosomal dominant RP and contains a mutated rhodopsin, which is truncated at the C-terminus and lacks the last 15 amino acid residues (Liu *et al.* 1999). There are five *S334ter* lines available, all are bearing the same mutation but contain different expression levels of the mutated opsin, with the fastest degeneration rate correlating to the highest expression level of mutated opsin.

The truncated rhodopsin is mislocalized and targeted non-specifically to various membrane domains (Lee and Flannery 2007). Additionally, arrestin is unable to deactivate the truncated rhodopsin. Rod degeneration in the *S33ter* line 3 was extremely fast, since TUNEL-staining showed a peak of degeneration already at P12. Similar to *rd1,* only one row of photoreceptors remained at P30, most of them being cones (Kaur *et al.* 2011).

1.3.5 The 661W cell line

Despite the fact that there is a large number of animal models available to study photoreceptor degeneration it is still difficult to study cone cell death at the cellular level.

In humans, rods outnumber cones 20:1, while in mice the percentage of cones is even lower with approximately 3% (Carter-Dawson and LaVail 1979). That makes it

difficult to analyze cone degeneration in animal models and in retinal explants. With the cone-like cell culture, called 661W, it would be possible to study cones only (Tan *et al.* 2004). These cells originate from transgenic mice expressing the simian virus 40 (SV40) large tumor antigen (T antigen) under the photoreceptor specific interphotoreceptor retinoid-binding protein (IRBP) promoter (Al-Ubaidi *et al.* 1992). 661W cells expressed several cone specific proteins like blue opsin, red/green opsin, transducin and cone arrestin, while they showed no expression for rhodopsin or rod arrestin. Other photoreceptor markers like phosducin or rod outer segment membrane protein1 (ROM1) were also not found to be expressed in 661W cells (Tan *et al.* 2004). The morphology of 661W cells differs from cones, since they do not build outer segments (Tan *et al.* 2004). The 661W cells appear to be light-sensitive and undergo cell death, when treated with light (Krishnamoorthy *et al.* 1999) or treated with light in the presence of the chromophore 9-cis retinal (Kanan *et al.* 2007). Another study with 661W cells examined the functionality of cone CNG channels. They found weak expression of the CNGB3 subunit, but no expression of CNGA3. Unfortunately, the CNG channel is not functional without the CNGA3 subunit, so they transfected the mouse *Cnga3* gene and could achieve channel functionality (Fitzgerald *et al.* 2008). To sum up the findings, this cell line seems to be more cone-like than any other available cell line and therefore may be used as a model system for cone degeneration studies under defined experimental conditions.

1.4 Photoreceptor degeneration mechanisms

This study is focused on the degeneration mechanisms in hereditary photoreceptor degeneration. Therefore, only these cell death mechanisms will be explained. Other causes of photoreceptor degeneration might be light damage (Wenzel *et al.* 2005), aging (AMD) (Hageman *et al.* 2008; http://webvision.med.utah.edu/; information retrieved February 27, 2012) or mechanical forces leading to injury of the eye and the retina.

1.4.1 Photoreceptor degeneration in rd1

RP is caused by various mutations, which have a strong influence on the progression and severity of the disease. However, findings from distinct animal models of RP indicate that the downstream events may be closely related. If similar degeneration pathways were triggered by different mutations then this might allow treating many patients independent of the causative mutation. As mentioned above,

the *rd1* mouse suffers from a loss-of-function of PDE6β, which leads to an accumulation of cGMP (Farber and Lolley 1974). Because of cGMP accumulation, CNG channels in *rd1* rods are thought to be open more frequently, leading to an increased intracellular Ca^{2+} level. An evidence for the impact CNG channels have on *rd1* degeneration was shown with a double mutant (DBM) animal made by crossbreeding of two RP-models, the *rd1* and *cngb1* knockout (KO). This DBM contained both, a non-functional PDE6 and a non-functional CNG channel. In line with the idea, that chronically opened CNG channels may be responsible for the severe degeneration in *rd1*, a strong delay of rod cell death was observed in the DBM (Paquet-Durand *et al.* 2011). Additionally increased cGMP may activate protein kinases (PKG). In photoreceptors, at least three different isoforms are expressed and PKGs are 100-fold more sensitive to cGMP than CNG channels are (Farber *et al.* 1979; Gamm *et al.* 2000; Feil *et al.* 2005). Strong activation of PKG is able to cause cell death in neural and non-neural cell types (Canals *et al.* 2003; Deguchi *et al.* 2004; Canzoniero *et al.* 2006). The excessive PKG activation in *rd1* photoreceptors was inhibited pharmacologically and a rescue effect was shown (Paquet-Durand *et al.* 2009). However, neither a non-functional CNG channel nor an inhibition of PKG was able to stop the rod degeneration completely, indicating that both pathways may be activated in parallel. Alternatively, the cell may be able to switch to another cell death mechanism, when one pathway is blocked.

Further downstream of CNG channels or PKG, various key players are involved in the cell death mechanism. The increased Ca^{2+} concentration (Fox *et al.* 1999; Doonan *et al.* 2005), originating either from external sources through CNG or voltage-gated Ca^{2+}-channels and/or from intrinsic stores in the endoplasmatic reticulum or mitochondria (Barabas *et al.* 2010), is able to activate calpain proteases (Sancho-Pelluz *et al.* 2008). Active calpains induce cell death via protein cleavage, like cytoskeletal proteins or proteins involved in cell death like Bcl-2 associated X protein (Bax), c-Jun N-Terminal kinase (JNK), and apoptosis inducing factor (AIF) (review Sancho-Pelluz *et al.* 2008). However, the inhibition of all Ca^{2+} channels by pharmacological substances is leading to contradicting results (for review see Nakazawa 2011). In some studies a rescue effect was noted, in others not, indicating that the influx of Ca^{2+} may not be the only cell death mechanism active in *rd1* rod photoreceptors (Frasson *et al.* 1999; Read *et al.* 2002; Sanges *et al.* 2006; Pawlyk *et al.* 2002; Takano *et al.* 2004). The above mentioned Ca^{2+}-dependent calpain proteases were shown to be activated and involved in *rd1* photoreceptor cell death (Paquet-

Durand *et al.* 2007a; Paquet-Durand *et al.* 2006; Kaur *et al.* 2011). One of the targets of activated calpains is AIF, which translocates into the nucleus after cleavage and induces DNA damage and eventually cell death. This nuclear translocation of AIF was shown to take place in degenerating rods of *rd1* mice (Sanges *et al.* 2006). DNA damage leads to PARP activation, which usually supports DNA repair (for review see Krishnakumar and Kraus 2010). However, over-activation of PARP, induced by massive DNA damage can lead to cell death, either by energy depletion or by AIF-dependent cell death. PARP overactivation was found in dying *rd1* rod photoreceptors (Paquet-Durand *et al.* 2007b). PARP activation may not only occur following calpain activation, but also after oxidative stress. Cellular oxidative stress occurs when reactive oxygen species (ROS) like hydrogen peroxide or nitric oxide are not counter-balanced by redox-regulating enzymes anymore. Oxidative stress leads to cell damage via for instance increased DNA oxidation and finally to cell death. In *rd1* high oxidative stress (Carmody *et al.* 1999; Hackam *et al.* 2004) as well as increased DNA damage (Sanz *et al.* 2007) was observed in photoreceptor cells, indicating that oxidative stress may be involved in photoreceptor degeneration. However, it is unclear which role oxidative stress play in cell death mechanisms. High levels of Ca^{2+} may induce oxidative stress (Sharma and Rohrer 2007), which in turn may cause DNA damage and PARP activation. Nevertheless, it is still controversial if oxidative stress is a cause of retinal neurodegeneration or a consequence (Andersen 2004).

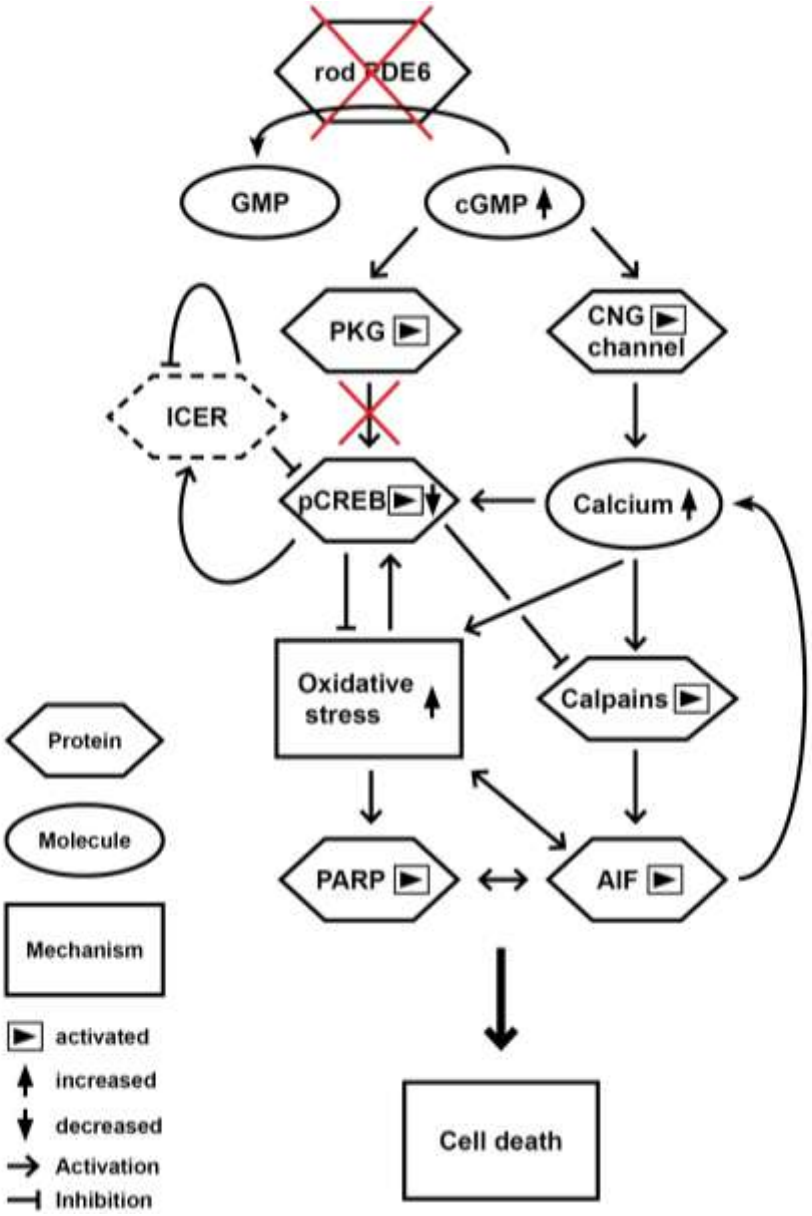

Figure 5: Potential mechanism leading to photoreceptor cell death in *rd1:* As a consequence of the *rd1* mutation, PDE6 is not working and unable to hydrolyze cGMP to GMP, leading to an accumulation of cGMP (Farber and Lolley, 1974). cGMP opens CNG channels, which leads to increased intracellular Ca^{2+} and activation of calpain proteases. Calpains cleave AIF, which translocates into the nucleus and induces DNA-damages, eventually leading to cell death. High cGMP activates PKG kinases, which should induce the activation of CREB dependent gene transcription. High Ca^{2+} and active AIF increase intracellular oxidative stress, which induces DNA damage. High oxidative stress and active AIF lead to an overactivation of the DNA-repair enzyme PARP, which causes massive energy depletion and finally cell death. Abbreviations: PDE6= phosphodiesterase; cGMP= cyclic guanosine monophosphate; PKG= protein kinase; CNG channel= cyclic nucleotide gated channel; ICER= inducible cAMP early repressor; pCREB= phosphorylated cAMP responsible element binding; PARP= poly (ADP-ribose) polymerase; AIF= apoptosis inducing factor (modified from Sancho-Pelluz *et al.* 2008)

1.4.2 Photoreceptor degeneration in different RP models

In other RP animal models, similar cell death mechanisms were found as in *rd1*. For example, in *S334ter* and *P23H* retinas, activated calpains and PARP as well as increased oxidative damage was shown (Kaur *et al.* 2011). Increased Ca^{2+} and activated calpains were detected in the spontaneous retinal degeneration rat model *WBN/Kob* as well as after MNU treatment of rat retinas (Azuma *et al.* 2004; Oka *et al.* 2006). Furthermore, active calpain as well as AIF translocation into the nuclei were shown in degenerating photoreceptors of *RCS* rats (Mizukoshi *et al.* 2010).

Hence, calpain activation was found in so many different RP models (Sancho-Pelluz *et al.* 2008; Paquet-Durand *et al.* 2006; Kaur *et al.* 2011; Azuma *et al.* 2004; Oka *et al.* 2006, Mizukoshi *et al.* 2010), while the activation of caspases was not found that often (Kaur *et al.* 2011; Doonan et al. 2005). These results may suggest that rod photoreceptors do not degenerate in a caspase-dependent fashion, which is a commonly associated with apoptotic cell death. However, it may be possible that photoreceptors degenerate in a calpain-dependent fashion, with increased Ca^{2+} and activated PARP. Interestingly, it is possible that more than one cell death pathway is active at the same time as was obtained in degenerating S334ter retina (Kaur *et al.* 2011). In this fast degeneration model not only calpains were active, but additionally also caspases.

1.4.3 Photoreceptor degeneration in cone degeneration

In a comparative study on the cell death mechanisms in *rd1* rods and the *cpfl1* cone-degeneration, again similarities of cell death pathways of photoreceptors were found. Increased cGMP levels, concomitant with activated PKG and increased calpain activity were detected. As well as in *rd1*, no activated caspase 3 was detectable, suggesting a non-apoptotic mechanism leading to cone degeneration in *cpfl1* mice (Trifunović *et al.* 2010). This suggests that in rod and cone photoreceptors similar or even the same mechanisms lead to degeneration. This would be of interest for the development of neuroprotective treatments, because it would open the possibility to save cones and rods with the same treatment.

1.4.4 cAMP-responsive element binding (CREB)

From neurodegenerative diseases like Huntington`s or Alzheimer it is known that the transcription factor cAMP-responsive element binding (CREB) is neuroprotective. Furthermore, disruption of CREB signaling may induce neurodegeneration in the

mouse (Mantamadiotis *et al.* 2002). CREB is activated by phosphorylation at the Serine 133 residue (pCREB) (Mayr and Montminy 2001) and may then bind to the cAMP-response element (CRE) sequence, which drives the transcription of numerous genes including neurotransmitters, growth factors and transcription factors (for review see Sakamoto *et al.* 2011). In *rd1*, CREB and pCREB expression was decreased at P11 (Paquet-Durand *et al.* 2006). This finding was surprising because activated PKG is able to phosphorylate CREB, plus the fact that oxidative stress induces CREB activation (Lee *et al.* 2009). Therefore, increased levels of pCREB would be expected in *rd1* photoreceptors. What caused the detected CREB reduction and is this decrease somehow involved in rod degeneration? One interesting study with 661W cells used a Ca^{2+} ionophore to increase the intracellular Ca^{2+}-level, which resulted in cell death, comparable with *rd1* rods (Arroba *et al.* 2009). This result could be repeated in wt retinal cultures and the cell death was correlated with a loss of pCREB. Furthermore, they correlated the loss of pCREB with the downregulation of calpastatin, the endogenous calpain inhibitor, which caused an upregulation of calpain-2 (Arroba *et al.* 2009). Possibly, pCREB protects photoreceptors against cell death via upregulation of calpastatin and inhibition of calpains. However, why is CREB decreased in *rd1* photoreceptors? One possible answer could be the prototypic inhibitor of CREB dependent transcription the inducible cAMP early repressor (ICER).

1.4.5 Inducible cAMP early repressor (ICER)

ICER is a member of the bZIP superfamily of transcription factors (Lonze and Ginty 2002). Included in this family are CREB, the cAMP response element modulator (CREM) and activating transcription factor 1 (ATF1). ICER is a transcript of the CREM gene, which encodes for various splice-forms of transcription activators and repressors (Borlikova and Endo 2009). CREM transcription repressors are known as ICER and are shorter than all other CREM transcripts, because they lack the activation domains and the kinase-inducible domain. There are four different ICER isoforms, namely ICER I, ICER II, ICER Iγ and ICER IIγ. ICER I contains the DNA-binding domain I, while ICER II contains the DNA-binding domain II, additionally ICER I + II have a γ-domain, which is missing in ICER Iγ and IIγ. The DNA-binding domains of ICER allow homo- and heterodimerization and binding to CRE-elements, where CREB and CREM transcription factors can bind as well. ICER competes with CREM and CREB and is a strong suppressor of CREB dependent transcription. Since it contains a CRE sequence, ICER transcription itself is CREB dependent, resulting in the fact, that ICER

is inhibiting its own transcription in a negative feedback loop (Molina *et al.* 1993a). The ICER isoforms have different half-lives, ICER I is the most stable and the γ-isoforms are the most short-lived (~3h) (Folco and Koren 1997). ICER transcription is strongly inducible by a various stimuli (Mioduszewska *et al.* 2003) and usually fast and transient. The time course of ICER transcription depends on the cell type (Borlikova and Endo 2009). ICER is expressed in various parts of the *rd1* brain, (for review see Kell *et al.* 2004) with the strongest expression in the pineal gland where ICER and CREB are regulating the circadian rhythm (Karolczak *et al.* 2005). In numerous cell cultures, ICER induction was shown after treatments that increased cAMP levels and activated PKA (Molina *et al.* 1993a; Stehle *et al.* 1993; Liu *et al.* 2006; Monaco and Sassone-Corsi 1997; Tinti *et al.* 1996; Hu *et al.* 2008). Alternatively, the Ras-dependent nerve growth factor pathway, the Janus kinase pathway, the PKC pathway; BDNF, or dopamine (Mioduszewska *et al.* 2003; Monaco and Sassone-Corsi 1997; Lund *et al.* 2008; Chang *et al.* 2006), induced PKA-independent ICER expression. In neurons, cardiomyocytes and vascular smooth muscle cells, ICER induction was leading to cell death (Jaworski *et al.* 2003; Mioduszewska *et al.* 2008; Ding *et al.* 2005; Ohtsubo *et al.* 2007) by repressing the pro-survival gene transcription of CREB. Therefore, an involvement of ICER in inhibition of CREB dependent transcription and activation in *rd1* photoreceptors appears plausible.

1.5 Neuroprotection and Therapy

Since RP was known in the middle of the 19th century, ophthalmologists have tried hard to find a cure to slow down disease progression. In a case study from as early as 1887, a woman was treated with electricity, unfortunately without permanent improvements of vision (Standish 1887). Since then much knowledge about the disease and its mechanisms has been gained, without any major advance for the therapy. Today, the recommended therapy is wearing sunglasses to protect the retina from UV light, while in some cases a Vitamin A uptake is recommended (www.pro-retina.de/netzhauterkrankungen/retinitis-pigmentosa; http://www.geteyesmart.org/eyesmart/diseases/retinitis-pigmentosa-treatment.cfm; information received 10/11/2011). Several fundamentally different concepts have been forwarded for RP therapy, namely gene therapy, neuroprotection or replacement (of cells or the whole retina). All concepts have different time windows for a medically sensible application.

1.5.1 Gene therapy

The idea of gene therapy is the correction of mutation-dependent defects or the protection of photoreceptors, using protein expression systems such as the adeno-associated virus vector (AAV). In some cases gene therapy was applied successfully (Gorbatyuk *et al.* 2010; Maguire *et al.* 2008; Simonelli *et al.* 2010) and could slow down degeneration in mutant animal models. Even some phase I clinical trials were made with human patients having LCA (Bainbridge and Ali 2008; Cideciyan *et al.* 2008; Maguire *et al.* 2008). Evaluating these studies is difficult, since all three studies used different treatment paradigms. Still, none of the used vectors had a negative effect and some patients had improved visual sensitivity. For patients, who had less severe disease symptoms at the beginning of the studies, the impact of therapy was better than in more advanced patients. Therefore, gene therapy should be applied as early as possible, before great damages occur, since the expression vector requires a more or less healthy target cell for protein expression. Consequently, gene therapy also requires an early disease diagnosis. Unfortunately, this is a problem, as the symptoms usually starting only after massive cell degeneration has taken place. For a review of gene therapy in ocular diseases, refer to Liu *et al.* 2011.

1.5.2 Replacement

Replacement therapy is aiming to bring back vision with a prosthetic device or by introducing functional photoreceptors. Since, there could be adverse effects caused by bringing a mechanical device into the eye, the patient should be already in a late disease stage to avoid additional vision impairment. Some promising studies were made with retinal implants in blind patients, who could divide patterns and were even able to read after implantation of a subretinal electronic chip (Zrenner 2002; Besch *et al.* 2008). Other attempts of replacement therapy would be reprogramming existing cells, like Müller glia cells, towards the photoreceptor cell fate (Bermingham-McDonogh and Reh 2011). Reprogramming of Müller cells happens naturally in fish or amphibian, but not in the mammalian retina, which makes it impossible to induce photoreceptor regeneration up to now. Instead of reprogramming Müller cells, other studies have used stem cells to replace lost photoreceptors. Either retinal sheets or single cell suspensions were transplanted into the subretinal space of animals or humans (Singh and MacLaren 2011). The cell numbers that were able to integrate into the host tissue are low and in some cases, inflammation after transplantation was

observed. Additionally, it is still unclear whether the vision of patients with a progressed diseased retina can be restored (Singh and MacLaren 2011).

1.5.3 Neuroprotection

Neuroprotection is aiming to protect retinal cells from cell death or at least to slow down cell degeneration by either interfering with cell death signaling or strengthening pro-survival mechanisms. In theory, neuroprotective substances could be applied in every stage of disease and be combined with other therapies. Moreover, and assuming that the principal degeneration processes are similar in patients with distinct mutations, neuroprotection might work independent of the degeneration-causing mutation.

Neurotrophic factors

The idea of protecting neurons from cell death started after Levi-Montalcini in the early 1950´s found the first neurotrophic factor, namely the nerve growth factor (NGF) (Levi-Montalcini *et al*. 1954; Aloe 2011). Neurotrophic factors are able to enhance neuronal cell growth and survival (Harada *et al.* 2002; Wen *et al.* 1995; Yu *et al.* 2004; Hackam 2008). For the neuroprotection of the retina, mainly three neurotrophic factors were studied: brain derived neurotrophic factor (BDNF), ciliary neurotrophic factor (CNTF) and pigment epithelium-derived factor (PEDF) (Trifunović *et al.* 2012). Combined treatment of *rd1* organotypic explant cultures with BDNF and CNTF resulted in neuroprotection of photoreceptors, which correlated with the downstream activation of pCREB (Azadi *et al.* 2007). CNTF alone was able to slow down retinal degeneration in at least 13 animal models of RP including *rd1* mice, *P23H* and *S334ter* rats (Sieving *et al.* 2006). Furthermore, PEDF and docosahexaenoic acid (DHA) had a synergistic protective effect in human RPE cells, when these cells were under oxidative stress (Bazan 2008). Unfortunately neurotrophic factors have some limitations like a short half live, which requires repeated administration. This fact may be responsible for contradicting results obtained for instance in a study on *Q344ter* mice which had received BDNF treatment via intravitreous injections and, where no protective effect (LaVail *et al.* 1998) was found. In another study, transgenic inducible BDNF expression delayed photoreceptor cell death in *Q344ter* mice (Okoye *et al.* 2003). The difference between both studies was the BDNF treatment period. A short increase of BNDF after the injections gave no effect, while a prolonged expression in the transgenic mice over three weeks up to three month did.

Additional disadvantages of neurotrophins are the large proteins size and serious systemic side effects that may occur when they are applied orally. Therefore, a special delivery system is required to increase neurotrophic factors locally and persistent (Trifunović *et al.* 2012).

Antioxidants

Antioxidant treatment may be another approach for the prevention of oxidative stress and neuroprotection. Oxidative stress is found in many age-related degenerative disorders like Alzheimer´s disease or Parkinson`s disease (Franco and Cidlowski 2009) as well as in ocular diseases like AMD (Komeima *et al.* 2007), glaucoma (Tezel 2006) and RP (Carmody *et al.* 1999; Usui *et al.* 2009a; Usui *et al.* 2009b). Neurotrophic factors can have neuroprotective effects, like the basic fibroblast growth factor (bFGF) which protected photoreceptor-like 661W cells against oxidative stress via a CREB dependent Bcl-2 upregulation (O'Driscoll *et al.* 2007). Apart from neurotrophins, various other substances have an antioxidant effect. In clinical trials the impact of Vitamin A, Vitamin E, DHA and lutein in combination or separated against retinal degeneration were validated (Berson *et al.* 1993; Pasantes-Morales *et al.* 2002). Unfortunately, the therapeutic success appeared to be dependent on the genetic background of the patient, the type of antioxidants used and the intervals of administration. In *rd1* a combined treatment with zeaxanthin, lutein, alpha-lipoic acid, glutathione and an extract from Wolfberry (Lyceum barbarum) was able to delay photoreceptor degeneration (Miranda *et al.* 2010), and similarly, glutathione S transferase (GST) protected retinal explant cultures of *rd1* (Ahuja *et al.* 2005). Despite the fact that neuroprotection with various antioxidants separated or combined was tried in various animal models of RP, the impact of antioxidant treatment was rather low. Hence, the observed improvements were only short lived and most likely eased unspecific symptoms rather than interfered with the degeneration mechanism itself (Baumgartner 2000).

Prevention of cell death via neuroprotection

Most of the recent strategies for neuroprotection focus on the prevention of cell death rather than unspecific support of the cellular metabolism (Trifunović *et al.* 2012). Prevention of cell death may be done by blocking either the initiation of cell death or its execution. Based on the cell degeneration mechanism in *rd1* photoreceptors (Sancho-Pelluz *et al.* 2008), one protective strategy would be the downregulation of cGMP to a regular level. One attempt to do so was a knock down of the guanylate cyclase (GC)

with siRNA in a PDE6 loss of function mouse (*Pde6b*^{H620Q}) (Tosi *et al.* 2010). The knock down of GC, the cGMP producing enzyme, in *Pde6b*^{H620Q} mice resulted in delayed photoreceptor loss and enhanced ERG response. Another neuroprotective strategy is the blockage of the CNG channels to decrease the intracellular Ca^{2+} level. This was done pharmacologically with more or less specific Ca^{2+} channel blockers like D-cis-diltiazem or L-cis-diltiazem, which resulted in minor rescue effects (Vallazza-Deschamps *et al.* 2005; Takano *et al.* 2004; Pearce-Kelling *et al.* 2001; Pawlyk *et al.* 2002; Bush *et al.* 2000; Barabas *et al.* 2010; Frasson *et al.* 1999). Significant rescue effects were seen after knockdown or knockout of CNG-channels in *Pde6b*^{H620Q} or *rd1* mice, respectively (Tosi *et al.* 2010; Paquet-Durand *et al.* 2011). Even in CNG-knockout mice, the rescue of the *rd1* phenotype was incomplete, implicating additional degeneration mechanisms independent of CNG channels. This mechanism may be PKG dependent and inhibition of the PKG with different inhibitors in two different RP models, *rd1* and *rd2*, resulted in a strong rescue effect. However, the degeneration was not stopped completely (Paquet-Durand *et al.* 2009), implying that the cell death mechanism may be more complex than expected.

Another protective approach would be the inhibition of cell death executing proteins like the calpain proteases. Inhibition of calpains with ALLN and/ or ALLM (Acetyl-L-Leucyl-L-Leucyl L-Norleucinal/ -Methionin) was successfully reducing cell death in *rd1* retinas (Sanges *et al.* 2006). Furthermore, the endogenous calpain inhibitor calpastatin was able to reduce cell death in *rd1* organotypic explant cultures and *in vivo* after injection of calpastatin into the vitreous body of PN10 *rd1* eyes (Paquet-Durand *et al.* 2010). Another cell death protein active in *rd1*, PARP1, was specifically inhibited, which resulted in reduced cell death in *rd1* retinal cultures until P25 (Paquet-Durand *et al.* 2007b). This result was confirmed with *Parp-1* KO retinal explants treated with zaprinast, a specific PDE5/6 inhibitor, to mimic the *rd1* degeneration. Compared to the correspondent wt, less photoreceptor degeneration was detectable in *Parp-1* KO retinas (Sahaboglu *et al.* 2010).

2 Experimental Questions and Aims

2.1 ICER and CREB signaling in photoreceptors

The neuroprotective factor CREB was downregulated in degenerating rd1 retinas (Paquet-Durand *et al.* 2006). This downregulation may be dependent on the CREB inhibitor ICER.

- What is the expression pattern of pCREB *C3H-rd1* retinas at different ages?
  - Quantification of pCREB in *C3H-rd1* retinas
- How is ICER expressed in *C3H-rd1* retina and in other retinal degeneration models?
  - Quantification of ICER expression in all used models
- How is pCREB and ICER expressed after zaprinast treatment in retinal explant cultures?
  - Quantification of pCREB and ICER expression in zaprinast treated *C3H-wt* retinal explant cultures

2.2 Using 661W cells to establish a screening-system for cone neuroprotection

Their limited number in the common used rodent animal models often hampers an investigation of cone degeneration on the cellular level. It would be beneficial to have a cell based cone degeneration screening system available to study cone degeneration mechanisms and cell protective treatment.

- Are 661W cells appropriate for a cone neuroprotection screening?
  - Expression study of retinal cell marker and proteins of the degeneration signaling pathway
- Is it possible to mimic the degeneration of *cpfl1* cones in 661W cells?
  - Comparison of the reliability of different cell death assays (TUNEL, AlamarBlue, Live/DEAD, Propidiumiodide)
  - Which pharmacological treatment induces a strong and *cpfl1* specific cell degeneration?
- Which putative neuroprotective substance is able to protect the 661W cells?
  - Testing of PKG inhibitors, antioxidants

3 Material and Methods

3.1 Material

Table 2: Materials and Devices:

Chemicals, Material, Devices and Software	Company	Product no.
(+/-)-α-Lipoic Acid (Thiotic Acid)	Sigma-Aldrich Chemie GmbH, Taufkirchen, Germany	T1395
0.5ml Save-Lock Microcentrifuge Tube	Eppendorf, Wesseling/Berzdorf, Germany	*0030121.023
1,4-diazabicyclo[2.2.2]octane (DAPCO)	Sigma-Aldrich Chemie GmbH, Taufkirchen, Germany	D-2522
1.5ml Save-Lock Microcentrifuge Tube	Eppendorf, Wesseling/Berzdorf, Germany	*0030120.086
15 ml Cell Star® Tubes	Greiner bio one, Frickenhausen, Germany	1880271
2.0ml Save-Lock Microcentrifuge Tube	Eppendorf, Wesseling/Berzdorf, Germany,	*0030120.094
2-Mercaptoethanol	Sigma-Aldrich Chemie GmbH, Taufkirchen, Germany	M-6250
50ml Cell Star® Tubes	Greiner bio one, Frickenhausen, Germany	210 261
8-Br-cGMP	BioLog live science institute	B004-250E
Acetic acid	Merck, Darmstadt, Germany	1099510001
Acetone	Merck, Darmstadt, Germany	1000142511
Adobe CS5 Design Standard Version12.0.3x32	Adobe Systems GmbH, Munich, Germany	—
Agar	Sigma-Aldrich Chemie GmbH, Taufkirchen, Germany	A-9915
AGFA Curix 60; film developing device	Siemens Healthcare, Erlangen, Germany	—
Almar Blue	Abderotec	719816
Albumin, from bovine serum	Sigma-Aldrich Chemie GmbH, Taufkirchen, Germany	A7906-50G
Amersham Hyperfilm™ ECL; chemiluminescence film	GE Healthcare Europe, Freiburg, Germany	28906837
Ammonium persulfate (APS)	Sigma-Aldrich Chemie GmbH, Taufkirchen, Germany	A3678
Ampicilin	Sigma-Aldrich Chemie GmbH, Taufkirchen, Germany	A5354-10ml
Anitbiotic-antimycotic	Invitrogen Life Technologies, Darmstadt, Germany	15240096
Anthos Labtec HT2 photometer	Anthos Mikrosysteme GmbH, Krefeld	—
Axio Imager Z1 Apo Tome Microscope	Carl Zeiss Micro Imaging GmbH, Göttingen	—
Axio Vision 4.7 Software	Carl Zeiss Micro Imaging GmbH, Göttingen	—
Axiovert 35M; inverted Microscope	Carl Zeiss Micro Imaging GmbH, Göttingen	—
Bradford Reagent	Sigma-Aldrich Chemie GmbH, Taufkirchen, Germany	B6916
Bromphenolblue	GE Healthcare Europe, Freiburg, Germany	17-1329-01
Canon PowerShot G9 digital Camera	Canon Deutschland GmbH, Krefeld, Germany	—
CMV-vector	Sigma-Aldrich Chemie GmbH, Taufkirchen, Germany	E 7398
Coomassie Blue R-250	Merck, Darmstadt, Germany	12553

Copper(II) sulfate pentahydrate ($CuSO_4(H_2O)_5$)	Merck, Darmstadt, Germany	1.02790
Corticosterone	Sigma-Aldrich Chemie GmbH, Taufkirchen, Germany	862290
Cryo.S™ 2ml Freezing Tubes	Greiner bio one, Frickenhausen, Germany	122263
culture membrane insert (for electroporation); 0,4µm pore size	Costar®; Corning B.V., Amsterdam, Netherland	3412
culture membrane insert (only culture); 0,4µm pore size;	Millipore GmbH, Schwalbach, Germany	PIHA03050
DABCO;1,4-Diazabicyclo(2,2,2)octane	Carl Roth, Karlsruhe, Germany	0718
DAPI	Sigma-Aldrich Chemie GmbH, Taufkirchen, Germany	D-9542
DHα Escherichia coli	Invitrogen Life Technologies, Darmstadt, Germany	18265017
Dimethyl Sulphoxide (DMSO; sterile filtered)	Sigma-Aldrich Chemie GmbH, Taufkirchen, Germany	D2650
Dithiothreitol (DTT)	Sigma-Aldrich Chemie GmbH, Taufkirchen, Germany	43817
DL-Tocopherol/-acetate	Sigma-Aldrich Chemie GmbH, Taufkirchen, Germany	T1539_25mg
Dulbecco's Modified Eagle Medium (DMEM)	PAA Laboratories GmbH, Cölbe, Germany	E15-843
Dulbecco's Modified Eagle Medium (DMEM)	Invitrogen Life Technologies, Darmstadt, Germany	41966-052
Dulbecco's Phosphate Buffered Saline (DPBS)	Invitrogen Life Technologies, Darmstadt, Germany	14040-083
ECL Plus; Amersham™	GE Healthcare Europe, Freiburg, Germany	RPN2132
Electroporation chamber A	self-made by the workshop of the Eye Hospital Tuebingen	—
Electroporation chamber B	self-made by the workshop of the Eye Hospital Tuebingen	—
Electroporation device CUY 21 EDIT	Nepa Gene Co.,LTD	—
Electroporation rings	self-made by the workshop of the Eye Hospital Tuebingen	—
Ethanol	Merck, Darmstadt, Germany	1009832511
Ethylenediaminetetraacetic acid (EDTA)	Sigma-Aldrich Chemie GmbH, Taufkirchen, Germany	E-9884
Fetal Bovine serum	Gibco, Karlsruhe, Germany	10500-064
Fiji image processing software, ImageJ, Java and plugin package	http://fiji.sc/wiki/index.php/Fiji	—
Whatsman, Chromatography paper, 3MM CHR, Filter paper for western blot	VWR, international GmbH, Bruchsal, Germany	3030-931
Fura-2, AM	Invitrogen Life Technologies, Darmstadt, Germany	F-1201
Glacial acetic acid	Merck, Darmstadt, Germany	1.00063
Glutamine/	Sigma-Aldrich Chemie GmbH, Taufkirchen, Germany	G8540
Glutathione	Sigma-Aldrich Chemie GmbH, Taufkirchen, Germany	G6013
Glycerol/Glycerin	Sigma-Aldrich Chemie GmbH, Taufkirchen, Germany	Sigma
Glycin	Carl Roth, Karlsruhe, Germany	3908.3
Heidolph DIAX 600 homogenizer	Heidolph, Schwabach, Germany	—
Wheaton konischer Gewebe-Handhomogenisator	NeoLab, Heidelberg, Germany	9-0936
IBMX	Sigma-Aldrich Chemie GmbH, Taufkirchen,	I5879-100 mg

	Germany	
Insulin	Sigma-Aldrich Chemie GmbH, Taufkirchen, Germany	I 6634
Isopropanol	Merck, Darmstadt, Germany	Merck
Jung; Tissue freezing medium®	Leica Microsystems Nussloch, Nussloch, Germany	0201 08926
L-Cystein HCL	Sigma-Aldrich Chemie GmbH, Taufkirchen, Germany	C7477
Linolic Acid	Sigma-Aldrich Chemie GmbH, Taufkirchen, Germany	L1012
Manganese(II) chloride tetrahydrate ($MnCl_2(H_2O)_4$)	Sigma-Aldrich Chemie GmbH, Taufkirchen, Germany	M-2670
Methanol	VWR Prolabo	20847.307
Monosodium phosphate (NaH2PO4)	Merck, Darmstadt, Germany	1063451000
Mowiol	Calbiochem	475904
Multifuge 3-S-R Centrifuge	Heraeus	—
Nanodrop 2000	Thermo scientific, Rockford, USA	—
Na-pyruvate	Sigma-Aldrich Chemie GmbH, Taufkirchen, Germany	P3662
NucleoBond® Xtra Maxi	Macherey-Nagel, Düren, Germany	—
Okadaic acid	Sigma-Aldrich Chemie GmbH, Taufkirchen, Germany	8,010
Paraformaldehyde (PFA)	Sigma-Aldrich Chemie GmbH, Taufkirchen, Germany	P 6148
phenylmethanesulfonylfluoride (PMSF)	Merck, Darmstadt, Germany	6367.1
Pierce® ECL Western Blotting Substrate	Thermo scientific, Rockford, USA	32106
Pluronic® F-127 *20% solution in DMSO	Molecular Probes, Invitrogen, Life Technologies Paisley, UK	P-3000MP
Poly-L-lysine solution	Sigma-Aldrich Chemie GmbH, Taufkirchen, Germany	P4832-50ML
Progesterone	Sigma-Aldrich Chemie GmbH, Taufkirchen, Germany	P-8783
Protein Assay Dye Reagent (Bradford)	Sigma-Aldrich Chemie GmbH, Taufkirchen, Germany	B 6916
Proteinase K	Sigma-Aldrich Chemie GmbH, Taufkirchen, Germany	P-6556
Proteinase K (for R16)	mpbio (MP Biomedicals)	193,504
PVDF transfer membranes; Amersham Hybond™-P	GE Healthcare Europe, Freiburg, Germany	RPN303F
R16 Powder Medium (Basal)	Invitrogen Life Technologies, Darmstadt, Germany	07490743
Retinol/Retinylacetate	Sigma-Aldrich Chemie GmbH, Taufkirchen, Germany	R 7632
Roswell Park Memorial Institute medium (RPMI)	PAA Laboratories GmbH, Cölbe, Germany	E15-840
Roti-Block	Carl Roth, Karlsruhe, Germany	A 151.1
Rotiphorese® Gel 30 (Acrylamid-Mix)	Carl Roth, Karlsruhe, Germany	3029.1
Sucrose	Clinic Pharmacy, Tübingen, Germany	1,076,511,000
Shaker; Heidolph unimax 2010	Heidolph, Schwabach, Germany	—
Shaking Water Bath 1086	GFL- Gesellschaft für Labortechnik mbH, Burgwedel, Germany	—
sodium chloride (NaCl)	Sigma-Aldrich Chemie GmbH, Taufkirchen, Germany	S-3014
Sodium dodecyl sulfate (SDS)	Fluka; Sigma-Aldrich Chemie GmbH, Taufkirchen, Germany	71,725

sodium phosphate monobasic monohydrate (NaH_2PO_4 x H_2O)	Merck, Darmstadt, Germany	1.06346
Sodium selenite pentahydrate ($NaSeO_3(H_2O)_5$)	Fluka; Sigma-Aldrich Chemie GmbH, Taufkirchen, Germany	00163
T3	Sigma-Aldrich Chemie GmbH, Taufkirchen, Germany	T6397-100 mg
TEMED	Carl Roth, Karlsruhe, Germany	2367.1
Thiamine HCL	Sigma-Aldrich Chemie GmbH, Taufkirchen, Germany	T1270
TILLVision Imaging Software	TILL Photonics, Gräfelfing, Germany	—
TILLVision Polychrome2 light source	TILL Photonics, Gräfelfing, Germany	—
Transferrin	Sigma-Aldrich Chemie GmbH, Taufkirchen, Germany	T-8027
Tris	Sigma-Aldrich Chemie GmbH, Taufkirchen, Germany	154563
Triton-X-100	Sigma-Aldrich Chemie GmbH, Taufkirchen, Germany	X-100
Trizma Base	Sigma-Aldrich Chemie GmbH, Taufkirchen, Germany	T-1503
Tryptone	Sigma-Aldrich Chemie GmbH, Taufkirchen, Germany	T7293
TUNEL®assay (In Situ Cell Death Detection Kit for Cell culture)	Roche Diagnostics Deutschland GmbH., Mannheim, Germany	1684809/1684817
Ultrafree-MG GV filter	Millipore GmbH, Schwalbach, Germany	UFC30GV0S
Vectashield	Linaris GmbH, Dossenheim, Germany	H-1000
Vitamin B12	Sigma-Aldrich Chemie GmbH, Taufkirchen, Germany	V6629
Vitamin C	Sigma-Aldrich Chemie GmbH, Taufkirchen, Germany	A4034
Yeast extract; Difco	Bacterius Ltd.; Houston, USA	66472JA
Zaprinast	Sigma-Aldrich Chemie GmbH, Taufkirchen, Germany	Z0878-25mg

3.2 Media and Buffers

Basal medium (R16)

For 800ml, basal medium one vial R16 powder was dissolved in 500ml ddH_2O. Then 32,5mM $NaHCO_3$, 60nM $NaSeO_3(H_2O)_5$, 5nM $MnCl_2$ x $4H_2O$, 20nM $CuSO_4$ x $5H_2O$, 0.1µg/ml Biotin and 1µg/ml Ethanolamine were added. With ddH_2O, it was brought to the volume of 800ml. Finally it was sterile filtered and aliquoted.

Complete medium

Into the Basal medium (R16) 0.2% BSA, 10µg/ml Transferrin, 0.0063µg/ml Progesterone, 2µg/ml Insulin, 0.002µg/ml T3, 0.02µg/ml Corticosterone, 2.77µg/ml ThiaminHCL, 0.31µg/ml Vitamin B12, 0.045µg/ml (+/-)-α-Lipoic Acid, 0.1µ/ml Retinol, 0.1µg/ml Retinyl acetate, 1µg/ml DL-Tocopherol, 1µg/ml Tocopherylacetat, 1µg/ml Linoleic Acid, 1µg/ml Linoleic-Acid, 7.09µg/ml L-CysteineHCl, 1µg/ml Glutathione, 50µg/ml Na-pyruvate, 25µg/ml Glutamine and 100µg/ml Vitamin C were added. For electroporation additionally 1% Antibiotic-Antimycotic was added.

Coomassie Blue solution

For 500ml Coomassie Blue solution 1.25g Coomassie Blue R-250, 250ml Methanol, 50ml Glacial acetic acid were dissolved in 100ml ddH_2O and it was brought to volume with ddH_2O.

EDTA

5mM EDTA was dissolved in PBS and the pH was adjusted to 8.5.

Adapted erythrocyte lysis buffer (ELB)

50mM Tris was dissolved in ddH_2O and pH was adjusted to 7.5, then 250mM NaCl, 0.1% Igepal (Nonidet P40), EDTA (pH 8.0) and Glycerol 20% v/v were added. Finally, fresh 5mM DTT, 2mM PMSF or 1x Proteinase Inhibitor was added.

Extracellular Solution (ES)

150mM NaCl, 5mM KCl, 2mM $CaCl_2xH_2O$, 2mM $MgCl_2xH_2O$, 10mM HEPES and 30mM GlucosexH_2O were dissolved in ddH_2O and pH was adjusted to 7.4.

Homogenization buffer

10mM Tris, 1mM EDTA, 150mM NaCl, 2% SDS, 10% Glycerol, 0,0625M Tris- HCl, 50nM Okadaic acid were dissolved in ddH_2O. The pH was adjusted to 6.8, and then 10µl/ml Proteases inhibitor cocktail was added.

5x Laemmli Buffer

1x Tris-HCL Buffer (1.5M; pH 6.8), 5% w/v SDS, 50% v/v Glycerol, 500mM beta-mercapto-ethanol, 0.05% Bromophenolblue were dissolved in ddH_2O.
Then the solution was homogenized, aliquots of 1ml were made and stored at -20°C.

LB-Medium

For 500ml LB-Medium 5g Tryptone, 2,5g Yeast extract and 5g NaCl were weighted. Then ddH_2O was added and pH was adjusted to 7.0. Finally it was brought to volume with ddH_2O and autoclaved.

PB

For the stock solution (20x) two solutions were prepared. For solution A 0.2M NaH2PO4xH_2O was dissolved in 250ml ddH_2O. For solution B 0.2M NaH_2PO4 was dissolved in 500ml ddH_2O. Then solution A was added into solution B until the pH was of 7.4. For experiments, the stock solution was diluted 1:20 to obtain an end concentration of 0,01M PB.

PBS

The stock solution of PB was diluted 1:20 with ddH_2O and 155mM NaCl was added. Finally, the pH was adjusted to 7.4.

10x Running Buffer

25mM Trizma Base, 190mM Glycin, 0.1% SDS were dissolved and brought with ddH2O to the end volume of 1l.

Transfer Buffer (10x)

25mM Trizma Base and 190mM Glycin were dissolved in 1l of ddH2O.

TE -Buffer

10mM Tris was dissolved in ddH_2O and the pH was adjusted to 8.0 with HCl. Finally, 1mM EDTA was added.

TBS (Immunohistochemistry)

50mM Tris was dissolved in 900ml ddH_2O and 155mM NaCl was added, then the pH was adjusted to 7.6 and ddH_2O was added.

TBS for western blot (10x)

13mM Trizma base was dissolved in 900ml ddH_2O and 150mM NaCl was added.
The pH was adjusted to 7.6 and with ddH_2O, it was filled up to 1l.

Tris-HCL Buffers

1.5M Tris was dissolved in ddH_2O and the pH was adjusted to 6.8.
0.5M Tris was dissolved in ddH_2O and the pH was adjusted to 8.8

5x Sample Buffer

10% w/v SDS, 10mM DTT or beta-mercapto-ethanol, 20% v/v Glycerol, 0.2M Tris-HCl, pH 6.8 and 0.05%w/v Bromophenolblue were dissolved in ddH2O.
The 5x stock solution was diluted to 1x concentration before used.

Stripping solution

Into 0,0625M Tris-HCl solution 2% of SDS and 0,007% beta-mercapto-ethanol were added.

Super optimal broth with catabolite repression (SOC-Medium)

2% w/v tryptone, 0.5% w/v yeast extract, 8.56mM NaCl and 2.5mM KCl were mixed and dissolved in ddH_2O. The pH was adjusted to 7.0 and the solution was autoclaved. Finally, 10mM $MgCl_2$ and 20mM glucose were added.44

3.3 Methods

3.3.1 Deoxyribonucleic acid (DNA) constructs

DNA constructs and plasmids

The oxidative stress sensors was kindly provided by PD Dr. Tobias Dick (German Cancer Research Center, Heidelberg, Germany) and were described in detail in (Gutscher *et al.* 2008).

Wt human CNGA3 expression construct was generated as described previously by (Trankner *et al.* 2004) and the co-transfected cyan fluorescent protein (CFP) expression vector (pECFP-C1; Clontech, Mountain View, CA, USA) was generated as described in Köppen *et al.* (2008).

For electroporation, an EGFP- expression vector was used (CMV-Vector; Sigma-Aldrich Chemie GmbH, Munich, Germany).

DNA purification (Maxi-prep)

DNA-purification was carried out with a NucleoBond® Xtra Maxi kit (Macherey-Nagel, Düren, Germany) according to provider`s manual. Every step was done at room temperature. After centrifugation at 6000g the bacteria-pellet was resuspended in “resuspension buffer” containing RNase A (60µg/ml) and lysis solution. After gentle shaking, the sample was incubated for 5min. In this time the “binding column” was equilibrated with “equilibration buffer”, “neutralization buffer” was added and after gentle shaking each sample was put into a “binding column”. When all liquid run through the column was rinsed with “equilibration buffer”. Then the column filter was discarded and “wash buffer” was added. Now the DNA was eluted by adding “elution buffer” and the elution was collected in 50ml tubes.

Isopropanol precipitation

Isopropanol was added to the eluted DNA samples at RT, after thorough vortexing the mixture was incubated for 2min. Afterwards the samples were centrifuged at 15000g for 30min at 4°C. The pellet was rinsed by addition of 70% ethanol and again centrifuged at 15.000g for 5min at RT. After the pellet was completely dried, it was diluted in TE and the plasmid yield was determined with spectrophotometry Nanodrop 2000 (Thermo scientific, Rockford, USA).

3.3.2 Bacteria

Strain

For all experiments competent DH5α-strain of Escherichia coli (E.coli) from a stock frozen at -80°C were used.

Transformation

Competent E.coli were thawed on ice and 50µl were pipetted into 2ml Tubes. All three vectors were added to different tubes and incubated on ice for 30min. All tubes were placed for 45sec in a 42°C water bath and were cooled for 2min on ice. Then 450µl SOC-medium was added to each tube and all samples were transferred to a 15ml Tube and let grow for 1h at 37°. LB-Agar plates with 0.02% Ampicillin were streaked with 100µl and 400µl transformed E.coli and incubated overnight at 37°C. To prepare an E.coli stock, one colony for each plate was transferred to 3ml LB containing Ampicillin and grown over night in 37°C while shaking.

Glycerol stock

60% Glycerol was sterile filtered and 250µl were pipetted into cryo-tubes. 750µl bacteria solution from an over-night culture was added and mixed extensively. All glycerol stocks were stored at -80°C.

Preculture

6ml of LB medium containing 0.2% Ampicillin were inoculated with *E.coli* directly from a glycerol stock and incubated overnight at 37°C while shaking at ca. 300rpm.

3.3.3 Cell culture

Cell lines

Human embryonic kidney cells 293 (HEK293) were maintained in DMEM containing 10% FBS and 1% Pen/Strep. Human cervical cancer cells (HeLa) were maintained in RPMI containing 10% FBS and 1% Pen/Strep. Murine cone-like 661W cell line was generously provided by Dr Muayyad Al-Ubaidi (Department of Cell Biology, University of Oklahoma Health Sciences Center, Oklahoma City, OK, USA) and were maintained either in DMEM or in RPMI to gain comparable conditions with both control cell lines. All cell lines were kept in a 25cm²-cell culture flask (PAA) at 37°C in a humidified atmosphere and 5% of CO_2 inside a Hera Cell incubator (Hereas).

Cell splitting

When the cells were confluent every 3rd or 4th day, the cells were seeded into a new cell culture flask. Every step was done under a sterile bench (Hereas) at sterile conditions. DPBS, Cell Medium and Trypsin were preheated in a 37°C water bath. All medium was aspirated from the cell culture flask and the cells were rinsed with DPBS. Afterwards 500µl Trypsin was added and the flask was shaken and incubated for 3-4min in the incubator at 37°C. Then 5ml of DPBS were added into the flask and with gently pipetting up and down every cell was detached. The DPBS containing the cells were added into a sterile 15ml tube and centrifuged at 4°C and 180g for 10min. The supernatant was aspirated and the pellet was resuspended in 2ml DPBS. 500µl of this cell suspension was added into a new flask containing 10ml medium. The cells were maintained at 37°C in a humidified atmosphere and 5% of CO_2 inside a Hera Cell incubator (Hereas).

Transfection

After cell splitting, the cell number was measured with an improved Neubauer chamber and 0.5-2 x 10^5 cells were seeded in 2ml medium without antibiotics/antimycotics and seeded into a 6-well plate. When the cells were approx. 90% confluent, transfection was done with Lipofectamin^{TM}2000 after provider´s manual. First, the DNA was diluted in medium without serum or antibiotics, as well as Lipofectamin^{TM}2000 was. After 5min incubation at RT both volumes were mixed and incubated at RT for 20min. Now 100µl of the transfection mix was added to every well, after 6h at 37° and 5%CO_2 medium was changed to normal cell culture medium.

Transfection efficacy was analyzed after 16-18h and for Ca^{2+} level measurement experiments, 3% or 1.5% sodium butyrate was added to HEK293 or 661W cells respectively, to increase the vector transcription.

AlamarBlue® cytotoxicity assay

Prior to the assay, 661W and HELA cells were seeded into a 96-well plate (5000cells/well) with 100µl Medium without antibiotics. 24h after cells were seeded, different treatment started by adding effector substances directly to the medium. AlamarBlue® was added aseptically in an amount equal to 10% of the volume in the well. After 4h of incubation at 37°C and 5% CO_2 in a humidified atmosphere, measurements were done using an Anthos Labtec HT2 photometer at 570nm and 620nm. Then the treatment was either prolonged or AlamarBlue® containing medium was replaced by fresh medium and the assay was repeated at a later time point.

***In Situ* Cell Death Detection Kit (TUNEL)**

Terminal deoxynucleotidyl transferase-mediated biotinylated UTP nick end labeling (TUNEL) staining was performed using an *in situ* cell death detection kit (Fluorescein or TMR; Roche Diagnostics GmbH, Mannheim, Germany). In short: Cells grown on a glass plate covered with Poly-L-lysine solution were fixed with 4% PFA for 15min at RT and rinsed with PBS. Permeabilization was done on ice with 0.1% Triton X-100 in 0.1% sodium citrate for 2min. Again, the cells were rinsed with PBS and blocked for 1h at RT in 0.003% PBST containing 10% normal goat serum, 1% BSA and 1% fish gelatin. The TUNEL label and the Enzyme provided with the kit were mixed 40:10 and an equivalent amount of block solution was added. The cells were incubated for 1h at 37°C, and then rinsed with PBS. Negative controls were done by omitting the enzyme. Finally, DAPI, diluted 1:10000 in PBS, were added for 5min at RT. All sections were mounted with Mowiol. Pictures were taken with the Axio Imager Z1 ApoTome Microscope using the 20x objective.

LIVE/DEAD® Viability/Cytotoxicity Kit *for mammalian cells*

Cells were seeded into 24-well plates, 4000cells/well for short treatment, 2000cells/well for long treatment. To stop treatment cells were rinsed in DPBS and DPBS containing 1µM Ethidium homodimer-1 and 2µM Calcein AM were added to all wells. After 45min incubation in dark at RT, every well was photographed with the inverted Axiovert 35M Microscope.

Ca^{2+}-Imaging

Ca^{2+} imaging in cells were done as previously published (Köppen *et al.* 2008), in short: 80% confluent cell cultures of HEK293 and 661W cells overnight grown were transfected with 8µg CNGA3 construct and 2µg CFP for each well. For transfection, the above-described Lipofectamin^{TM}2000 protocol was used. 6h after transfection the cells were transferred on Poly-L-lysine covered glass plates in 24-well plates and cultured overnight in 500µl DMEM containing 10% FBS and 1% Pen/Strep. To increase the transfection rate 0.6% or 0.3% butyrate were added to the HEK293 or 661W cells respectively and the cells were incubated overnight. To load the Ca^{2+}-sensitive dye Fura-2, each glass plate was incubated for 40min in a mixture of the detergent Pluronic® (0.2%) and 0.2% Fura-2 (Grynkiewicz *et al.* 1985) in 1ml extracellular solution (ES) at 37°C and 5% CO_2. The cells were transferred to the Ca^{2+} imaging set-up (Zeiss microscope connected to a TILL Vision Polychrome 2 light source) in 1ml ES. Pictures were taken every 5sec at 340 and 380nm for a minimum of 15min and up to 60min. After two minutes, 8-Br-cGMP at a final concentration of 1mM was added to elicit the Ca^{2+} influx in a CNG dependent manner. After 15min the measurement was stopped.

Immunohistochemistry

Cells were grown in a 24-well plate on glass plates covered with Poly-L-lysine. The cells were fixed with 4% PFA for 15min at RT, then rinsed with PBS and blocked for 1h at RT with PBS containing 0.3% Triton, 1% BSA and 10% normal serum from host animal of the second antibody. The first antibody was diluted in block solution like described in Table.2 and added to the wells overnight at 4°C. After rinsing with PBS the second antibody, diluted in 0.3% PBST was added for 1h at RT. Nuclear staining was done with DAPI 1:10000 in 0.3% PBST for 10min at RT. After rinsing with PBS all glass plates were placed onto a microscope slide, covered with Mowiol containing DABCO and mounted with a cover slip. Pictures were taken with the Axio Imager Z1 ApoTome with 20x and 63x objectives.

Microscopy, cell counting, and statistical analysis

Light and fluorescence microscopy was performed with the Axio Imager Z1 ApoTome Microscope. Images were captured using a Zeiss Axiocam digital camera and the Zeiss Axiovision 4.7 software. Pictures of the LIVE/DEAD® Viability/Cytotoxicity assay were done with the Axiovert 35M Microscope, which was

equipped with the Canon PowerShot G9 digital Camera (Canon Deutschland GmbH, Krefeld, Germany). Every well was photographed with a GFP and a Cy3 filter.

Further analysis of fluorescence pictures (not LIVE/DEAD® Viability/Cytotoxicity assay) were done with ImageJ 1.44 (http://imagej.nih.gov/ij; Java1.6.9_10 (32-bit)) or Fiji (http://pacific.mpi-cbg.de/wiki/index.php/Fiji; (64bit) information retrieved July 15, 2012). For image processing, the Adobe Creative suite CS5 standard was used. (Adobe Systems Incorporated, San Jose, CA).

AlamarBlue® cytotoxicity assay was analyzed as suggested by manufacturer: (http://www.abdserotec.com/about/company_profile-483.html, information retrieved June 14, 2010) and the averaged results were analyzed for significant differences with unpaired, unequal students T-test. Significance levels were p=0.05; p=0.01; p=0.001.

In Situ Cell Death Detection Kit (TUNEL) All TUNEL positive cells and the total cell number (all DAPI stained cells) were manually counted using the ImageJ software. The total cell number divided by the TUNEL positive cell number was multiplied with 100 to obtain the percentage of TUNEL positive cells.

Pictures of cells treated with LIVE/DEAD® Viability/Cytotoxicity Kit *for mammalian cells* were loaded into Photoshop CS5 to get an overlay of green stained alive and red stained dead cells. All live and all dead cells were counted manually in the ImageJ software. The live cell number divided by the cell number of dead cells was multiplied with 100 to obtain the percentage of dead cells for each well. The percentage of all treated cells were normalized to the DMSO control percentage and analyzed for significant differences with unpaired, unequal students T-test. Significance levels were defined as $p>0.05$.

After Ca^{2+}-Imaging the data was loaded into the TILL Vision Imaging Software. From regions of interest, the ratio of the fluorescence intensity after excitation of 340nm and 380nm were calculated. The cells were sorted into different groups, after the fluorescent transfection control or after strong or weak responses to the signal (cGMP). Three groups were built: not transfected, transfected with strong response and transfected with weak response. The ratios of the grouped cells were averaged for every time point. For all averaged time points, the significant differences were analyzed with unpaired, unequal students T-test. Significance levels were defined as $p>0.05$.

3.3.4 Animal experiments

Animals

All used animal were housed under standard white cyclic lightning, had free access to food and water and were used irrespective of gender. Homozygous *C3H-rd1*/*C3H-rd1* and congenic *C3H-wt* mice (Sanyal and Bal 1973), as well as homozygous *C57Bl6 cpfl1*/*cpfl1* and congenic *C57-wt* were used. The latter animals were a kind gift from Bo Chang (Jackson Laboratory, Bar Harbor, Me, USA). Homozygous *P23H* and *S334ter* rhodopsin transgenic rats (produced by Chrysalis DNX Transgenic Sciences, Princeton, NJ) of the line *Tg(P23H)1Lav* and *Tg(S334ter)3Lav* (*P23H-1* and *S334ter-3*) were kindly provided by Dr. M. M. LaVail (University of California, San Francisco, CA). Heterozygous *P23H* and *S334ter* rats were obtained by crossing with *CD-wt* [*CD*: CD® IGS Rat, Crl:CD(SD)] rats to reflect the genetic background of autosomal dominant RP (ADRP). Age matching *CD-wt* animals were used as control. All procedures were approved by the Tübingen University committee on animal protection and performed in compliance with the ARVO statement for the use of animals in Ophthalmic and Visual Research. Protocols compliant with § 4 paragraph 3 of the German law on animal protection were reviewed and approved by the "Einrichtung für Tierschutz, Tierärztlichen Dienst und Labortierkunde" (Anzeige/Mitteilung nach § 4 vom 28.04.08, 16.12.08, 10.02.09). All efforts were made to minimize the number of animals used and their suffering.

Retinal explant cultures

Organotypic retinal cultures with or without retinal pigment epitheliums (RPE) were prepared as published by (Sahaboglu *et al.* 2010). Briefly, the animals were sacrificed, the eyes enucleated and for maintaining RPE pretreated with 12% Proteinase K in R16 Basal medium for 15 minutes at 37°C. Proteinase K activity was blocked by addition of 10% fetal bovine serum for 2min, followed by rinsing in R16. In the following, cornea, lens, sclera and choroid were removed carefully under a sterile bench, with only the RPE remaining attached to the retina. For electroporation experiments, no Proteinase K treatment was done, in order to remove the RPE from the retina to be able to see if the photoreceptors are showing GFP as a transfection control. Finally, the explant was cut into four wedges, to assure a flat connection for a better nutrition supply on the culture membrane. With a big, cut pipette tip the explants were transferred into a culture membrane insert (Millipore AB, Solna, Sweden; PIHA03050) the RPE facing the membrane. For electroporation, either the photoreceptors or the ganglion cells

faced the membrane. The membrane inserts were placed into six well culture plates and 1.5 ml of R16 Powder Medium (Basal medium) with supplements (Caffé *et al.* 2001a) was added. The cultures were incubated at 37°C in a humidified 5% CO_2 incubator (Heraeus Cytoperm 2 Gassed Incubator; 51011659; Thermo Scientific). The culture medium was changed every second day.

Histology

Animals were euthanized in compliance with the ARVO Statement for the use of Animals in Ophthalmologic and Vision Research. All animal models were euthanized at two different stages, shortly before photoreceptor degeneration is at maximum and at adult age (see Tab.3). The eyes were enucleated, and the anterior parts and lenses were removed.

Table 3: Stages of all animal models used for experiments:

Animal	Maximal/beginning* degeneration	Adult
C3H-rd1* and *C3H-wt	PN11*	PN30
cpfl1/cpfl1* and *C57-wt	PN14*	PN30
S334ter* and *CD-wt	PN12	PN30
P23H* and *CD-wt	PN15	PN30

Fixation and Cryo-embedding

Eyecups as well as organotypic retinal cultures were fixed in 4% paraformaldehyde (PFA) in 0.1M PBS (pH 7.4) for 30min at RT. After rinsing with PB the tissue was incubated in graded sucrose-solutions (10min in 10%; 20min in 20%, 30min in 30%) and incubated overnight in a tissue freezing medium at 4°C. After embedding in tissue freezing medium and freezing at -20°C, the eyes or retinas were cut with a cryostat (Leica, CM3050S) into radial 12µm sections. Three to four sections were placed onto a microscopic slide and stored at -20°C.

Table 4: Antibodies used in Immunohistochemistry and in western blot:

Antigen	Host	Source / Cat. number	IHC	WB
Actin	mouse	Milipore; MAB 1501	1:200	1:4000
Actin	rabbit	Abcam; ab1801	———	1:4000
Calbindin	mouse	Swant; 300	1:500	———
Calmodulin (CALM)	rabbit	Acris; ABIN460749	1:100	———
Calretinin	mouse	Chemicon; MAB 1568	1:300	———
CBP-NT	rabbit	Upstate; 06-297	1:300	———
cGMP	sheep	Kind gift of Prof. Dr. Harry Steinbusch	1:500	———
Connexin36	rabbit	Zymed; 51-6200	1:500	———
CREB	rabbit	Cell Signaling; #9197	1:400	1:1000
CREM	rabbit	Aviva Systems; ARP34777	1:200	1:1000
Fluorescein Peanut Agglutinin		Linears; FL-1071	1:500	———
GABA	rabbit	Biotrend; GA-1159	1:100	———
GFAP	mouse	Sigma; G-3893	1:400	———
Glutamine Synthetase	mouse	Chemicon; MAB 302	1:1000	———
Glycogen phosphorylase	guinea pig	Kind gift of B.Pfeiffer-Guglielmi	1:500	———
HNE	rabbit	Alpha Diagnostic; HNE11-S	1:100	———
ICER	rabbit	Kind gift of Molina	1:10000	1:1000
JH 455 (blue Opsin)	rabbit	Kind gift of Jeremy Nathans	1:1000	———
Neuron specific enolase	rabbit	Polyscience; 16625	1:3000	———
Nitro Tyrosine	rabbit	Millipore/Chemicon; AB 5411	1:100	———
Opsin red/green	rabbit	Milipore/Chemicon; AB 5405	1:200	———
Parvalbumin	mouse	Sigma; P 3088	1:300	———
pCREB S133	rabbit	Santa Cruz; sc-101663	1:500	———
pCREB S133	rabbit	Cell Signaling; #9198	1:100	1:1000
pCREB S142	rabbit	Abcam; ab51113	1:100	———
PDE6beta	rabbit	ABR; PA1-722	1:400	———
PKG1	rabbit	Kind gift of Prof. Dr. Robert Fail	1:500	———
PKG1/ PKG2	rabbit/ rabbit	Kind gift of Prof. Dr. Peter Ruth	1:500/ 1:500	———
Rhodopsin	mouse	Chemicon; MAB 5316	1:400	———

Immunohistochemistry

Fluorescence immunostaining was performed on 4% PFA fixed retinal cryo-sections on a microscopic slide. The sections were dried for 1h at 37°C and rinsed with 0,01M phosphate buffer saline (PBS) to remove the tissue-freezing medium. For blocking unspecific binding sites PBS containing 0.3% Triton, 1% bovine serum albumin and 10% normal serum from host animal of the second antibody (blocking solution) was applied at room temperature (RT) for 1h. The first antibodies were diluted in blocking solution as listed in Table 4 and added to the tissue overnight at 4°C. After rinsing with PBS the second antibody against the host of the first antibody was diluted like listed below and were applied for 1h at RT. For nuclear staining DAPI diluted 1:10000 in PBS was applied for 10min at RT. After rinsing with PBS, all sections were mounted with Vectashield. Controls for all reactions were carried out by omitting the first antibody. Pictures were taken with the Axio Imager Z1 ApoTome Microscope.

Propidiumiodide (PI) staining

PI was diluted 1:10 in complete medium and added into the retina culture chamber for 3h at 37°C and 5% CO_2. Afterwards the standard fixation protocol for cryo-embedding was done and the cryo-sections were analyzed with the Axio Imager Z1 ApoTome Microscope.

***In Situ* Cell Death Detection Kit (TUNEL)**

Terminal deoxynucleotidyl transferase-mediated biotinylated UTP nick end labeling (TUNEL) staining was performed using an *in situ* cell death detection kit (Fluorescein or TMR; Roche Diagnostics GmbH, Mannheim, Germany). In short: fixed cryo-sections on a microscopic slide were rinsed with PBS to remove the tissue-freezing medium. Afterwards all slides were incubated for 5min at 37°C in 0.05M TBS pH 7.6 containing 0.01% Proteinase K. The slides were rinsed with TBS and incubated for 5min with pre-cooled -20°C Ethanol/Acetic acid solution. Again, the slides were rinsed with TBS and blocked for 1h at RT in 0.003% PBST containing 10% normal goat serum, 1% BSA and 1% fish gelatin. The TUNEL label and the enzyme provided in the kit were mixed 40:10 and an equivalent amount of block solution was added. The mixture was pipetted onto the sections, for negative controls the enzyme were omitted and the slides were incubated for 1,5h at 37°C or overnight at 4°C. Again all sections were rinsed with PBS, then DAPI, diluted 1:10000 in PBS was applied on the sections. Finally, the slides were mounted with Vectashield and pictures were taken with the Axio Imager Z1 ApoTome Microscope.

Western blot (WB)

Ten retinas were homogenized in ELB-buffer using a manual homogenizer (glass to glass) or the Heidolph DIAX 600 homogenizer (Heidolph, Schwabach, Germany). Samples were mixed with Laemmli or sample buffer, boiled for 5min, separated on 10% SDS-polyacrylamide gels, and were electro-transferred to PVDF transfer membranes. Unspecific binding on the samples was blocked using 1x Roti-Block and incubated overnight at 4°C with primary antibody (see Tab.2) diluted in TBS buffer containing 0.02% Triton-X-100 (TBST) and 5% dry milk. After rinsing with TBST, horseradish peroxidase–conjugated secondary antibody against the host of the first antibody was diluted 1:4000 in TBST and applied for 1h at RT on a rotating platform (Heidolph unimax 2010) with ca. 40rpm. The membrane was thoroughly rinsed with TBST and incubated with ECL or ECL plus detection kit, following the provided manual. The membrane was sealed into a plastic bag and put into dark box. In a dark room a chemiluminescence film was placed on the membrane and for protein band detection the film was developed with the AGFA Curix 60 (Siemens Healthcare, Erlangen, Germany). After detection, the membrane was rinsed in TBST and the antibodies were removed. For this, the membrane was placed into a shaking water bath (GFL, Burgwedel, Germany) in stripping buffer for 15min at 50°C. The above-described protocol was repeated with anti-Actin as the first antibody to obtain a loading control. For quantification, every Western blot was repeated at least three times.

Microscopy, cell counting, and statistical analysis

Light and fluorescence microscopy was performed with the Axio Imager Z1 ApoTome Microscope. Images were captured using a Zeiss Axiocam digital camera and the Zeiss Axiovision 4.7 software. Transfected live explant cultures were surveyed with the Axiovert 35M Microscope, which was not equipped with a camera.

Further analysis like cell counting or fluorescence intensity measurements were done with ImageJ 1.44 (http://imagej.nih.gov/ij; Java1.6.9_10 (32-bit)) or Fiji (http://pacific.mpi-cbg.de/wiki/index.php/Fiji; (64bit)). For image processing, the Adobe Creative suite CS5 standard was used. (Adobe Systems Incorporated, San Jose, CA). Quantification of the relative intensities of WB bands was done following a tutorial written by Luke Miller (http://lukemiller.org/index.php/2010/11/analyzing-gels-and-western-blots-with-image-j/).

For fluorescence intensity measurement, at least three different animals were used and at least three cryo-sections were pictured with the Axio Imager Z1 ApoTome Microscope. Into the Fiji software, the pictures showing the protein staining of interest were loaded and five line-plots were analyzed for each picture. From one line plot the maximal gray value intensity of one cell of the inner nucleus layer (INL) and of one cell of the outer nucleus layer (ONL) was noted for further analysis. The INL values were used as an internal control and the ONL values were normalized by dividing the ONL values by the INL values and multiplying it with 100. The normalized results of age matching controls and mutants were analyzed with unequal, unpaired students T-test for significant differences. Significance level was defined as $p>0.05$.

4 Results

4.1 cAMP response element-binding (CREB) and inducible cAMP early repressor (ICER)

4.1.1 CREB expression in C3H-rd1

For many neuronal cells types, the transcription factor CREB was shown to be neuroprotective and needed for survival and plasticity of mature neurons (Sakamoto *et al.* 2011). In retinas of the RP mouse model *rd1*, CREB expression was downregulated and the level of active CREB (pCREB), which is phosphorylated at Serine 133 (Mayr *et al.* 2001), decreased (Paquet-Durand *et al.* 2006; Azadi *et al.* 2007; Arroba *et al.* 2009). In this thesis, fluorescent immunohistochemistry (IHC) on frozen, retinal sections of *rd1* at P11 and P30 was performed. At P11, the onset of rod degeneration took place, while at P30, most rods are already gone (Carter-Dawson and LaVail 1979). The IHC staining for CREB looked similar in *rd1* and corresponding wt retinas, presenting a weak nuclear staining for cells in the ganglion cell layer (GCL) and for some cells in the inner nuclear layer (INL) and a strong staining of all connecting fibers throughout all layers of the retina (Fig.6 A-D). In conclusion, no obvious difference of CREB expression was observed in *C3H-rd1* mutant retinas compared with the corresponding *C3H-wt*.

Immunolabeling against pCREB showed a nuclear staining in nearly all cells of the GCL and most cells of the INL (Fig.6 E-H). A similar nuclear staining was already described (Kim and Park 2005) and is in line with the fact that CREB is a nuclear transcription factor (Lonze and Ginty 2002). Only in *C3H-wt* (Fig.6 F and H), but not in *C3H-rd1* (Fig.6 E and G) labeling of photoreceptor segments and pedicles was observed. Another difference between the wt and the mutant was seen in the ONL labeling. In both, P11 and P30 *C3H-rd1* retinas, some photoreceptor cell bodies showed pCREB staining (Fig.6 E and G); while in the age-matching *C3H-wt*, this was not found (Fig.6 F and H).

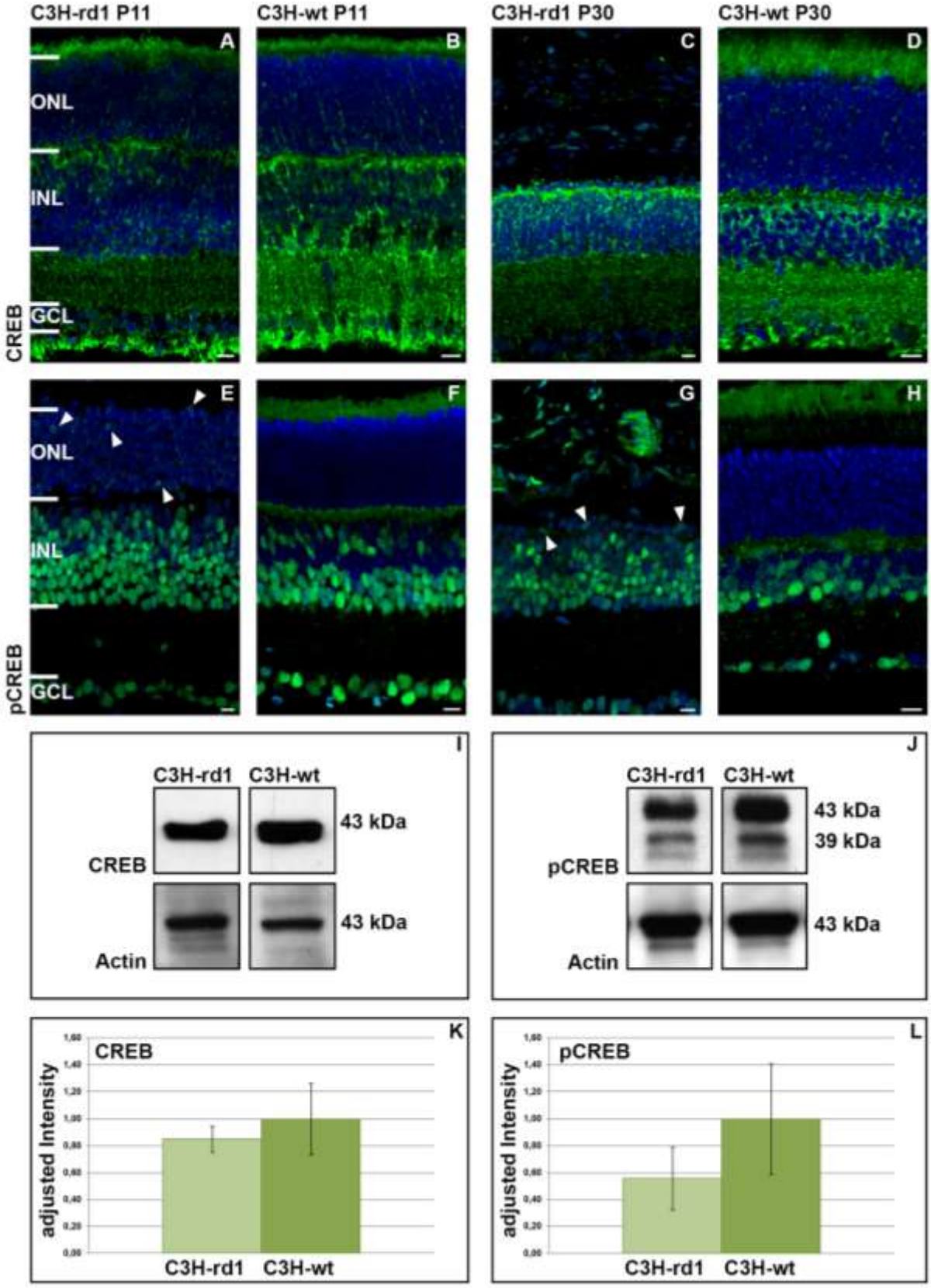

Figure 6: CREB and activated CREB expression in *C3H-rd1:* A-D) CREB expression (green) in *C3H-rd1* and *C3H-wt* retinas at P11 and P30 was found in GCL and some cells in the INL, but not in the ONL. A strong staining was visible in the OPL, IPL, and in GCL connecting fibers. E-H) pCREB expression (green) was found in nearly all GCL nuclei, in most nuclei of INL-cells in both *C3H-rd1* and *C3H-wt*. Nuclear staining of photoreceptors was found only in *C3H-rd1* (arrowheads in E and G) while photoreceptor segments and pedicles were stained in *C3H-wt* only (F and H). I-L) Western blot of total retina protein for CREB and pCREB did not show a significant decrease of both CREB forms in *C3H-rd1*. Western blot data are representative for 3 independent experiments each with at least 4 different animals. Scale bar=10µm; Blue staining= nuclear marker DAPI

Consequently, western blot was performed to quantify the protein levels of CREB and pCREB. However, western blot of total retinal homogenates failed to show significant decrease for CREB expression compared with the corresponding *C3H-wt* (adjusted density *C3H-rd1*, P11:0.85; SEM 0.1; t-test: p<0.195). The same was true for pCREB levels compared with the *C3H-wt* (adjusted density *C3H-rd1*, P11: 0.6; SEM 0.2; t-test: p<0.129) in *C3H-rd1* at P11 (Fig.6 K and L). This may mirror the fact that a difference of the pCREB staining was restricted to the ONL, while the most prominent staining in GCL and INL displayed no changes between *C3H-wt* and *C3H-rd1*. A more ONL restricted approach might show a significant difference of pCREB levels.

4.1.2 ICER expression in C3H-rd1

ICER, a potent endogenous repressor of CRE-mediated gene transcription is known to regulate circadian rhythm, neuroendocrine function and is involved in several degenerative diseases (Borlikova and Endo 2009; Wang *et al.* 2010). Commercially available antibodies against CREM, the gene family to which ICER belongs, do not specifically bind to ICER. Therefore, we chose an anti-CREM antibody detecting ICER as well as other CREM isoforms (Kimura *et al*. 2006). CREM-IHC on frozen, retinal slices at P11 and P30, labeled nearly all cells in every layer of *C3H-rd1* and *C3H-wt* retina, however the staining was more prominent in GCL and INL compared to the ONL staining (Fig.7 A-D). To get an ICER-specific staining, an antibody raised directly against ICER was used (kind gift from Dr. Carlos Molina, Montclair State University, USA). Both antibodies produced a comparable staining at P11 and P30 in cells in the GCL and INL. However, with the specific ICER antibody a number of cells were strongly labeled in the ONL at P11 and at P30 (Fig.7 E-H). Surprisingly, the number of labeled photoreceptors observed at P11 was similar at P30, when nearly all rod photoreceptors are gone. This led to the question whether ICER was expressed in rod or in cone photoreceptors. To answer this question, double staining with the cone marker glycogen phosphorylase (GlyPhos) and ICER was performed. GlyPhos is expressed in Müller cells, astrocytes and in cone photoreceptors in mammalian retinas (Nihira *et al.* 1995; Pfeiffer *et al.* 1995; Pfeiffer-Guglielmi *et al.* 2005). The double staining of ICER and GlyPhos showed a complete overlap of all ICER positive nuclei in the ONL with GlyPhos labeled cones (Fig.7 I-P). Hence, the double staining confirmed an ICER expression in cone nuclei in both *C3H-rd1* and *C3H-wt,* at P11 and P30.

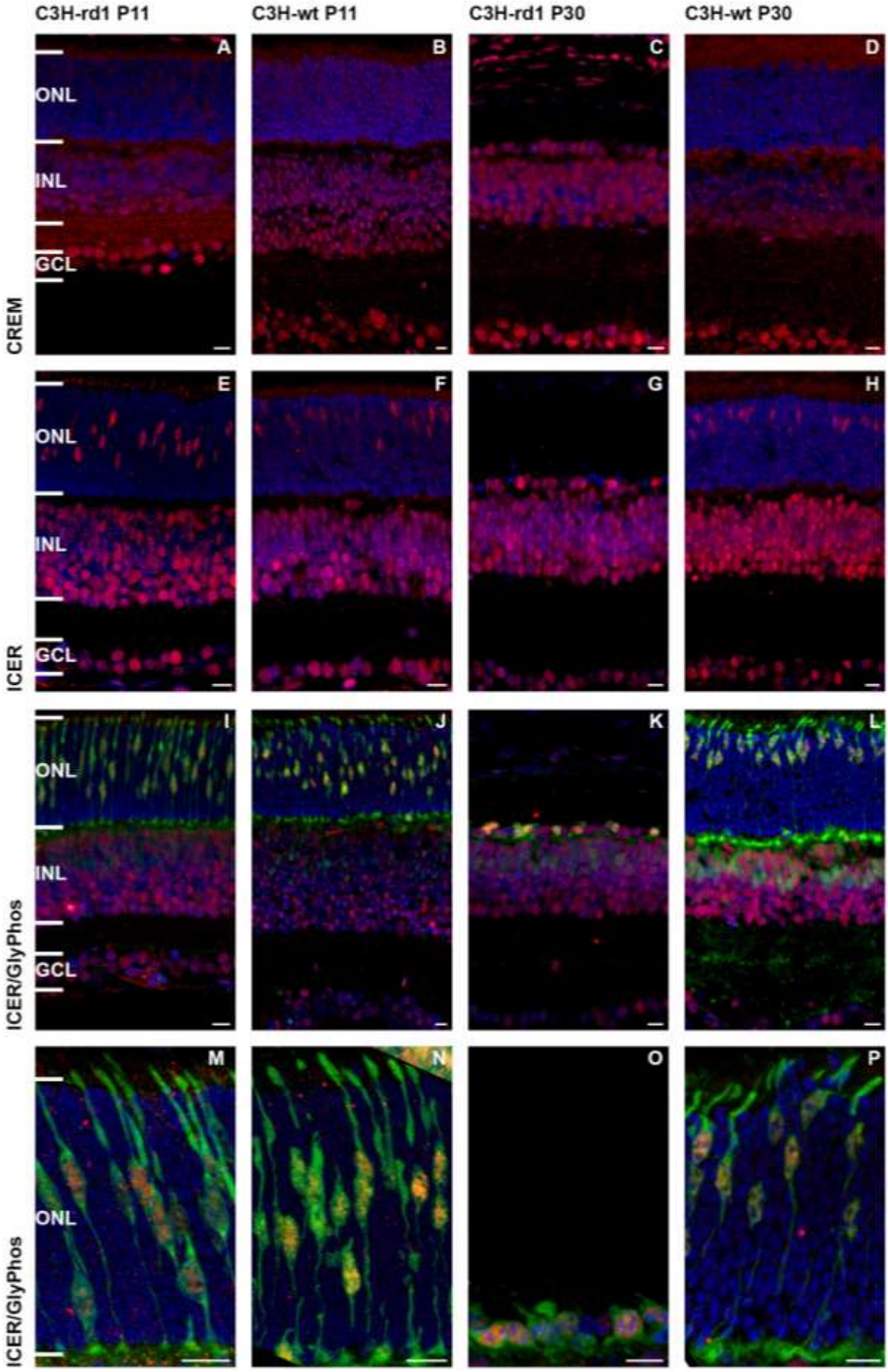
C3H-rd1 P11
C3H-wt P11
C3H-rd1 P30
C3H-wt P30
A
B
C
D
ONL
INL
GCL
CREM
E
F
G
H
ONL
INL
GCL
ICER
I
J
K
L
ONL
INL
GCL
ICER/GlyPhos
M
N
O
P
ONL
ICER/GlyPhos

Figure 7: CREM/ICER expression in *C3H-rd1* and ICER localization in cones: A-D) IHC against CREM (red) stained nearly all cells of the retina with no obvious difference between P11 and P30. Strongest CREM expression was found in GCL and some cells of the INL. E-H) ICER staining (red) showed a similar expression pattern in GCL and INL, but additionally some ONL cells were labeled. I-L) Co-labeling with antibodies against the cone marker glycogen phosphorylase (GlyPhos) (green) and ICER (red) gave a complete overlap of ICER and GlyPhos in the ONL suggesting that ICER expression in the ONL was restricted to cones. M-P) Magnifications of the ONL, which were double-stained for GlyPhos (green) and ICER (red). ICER was expressed in cone cell bodies. Scale bars=10µm; Blue staining= nuclear marker DAPI

4.1.3 ICER expression in other neurodegeneration models

Since, retinal ICER expression was never investigated before; we wanted to see whether it was expressed in other species as well. Two RP rat models, *S334ter* and *P23H* were examined, both carrying mutations in the rhodopsin gene; (Dryja *et al.* 1990b; Liu *et al.* 1999). Additionally, ICER expression in the primary cone photoreceptor function loss (*cpfl1)* mouse model was investigated (Chang *et al.* 2002).

Frozen retinal sections of *S334ter* rats were examined at P12 at the peak of rod degeneration (Kaur *et al.* 2011) and at P30 when only cones remained in the ONL. In *S334ter* retinas, ICER was expressed in cells of the GCL and INL and in photoreceptors (Fig.8 A-D). When the ICER staining pattern of *S334ter* was compared with *C3H-rd1* retinas (Fig.7 E and Fig.8 A), the number of stained cells seemed to be lower in the rat retinas, especially in cells of the INL. In *S334ter* retinas at P30, the intensity of ICER expression seemed to be increased (Fig.8 A and C).

In the slower degeneration model *P23H*, the peak of degeneration was at P15 (Kaur *et al.* 2011), while at P30 some rods were still left. In frozen retinal sections, ICER was found to be expressed in cells in the GCL, some cells in the INL and in some photoreceptor nuclei (Fig.8 E-H). The increased ICER expression was even stronger in *P23H* retinas at P30, compared with *S334ter* retinas (Fig.8 E and G).

Since the cone marker GlyPhos was not suitable for rat tissue, we were unable to perform GlyPhos/ICER double staining in the two rat models. However, it is known that in *S334ter* retinas at P30 only cone photoreceptors are left in the ONL (Lee *et al.* 2011). The observation that ICER was expressed in most ONL cells at this stage indicated selective expression of ICER also in rat cone photoreceptors. Since ICER appeared to be cone photoreceptor specific, its expression in a primary cone-degeneration model was investigated. Here, the *cpfl1* cone degeneration model was chosen, which, similar to the rod photoreceptor situation in *C3H-rd1* mouse, is characterized by a dysfunctional cone PDE6 (Trifunović *et al.* 2010).

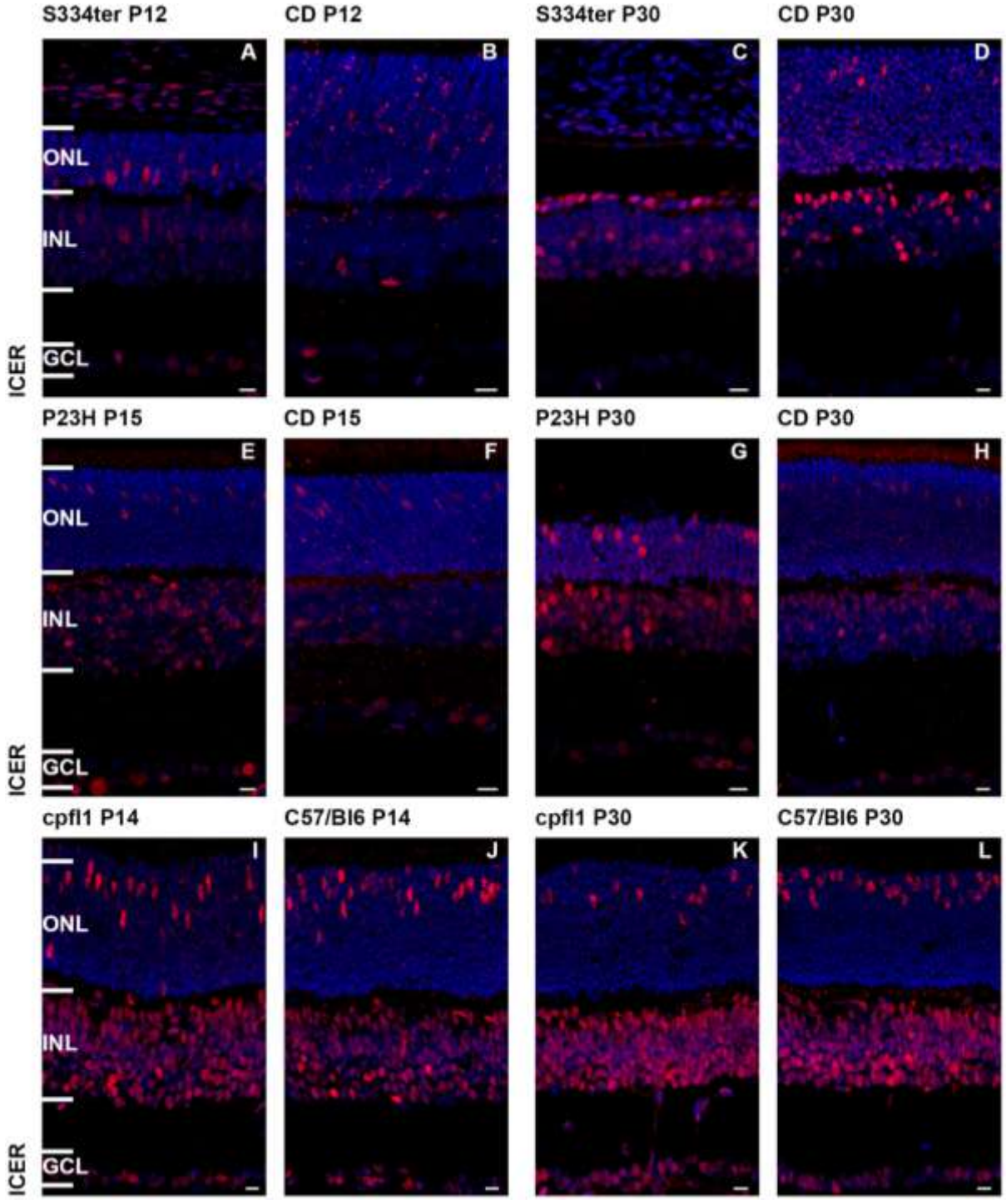

Figure 8: Expression of ICER in other degeneration models: A-D) ICER was expressed in *S334ter* and *CD-wt* retinas at P11 in some GCL and INL cells, and in cones. The expression seemed to be increased at P30 in *S334ter* and *CD-wt* retinas. E-H) ICER expression in *P23H* retinas and *CD-wt* at P15 and P30 was found in GCL, some cells of the INL and in cones. I-L) ICER expression in *cpfl1* mouse and C57-*wt* was found in most GCL, most cells of the INL and in cones. In *cpfl1* retina at P30 some cones are already gone, hence the number of labeled cones was reduced compared to corresponding *C57-wt* (K and L). Scale bars=10µm; Blue staining= nuclear marker DAPI

Frozen retinal sections of *cpfl1* mice at P14 and at P30 were further examined, corresponding to the onset of cone degeneration and late-stage cone degeneration, respectively. Similar to the other degeneration models, ICER was expressed in cells of the GCL, most INL-cells and in photoreceptor cells (Fig.8 I-L). In *cpfl1* retinas at both analyzed ages, more cells were stained compared with both mutant rats, but the staining was similar to *C3H-rd1* retinas at both ages (Fig.7 E and G; Fig.8 I and K). Again, colabeling of GlyPhos and ICER showed that ICER expression in the ONL was restricted to cone photoreceptors (Data not shown). In *cpfl1* mice, the number of cones was reduced at P30 when compared to *C57/Bl6-wt* (Fig.8 K and L).

4.1.4 Quantification of ICER expression

Immunohistochemistry showed that ICER was expressed in the retina of all four examined animal models. In these images, we quantified ICER expression by measuring the intensity of the staining using the ImageJ software. The pictures of every stage were made with the same settings (*e.g.* exposure time) for each mutant and its corresponding control. In ImageJ a line was drawn through the retina and the line plot option of the software was used (Fig.9 AI). The line plot depicted the maximum grey value for all three retinal layers (Fig.9 AII; maximum value for GCL encircled in green), which were listed as an exact value, as well (Fig.9 AIII; the maximum value from AII marked in green). The maximum value of the INL was used as an internal control, to minimize methodological or tissue specific variation of fluorescence intensity. Thereafter, the ratios of ONL to INL, or ONL to GCL were calculated and depicted in a chart (Fig.9 AIV). To make the measurement statistically relevant it was repeated with three different animals for each mutant stage and matching wild type. Furthermore, for each animal three to five images were made, so that at minimum 15 lines for each animal were analyzed. The ratios ONL/INL and ONL/GCL led to the same results, here, only ONL/INL ratio is shown (Fig.9).

In *C3H-rd1* mice no significant increase of ICER intensity was found at P11 (ratio 112.8 in *C3H-rd1* and 87.8 in *C3H-wt*; SEM 4.8 and 6.5; t-test: $p<0.383$), but at P30 the ICER intensity increase was highly significant (ratio 157.2 in *C3H-rd1* and 103.4 in *C3H-wt*; SEM 10.2 and 3.8; t-test: $p<0.001$) when compared with *C3H-wt* (Fig.9 B). In *S334ter* rats, the increase of ICER expression in the ONL was confirmed. At both time points, ICER expression was highly significantly increased compared with *CD-wt* rats (Fig.9 C; P12, ratio 238.9 in *S334ter* and 133.8in *CD-wt*; SEM 17.5 and 8.0; t-test: $p<0.001$; P30, ratio 299.0 in *S334ter* and 112.2 in *CD-wt*; SEM 21.7 and 6.7; t-test:

p<0.001). In *P23H* rats, ICER intensity was not increased at P15 (ratio 133.6 in *P23H* and 139.9 in *CD-wt*; SEM 5.5 and 6.8; t-test: p<0.451), while it was significantly increased at P30 (Fig.9 D; ratio 137.7 in *P23H* and 93.5 in *CD-wt*; SEM 6.4 and 6.6; t-test: p<0.001). ICER expression in *cpfl1* cone photoreceptors was significantly increased at P14 (ratio 190.2 in *cpfl1* and 141.3 in *C57/Bl6-wt*; SEM 7.2 and 7.4; t-test: 0.000) while no significant increase was found at P30 (Fig.9 E; ratio 150.3 in *cpfl1* and 114 in *C57/Bl6-wt*; SEM 23.7 and 9.8; t-test: p<0.155). This finding was to be expected, since ICER is expressed in cones only and at this age most cones are gone or dying, which may have influenced ICER intensity.

In summary, our results suggest that *C3H-rd1* and *P23H* retinas showed an increase of ICER expression in later stages, while in the fast degeneration model *S33ter* ICER was increased in both analyzed time points. On the other hand, the ICER expression was increased in *cpfl1* retinas, at the onset of cone degeneration (P14), while at P30 no increase was found. This may suggest a role for ICER in cone degeneration.

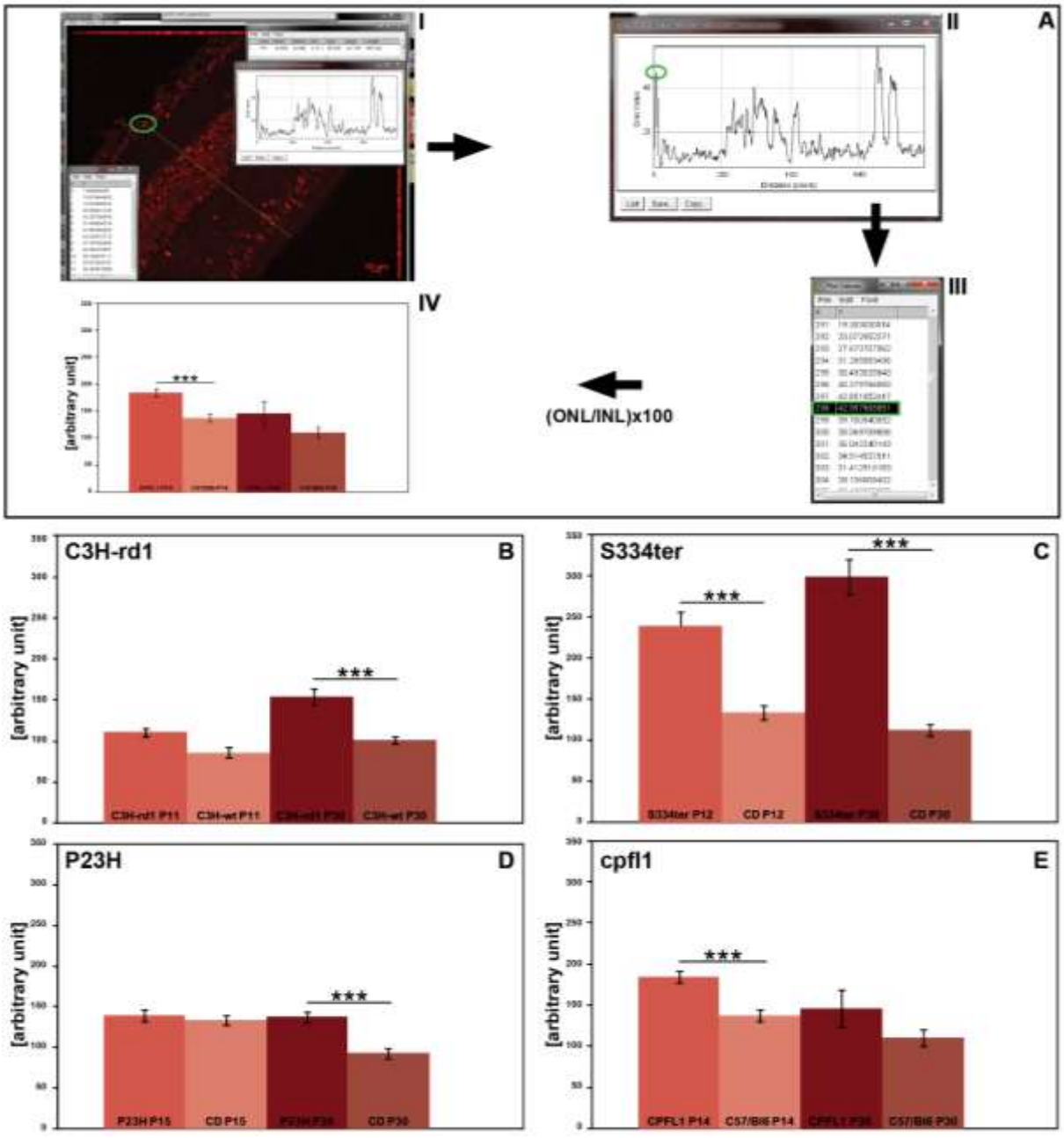

Figure 9: ICER quantification in four distinct degeneration models: A) Schematic overview of ICER quantification. Fluorescent pictures were loaded into ImageJ and the line plot option (AI and II) was used to obtain maximum intensity values (AIII) for cells in all three retinal layers. The mean ratios of the INL and the ONL, are depicted in chart (AIV). B) ICER quantification for *C3H-rd1*. ICER was significantly higher expressed at P30. C) ICER quantification for *S334ter*. In both stages, ICER expression was stronger in the mutant. D) ICER quantification in *P23H* retinas. Only at P30 a significantly higher expression of ICER was found. E) ICER quantification in *cpfl1* retinas. At P14 ICER was significantly higher expressed, while it was not measurable anymore at P30. All charts represent three independent experiments and three different animals for each degeneration model and wt.

4.1.5 pCREB and ICER expression in retinal culture explants treated with zaprinast

The addition of the specific PDE5/PDE6 inhibitor zaprinast mimics the *C3H-rd1* photoreceptor degeneration in *C3H-wt*-cultured retinas (Sahaboglu *et al*. 2010). For this experiment, *C3H-wt* retinas at P5 were harvested and the retinal culture explants were incubated for two days (P7) (see Material and Methods). At P7, 100µM zaprinast diluted in DMSO was applied to the medium. Cultures treated with DMSO only, served as control. Retinal explants were fixed after 4 days treatment, corresponding to P11 and cryo-sections were performed (Sahaboglu *et al.* 2010); All retinal cultures, the treatment procedure, fixation and cutting were done by Ayse Sahaboglu, Division of Experimental Ophthalmology, Institute for Ophthalmic Research, University of Tübingen, Germany). In this *in vitro* model of retinal degeneration, the immunostaining intensities of pCREB and ICER was analyzed.

In retinal cultures, pCREB staining was found in cell bodies in the GCL, most cell bodies in the INL and in the ONL (Fig.10 B), similar to what was previously found in *C3H-wt* retinas at P11 (compare Fig.10 B and Fig.6 F). After zaprinast treatment, nearly no pCREB was detected in the ONL, while the staining pattern in the GCL and INL remained the same (Fig.10 A). This was confirmed by measuring the fluorescence intensity in pCREB immunolabeled images (Fig.9 A), where a significant reduction of pCREB staining in the ONL was observed (Fig.10 C).

In retinal explants, ICER was expressed in cells in the GCL, INL and in photoreceptor cells (Fig.10 D and E). The staining was comparable with the *in vitro* expression pattern of ICER in *C3H-wt* at P11 (compare Fig.10 D and E with Fig.7 E). No significant difference in ICER expression after zaprinast treatment was noted and confirmed with the quantification data (Fig.10 F).

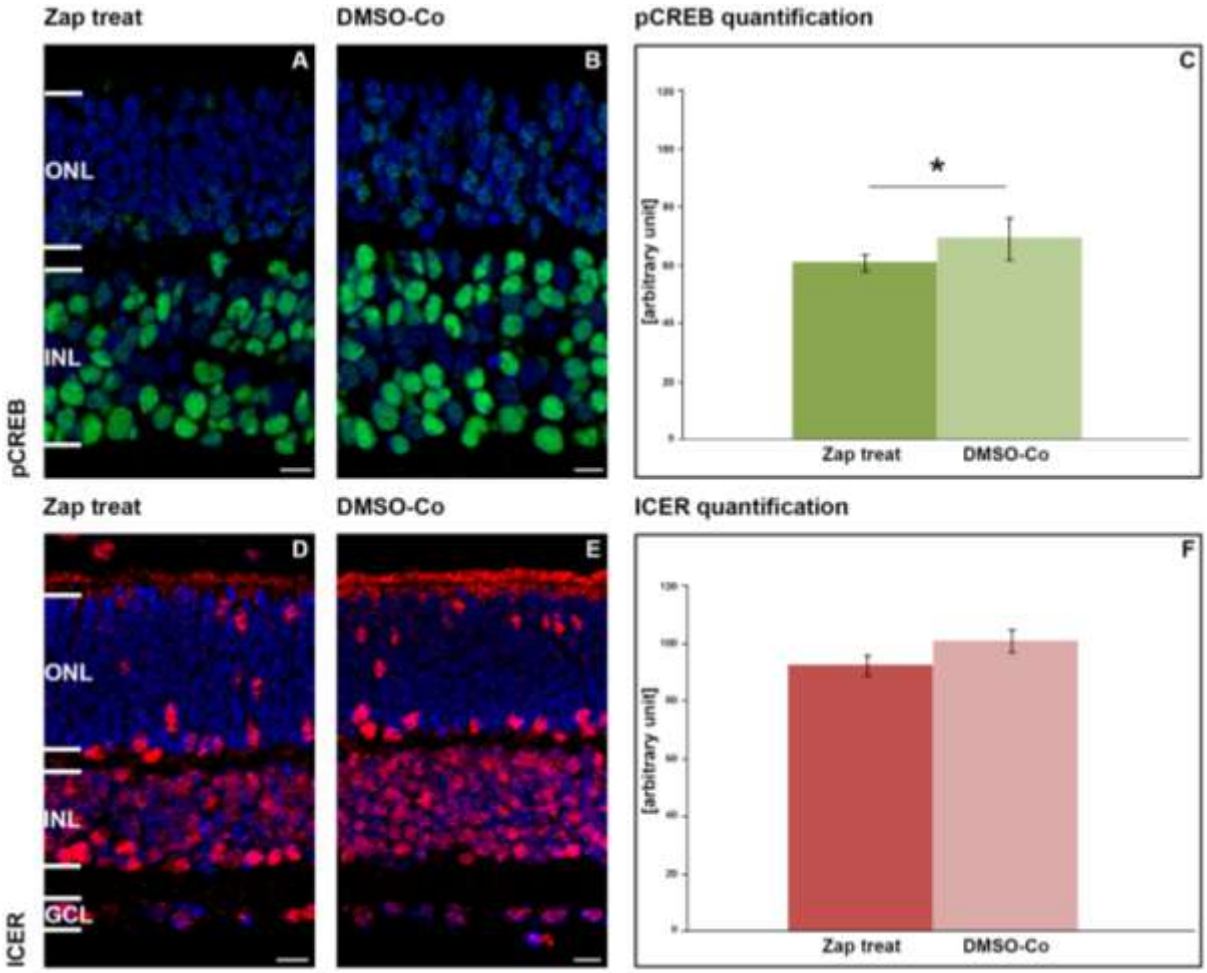

Figure 10: ICER and pCREB expression and quantification after zaprinast treatment in retinal cultures: A-F) pCREB expression in zaprinast treated retinal cultures and quantification. Retinal explants were cultured from P5-P11 and treated from P7-P11 by Ayse Sahaboglu. A) pCREB expression in zaprinast treated cultures was found in GCL, most INL cells and some photoreceptors. B) pCREB expression in DMSO-treated control (Co) cultures was detected in GCL, most INL cells and in photoreceptors C) Ratio ONL to INL of pCREB maximum grey value intensity after zaprinast treatment retinal cultures. After zaprinast treatment, less pCREB expression was found; D) ICER expression after zaprinast treatment of retinal cultures. Expression was found in GCL, most INL cells and in some ONL cells E) ICER expression in DMSO-Co; Expression was similar as in D); F) Ratio ONL to INL ICER maximum grey value intensity after zaprinast treatment of retinal cultures. ICER expression was not changed after zaprinast treatment; Both charts represent measurements from three independent experiments and 3 different animals. Scale bars=10µm; Blue staining= nuclear marker DAPI

4.2 Development of a 661W cell cone degeneration model for testing putative neuroprotective substances

4.2.1 Marker study for 661W cells

Before we started to set up our screening system, we performed a study on retinal cell type specific markers for 661W cells. It was already shown previously, that 661W cells express blue and red/ green cone opsins as well as transducin and cone arrestin, but not rod opsin or rod arrestin (Tan *et al.* 2004). We wanted to see, if the cells express further proteins of the phototransduction cascade, and additionally, whether they express markers for inner retinal cells.

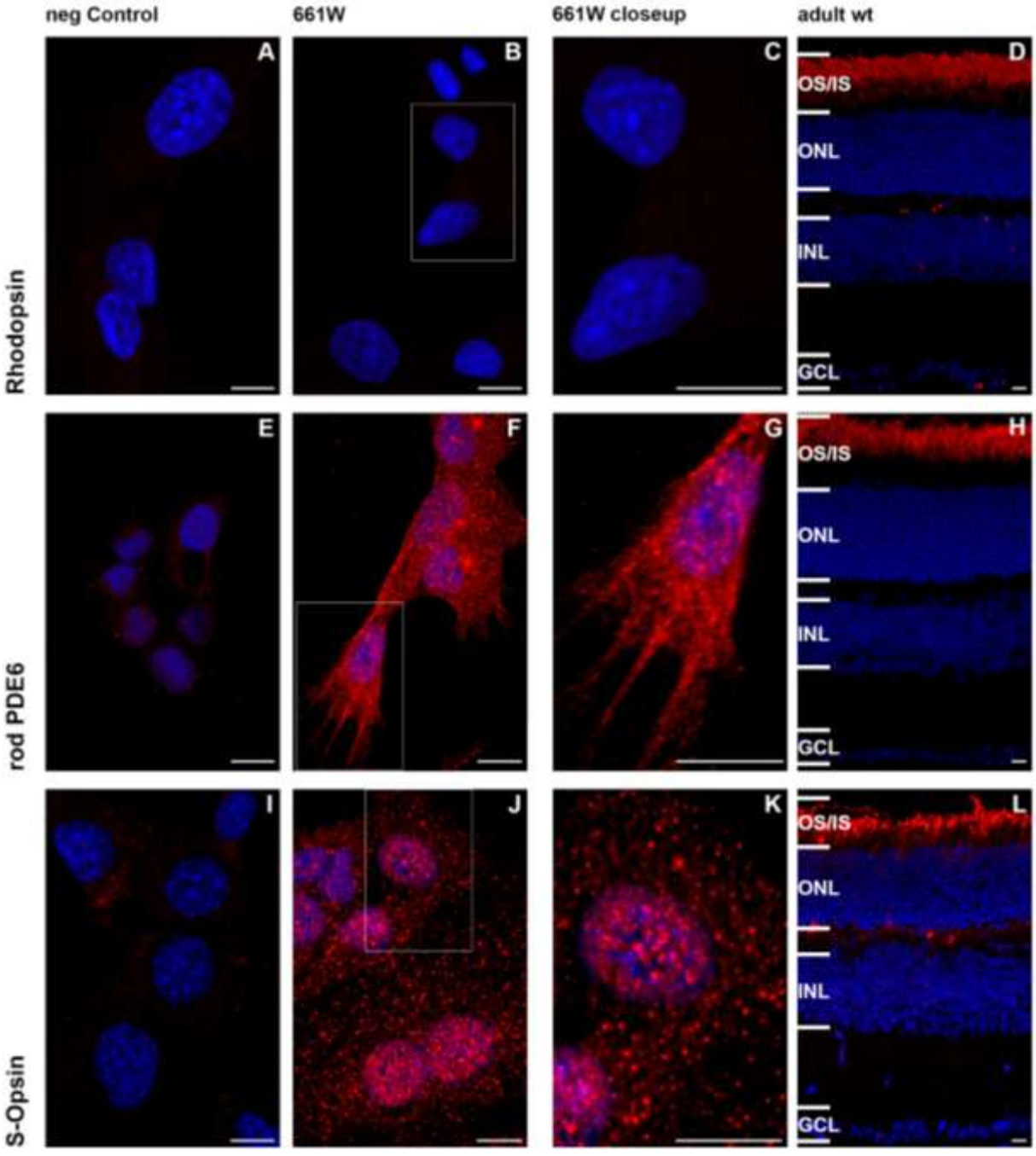

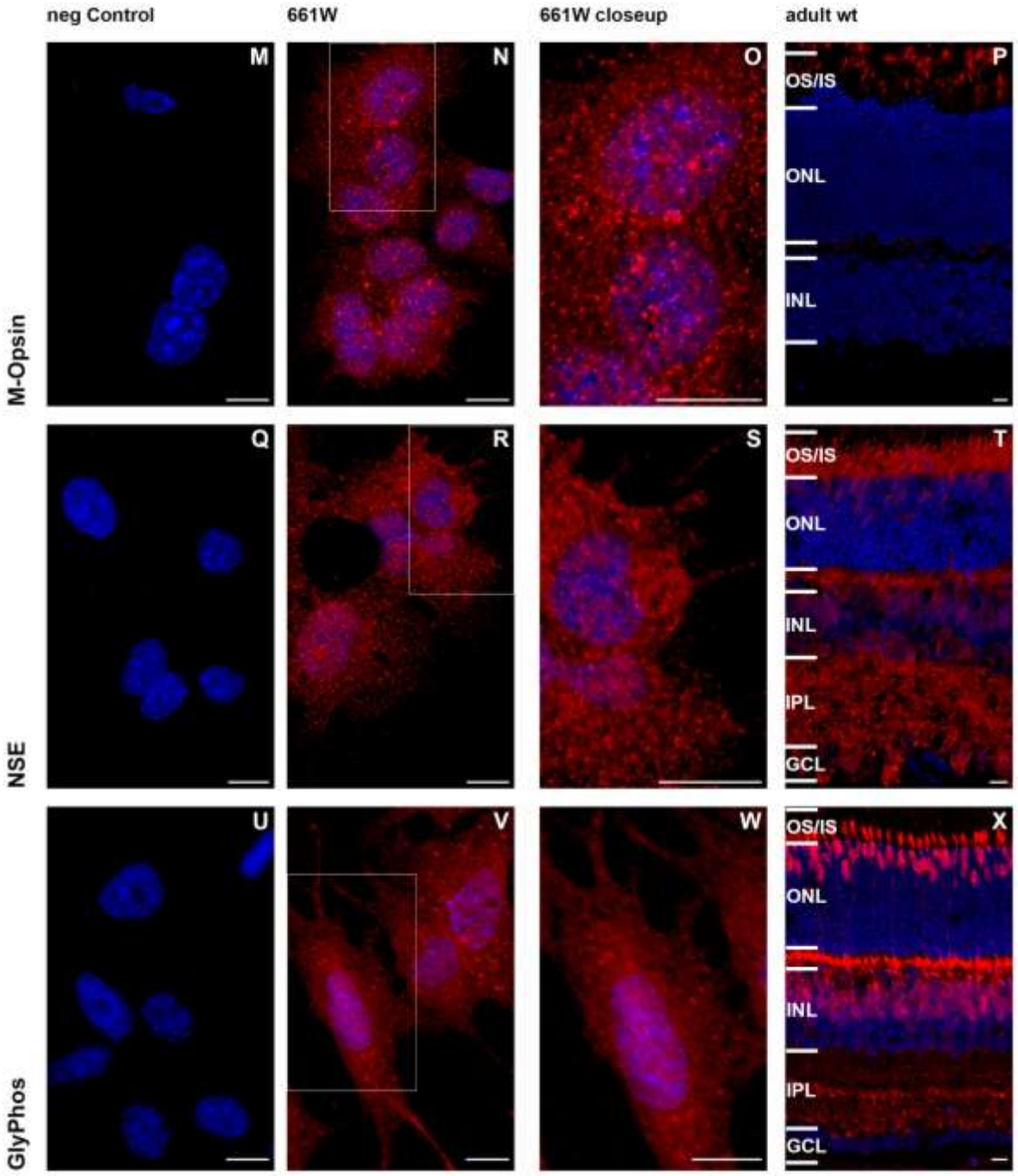

Figure 11: Retinal marker expression in 661W cells: A-D) Rhodopsin expression in 661W cells. A) For the negative (neg) control the primary antibody was omitted. B) No expression of rhodopsin was found in 661W. C) Magnification of the area highlighted in B). D) Rhodopsin expression in wt retina at P30. Rhodopsin was expressed in rod outer segments. E-H) Rod PDE6 beta expression. E) Negative control; F) Rod PDE6β was abundantly expressed in 661W cells. G) Magnification of the area highlighted in F). H) Rod PDE6β expression was found in outer segments in wt retina at P30. I-L) S-opsin expression in 661W as a cone marker. I) negative control; J) Cone s-opsin was abundantly expressed in 661W cells. K) Magnification of the area highlighted in J). L) S-opsin expression in wt retina was found in outer segments. M-P) M-opsin expression in 661W as a cone marker. M) Negative control; N) Cone m-opsin was abundantly expressed in 661W cells. O) Magnification of the area highlighted in N). P) M-opsin expression in wt retina was found in outer segments. Q-T) NSE expression in 661W as a cone marker. Q) Negative control; R) NSE was abundantly expressed in 661W cells. S) Magnification of the area highlighted in R). T) NSE expression in wt retina was found in all parts of cone photoreceptors, in some inner retina cells, in the inner plexiform layer and in some ganglia cells. U-X) GlyPhos expression in 661W; U) Negative control; V) The cone marker GlyPhos was abundantly expressed in 661W cells; W) Magnification of the area highlighted in V). X) GlyPhos expression in wt retina at P30 was found in all parts of cone photoreceptors, in some inner retina cells, in the inner plexiform layer and in some ganglia cells. In blue color: DAPI stained nuclei; red color: marker staining; all scale bars represent 10µm; Abbreviations: OS/IS=Outer and inner segments; ONL= outer nuclear layer; INL= inner nuclear layer; IPL= inner plexiform layer; GCL= ganglia cell layer; NSE= Neuron specific enolase; PDE6= phosphodiesterase 6; GlyPhos=glycogen phosphorylase

We tested whether 661W cells expressed rhodopsin under our culture conditions and confirmed that these cells did not express rhodopsin (Fig.11 A-C; Tab.5). However, they did show abundant expression of rod PDE6β (Fig.11 E-G, Tab.5), as well as abundant expression of the cone PDE6 (Fig.12 cone PDE6h). As cone marker, we used anti-S and M-opsin antibodies, which showed abundant expression of both opsins in 661W (Fig. 11 I-K and M-O; Tab.5). Furthermore, the cone marker neuron-specific enolase (NSE) (Rich *et al*. 1997) as well as glycogen phosphorylase (GlyPhos) (Nihira *et al.* 1995;Haverkamp *et al.* 2005) were abundantly expressed (Fig.11 Q-S and U-W; Tab.5). Another cone marker, peanut agglutinin (PNA), a lectin with a high affinity for galactose-galactosamine disaccharide residues, marks specifically cone inner and outer segments in various species (Blanks and Johnson 1984). In 661W cells, PNA stained preferably around the nucleus, while other cell cytoplasm and cell extensions were only slightly labeled (results not shown, Tab.5). Connexin36, a channel protein, is involved in rod and cone photoreceptor coupling (Trumpler *et al.* 2008), but the expression of connexin36 was only found to be restricted to the cones in the outer retina (Feigenspan *et al.* 2004;Bloomfield and Volgyi 2009). In 661W cells, a strong membranous or cytoplasmic expression of connexin36 was detected (results not shown; Tab.5).

Table 5: Expression of all retinal cell markers tested in 661W cells:

Protein/ Enzyme	Rod Marker	Cone Marker	Other Cell Marker
rhodopsin	**negative**	**—**	**—**
rod phosphodiesterase 6	**positive**	**—**	**—**
cone phosphodiesterase 6	**—**	**positive**	**—**
neuroenolase	**—**	**positive**	**—**
glycogen phosphorylase	**—**	**positive**	**—**
S-opsin	**—**	**positive**	**—**
M-opsin	**—**	**positive**	**—**
lectin/ PNA	**—**	**positive**	**—**
connexin36	**—**	**positive**	**—**
ICER	**—**	**positive**	**—**
calbindin	**—**	**—**	**negative**
calmodulin	**—**	**—**	**positive**

The transcription factor ICER (see above), was expressed in cone photoreceptor nuclei in both mouse and rat retinas. In 661W cells, we found a nuclear expression of ICER as well (results not shown; Tab.5). As a marker for inner retinal cells, an antibody directed against calbindin was used, which is expressed in horizontal cells, amacrine cells and in ganglion cells (Haverkamp and Wässle 2000). No calbindin expression in 661W cells was obtained (results not shown, Tab.5). An antibody against calmodulin, which labels bipolar and amacrine cells in mouse retina, was, however, expressed in the cytoplasm of 661W cells (results not shown, Tab.5). Furthermore, the 661W cells were maintained in R16 medium supplied with or without serum to see if this medium can induce further differentiation towards the cone cell fate. Unfortunately, no difference in protein expression or morphology was obtained, only cell growth was impaired (data not shown). Therefore normal cell medium was used for maintaining the cells.

In summary, the rod specific phosphodiesterase and calmodulin were expressed in this cell line as well as eight cone specific proteins, while rhodopsin and calbindin were not expressed (Tab.5). Taken together, the 661W cell line appeared cone-like and hence suitable for studies into cone-degeneration mechanisms.

4.2.2 Induction of cpfl1-like cone degeneration in 661W cells

Cone photoreceptors of the *cpfl1* mouse have a non-functional PDE6, which leads to an accumulation of cGMP. As described earlier for the *C3H-rd1* mouse, this leads to permanent opening of CNG channels, activation of cGMP-dependent PKG, and eventually cell death (Fig. 7 A). In order to test different cell death assays, the 661W cells were treated with H_2O_2, which is lethal to 661W (Mandal *et al.* 2009) (Fig. 7 F). After we found a reliable and fast cell death assay, we intended either to activate PKG pharmacologically or to inhibit the PDE6 to emulate a situation similar to the *cpfl1* degeneration.

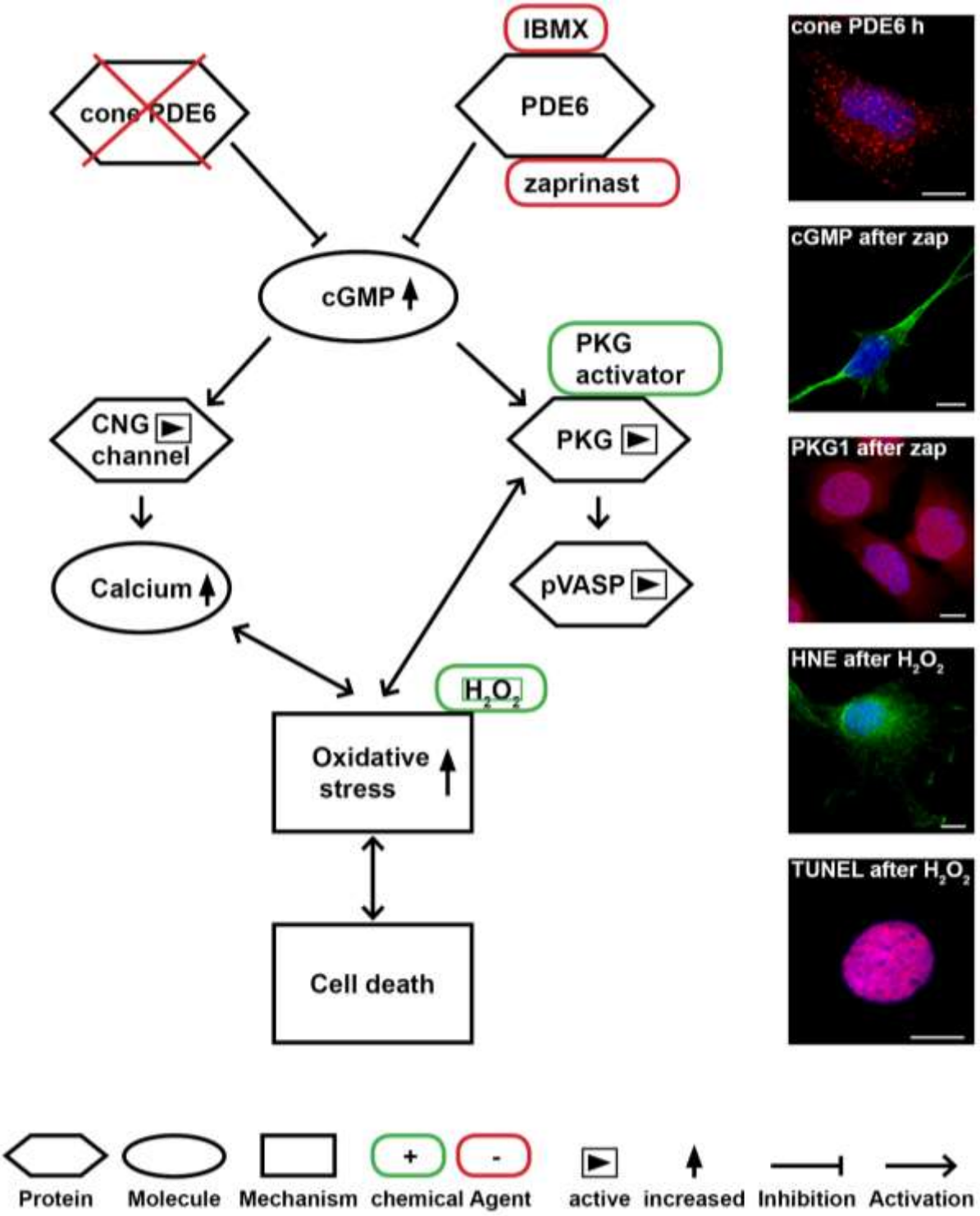

Figure 12: Potential cell death signaling in *cpfl1* cones and in 661W cells: A) cone cell death in *cpfl1* cones is induced by a non-functional PDE6 leading to PKG activation and accumulation of cGMP, followed by the opening of CNG channels, Ca^{2+} increase, and finally cell death. This degeneration mechanism was mimicked in 661W cells with H_2O_2 treatment, activation of PKG, or inhibition of PDE6. B) Cytoplasmic expression of the cone PDE6 in 661W. C) Anti-cGMP antibody showed abundant cGMP in the cytoplasm of 661W cells after inhibition of the PDE6 with the specific inhibitor zaprinast. D) PKG1 expression was observed in/or around the nuclei of 661W cells after zaprinast treatment. E) Staining of 4-Hydroxynonenal, a product of lipid oxidation, after H_2O_2 treatment. F) TUNEL staining after treatment of 661W with H_2O_2. Scale bar=10µm

4.2.3 Oxidative stress in 661W cells

For measuring oxidative stress in live 661W cells, we transfected them with an oxidative stress sensor (Gutscher *et al.* 2008). This sensor was made by combining the human glutaredoxin-1(Grx1) with a conventional redox-sensitive GPF (roGFP). The Grx1-roGPF2 fusion protein was previously transfected into human HeLa cells and had been used to image the intracellular glutathione redox potential. In the transfected HeLa cells, sensor was tested by adding either hydrogen peroxide to induce oxidative stress or dithiothreitol (DTT), which is a strong reducing agent. The sensor underwent conformational changes when it was oxidized, altering the emission wavelength. After excitation at 408nm and 488nm wavelength, the ratio of the emission in the green channel (500-530nm) was calculated. This ratio is depicting the redox level of the sensor.

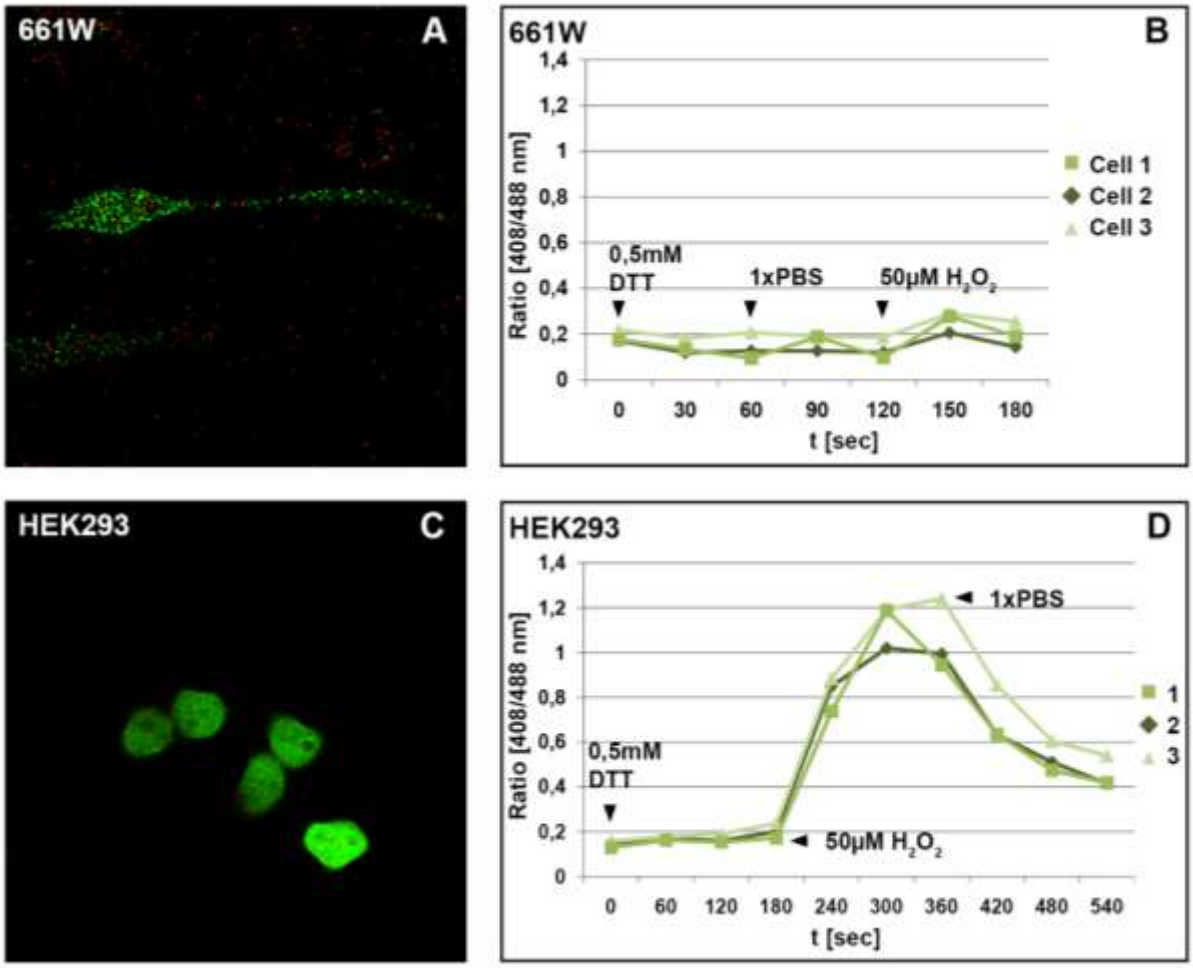

Figure 13: The oxidative stress sensor expression and measurement of oxidative stress in 661W cells: A) Expression of the oxidative stress sensor Grx1-roGPF2 in 661W cells. B) Transfected cells were excited with a laser at 408nm and 488nm and the emission was measured at 500-530nm for the following 3min. The ratio of 408nm and 488nm was calculated and plotted against the time to see redox changes. To reduce the sensor maximally DTT was added. After PBS rinsing, H_2O_2 was added, but only minimal changes in the ratio were seen. C) Expression of Grx1-roGPF2 in HEK293 cells. D) Ratio of Grx1-roGPF2 plotted against time. DTT were added to induce maximal reduction, while after H_2O_2 slowly the ratio was raised. PBS was able to reduce the ratio again. All measurements were repeated three times with 3 different cells.

The murine 661W cells showed a much weaker expression of human Grx1-roGPF2, 24h after transfection (Fig.13 A), when compared with the strong expression in human HEK293 cells (Fig.13 C). We measured transfected 661W cells, cultivated on a glass plate under a microscope setup (Nikon D-Eclipse C1). To reduce the sensor maximally, we added 0.5mM DTT to the medium and measured the emission (500-530nm) after excitation at 408 and 488nm. The ratio of 408/488nm was calculated, with the maximally reduced sensor displaying a ratio of 0.2, similar to what was shown in Gutscher *et al* (2008). However, in 661W cells treated with 50µM H_2O_2, the maximum ratio observed was 0.3. This result was interpreted as a non-functional sensor. In HEK293 cells, the ratio at maximal reduction was 0.2 as well, but after H_2O_2, it rose to 1 or 1.2, which was even higher than in HeLa cells. Surprisingly, the response was much slower in HEK293 cells as expected. In our system, it took roughly 2min before the ratio reached the maximum oxidation while in Gutscher *et al.* (2008) the oxidative stress sensor was shown to react within 15sec. Even in HEK293 cells the sensor was not reacting as expected, while in murine 661W cells, the human Grx1-roGPF2 sensor was not expressed in high levels and the oxidative stress measurement was therefore not possible with our system. Therefore, we stopped this approach at this point.

4.2.4 Induction and measurement of cell death in 661W cells

Work on the 661W degeneration model system required availability of a reliable assay to measure cell death. Therefore, a number of different commercial and non-commercial assays for the detection of cell death were tested. With the TUNEL method essentially all 661W cells were stained positive and no difference between control and treated cells were observed. This effect was not seen in the HEK293 control cell line (data not shown). As a consequence, this method was deemed inappropriate to determine cell death in 661W cells. We then compared three different methods to measure the cell death 24h after treatment with 100µM H_2O_2 (Fig. 14). The Live/Dead assay labeled live cells with Calcein dye in green and dead cells with Ethidiumbromide dimer-1 in red (Fig.14 A and B). Images were made with a fluorescence microscope (Zeiss Axiovert) and dead and live cells were counted. After treatment with 100µM H_2O_2 for 15min and further cultivation of the 661W cells for 24h, nearly every cell was dead. Compared with untreated cells (percentage of dead cells: 14.7%; SEM 8.9), the percentage of dead cells (92.9%; SEM 5.5) was highly significantly increased (t-test: $p<0.0001$) (Fig.14 C). After the same treatment, fixed cells were labeled with

propidiumiodide, to count the total number of cells remaining attached in the petri dish (Fig.14 D and E). In the H_2O_2 treated cells the mean value of total cell number was 0.83 (SEM 0.4) while in untreated cells it was 75.71 (SEM 2.15), this reduction was again highly significant (t-test: $p<0.0001$).

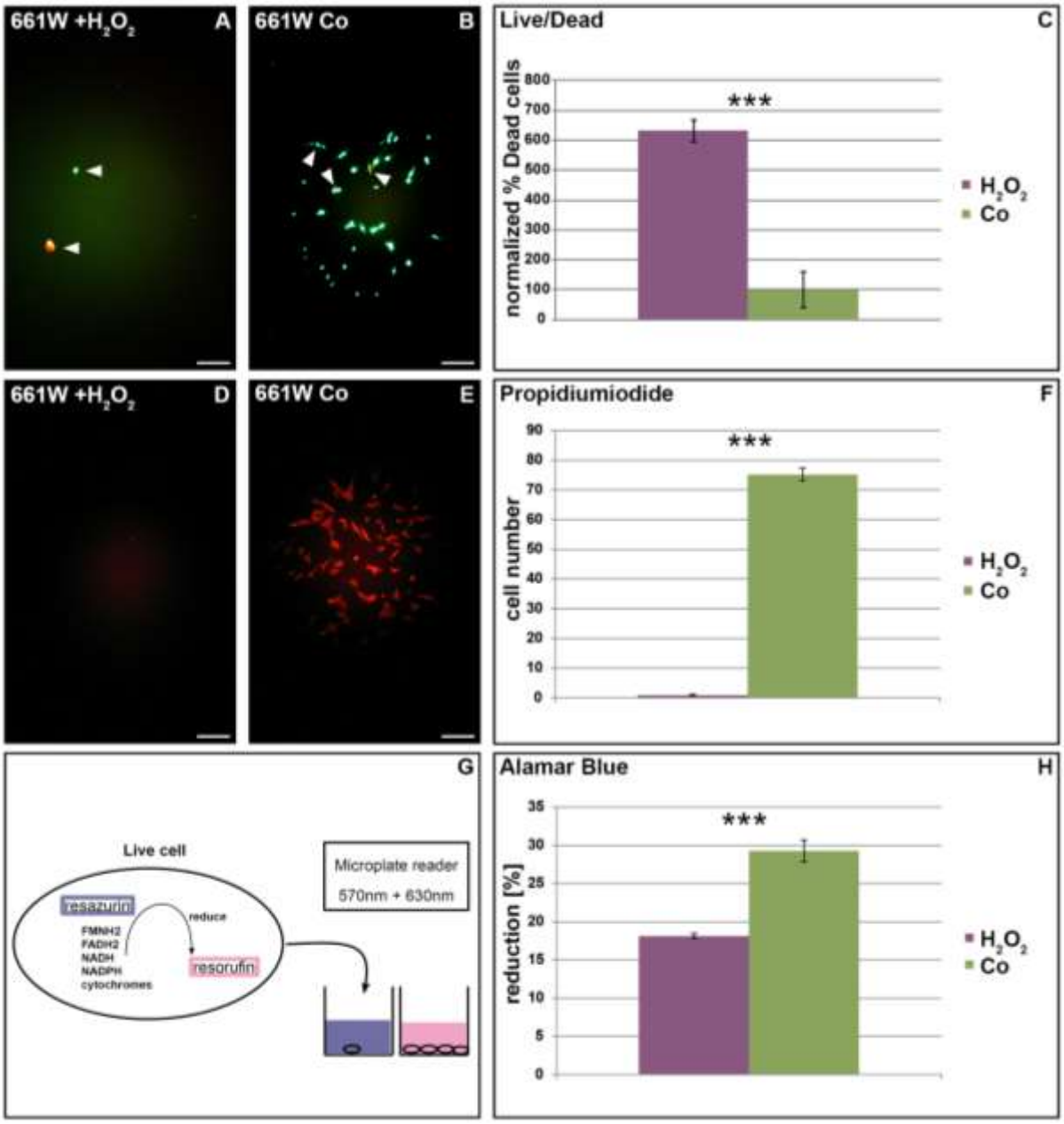

Figure 14: Comparison of different cell death/viability assays: A-C) Live/Dead assay A) H_2O_2 treated cells with two 661W cells (arrowheads) remained, one cell was alive (green) the other was dead (red); B) Live/Dead assay staining of untreated 661W cells with 3 dying cells (arrowheads). C) Normalized percentage of dead cells after H_2O_2 treatment was significant increased compared to untreated control. D-F) Propidiumiodide (PI) staining; D) H_2O_2 treated cells; E) untreated control F) mean of absolute cell numbers for H_2O_2 treated cells and untreated cells showed that significantly less cells remained after treatment. G and H) AlamarBlue cell viability assay G) The blue dye resazurin is reduced to resorufin in live cells. This reduction changes the color from blue to pink, which is measured in a photometer. H) percentage of AlamarBlue dye reduction for treated and untreated group was significantly higher in untreated group, where more cells were alive than after treatment; Scale bars= 10µm; All experiments were repeated in 6 independent wells for Live/Dead and PI or in 11 independent wells for AlamarBlue.

The third test, AlamarBlue is a blue dye, which is reduced by live cells causing a color change from blue to pink. This change in color was measured with a spectral photometer to then calculate the reduction of the dye, which displays indirectly the extend of cells alive or death (Fig.14 G). The nontoxic dye was added to the medium and incubated for 4h before the first measurement was performed. Cell viability measurements with AlamarBlue after H_2O_2 treatment showed significantly less reduction of the indicator dye (t-test: $p<0.0001$) in treated cells (18.1%; SEM 0.3) compared with the reduction in untreated cells (23.3%; SEM 1.5). This implies that fewer cells were alive after treatment compared with the untreated control. As expected, all three cell death measurements proved a highly significant induction of cell death after H_2O_2 treatment, which was to be expected. For further measurements, I used the Live/Dead assay, because it was easier to apply, gave fast and clear staining and was easy to measure. This assay did not only show live cells, like the AlamarBlue assay but rather living and dead cells. Additional, it gave the absolute cell numbers (as with propidiumiodide staining), which may be more convincing than measuring a color change in the medium.

After the unspecific cell death initiation with H_2O_2, I used the PKG activator 8-pCPT-PET-cGMP to trigger cell death in 661W cells (Fig.15 A). Following 24h treatment with 50µM PKG activator, a significantly higher percentage of dead cells (6.5%; SEM 0.3; t-test: $p<0.0001$) was measured compared to the untreated control (2.3%; SEM 0.8).

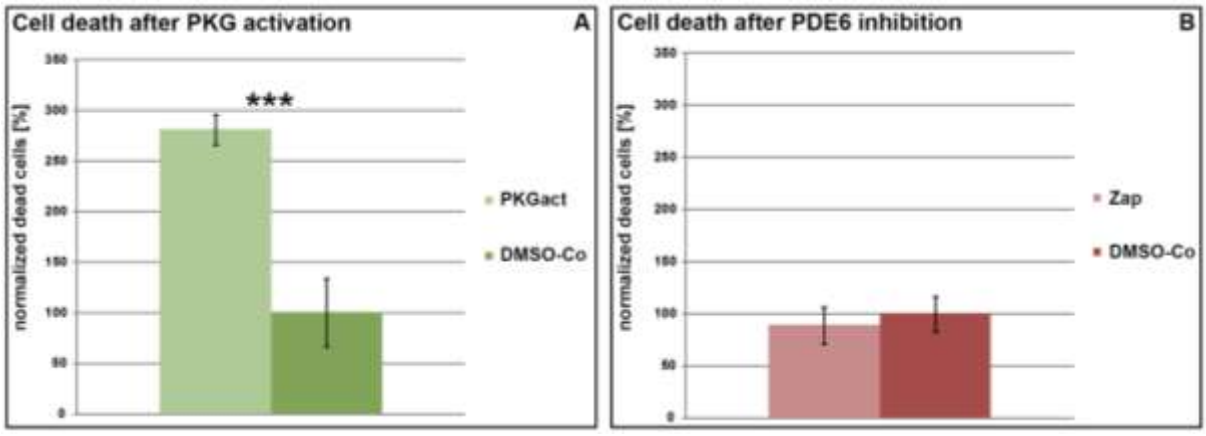

Figure 15: *cpfl1*-like cell death induction in 661W: A) After PKG activation with 8-pCPT-PET-cGMP cell death was significantly increased. B) After PDE inhibition with zaprinast no increase in cell death was found; both experiments were repeated three times.

As a second, independent cell death induction protocol, we specifically inhibited PDE6 with zaprinast (Fig.15 B). After 24h of 500µm zaprinast treatment no significant difference between treated (5.4%; SEM 1.1; t-test: $p<0.656$) and control group (6.1%; SEM 1.0) was detected. This was surprising because we saw expression of rod and cone PDE6 in 661W cells (Fig.11 E-H) and zaprinast inhibits both PDE6 isoforms (Zhang *et al.* 2005). Therefore, zaprinast treatment was expected to have an effect on the cells.

However, 661W cells are not expressing the *Cnga3* subunit of the CNG channels (Fitzgerald *et al.* 2008) and without this subunit the channel is not functional. Therefore, even higher cGMP levels caused by inhibition of PDE6 may not be able to induce a sufficient influx of Ca^{2+} ions through the CNG channel to cause cell death. To test for this hypothesis, we transfected the cells with a *Cnga3* expression vector and measured the channel functionality after transfection (Köppen *et al.* 2008). To this end, we performed Ca^{2+} measurements before and after treatment with a cGMP analog (8-bromo-cGMP). A functional CNG channel would be opened by cGMP causing Ca^{2+} to flow in and the Ca^{2+} concentration to rise. We transfected HEK293 and 661W cells with *Cnga3* and measured the intracellular Ca^{2+} with the Ca^{2+} indicator Fura2-AM. Transfected HEK293 (n=12; 10 cells showed functional CNG channel) and 661W cells (n=12; 8 cells showed functional CNG channels) showed Ca^{2+} influx after cGMP was added, while untransfected 661W cells did not show any cGMP dependent Ca^{2+} increase (Fig. 16 A).

Cnga3 transfected 661W cells were treated with 100µM zaprinast for 30min or 1h followed by a cGMP immunohistochemistry to test for cGMP accumulation. A 30min zaprinast treatment resulted in accumulation of cGMP in some cells (Fig.16 B, arrowheads), while others were not labeled. The untreated control showed a less intensive staining of cGMP in most cells (Fig. 16 C). After 1h of zaprinast treatment, increased staining of cGMP was not detectable (Fig.16 D) compared with untreated control cells (Fig.16 E). However, some cells became rounded which may indicate anoikis and the beginning of cell death (Hou *et al.* 2006) (Fig.16 D, arrowheads). This result implied that after *Cnga3* transfection zaprinast treatment was able to increase the cGMP concentration in the cells and induce cell death in 661W cells.

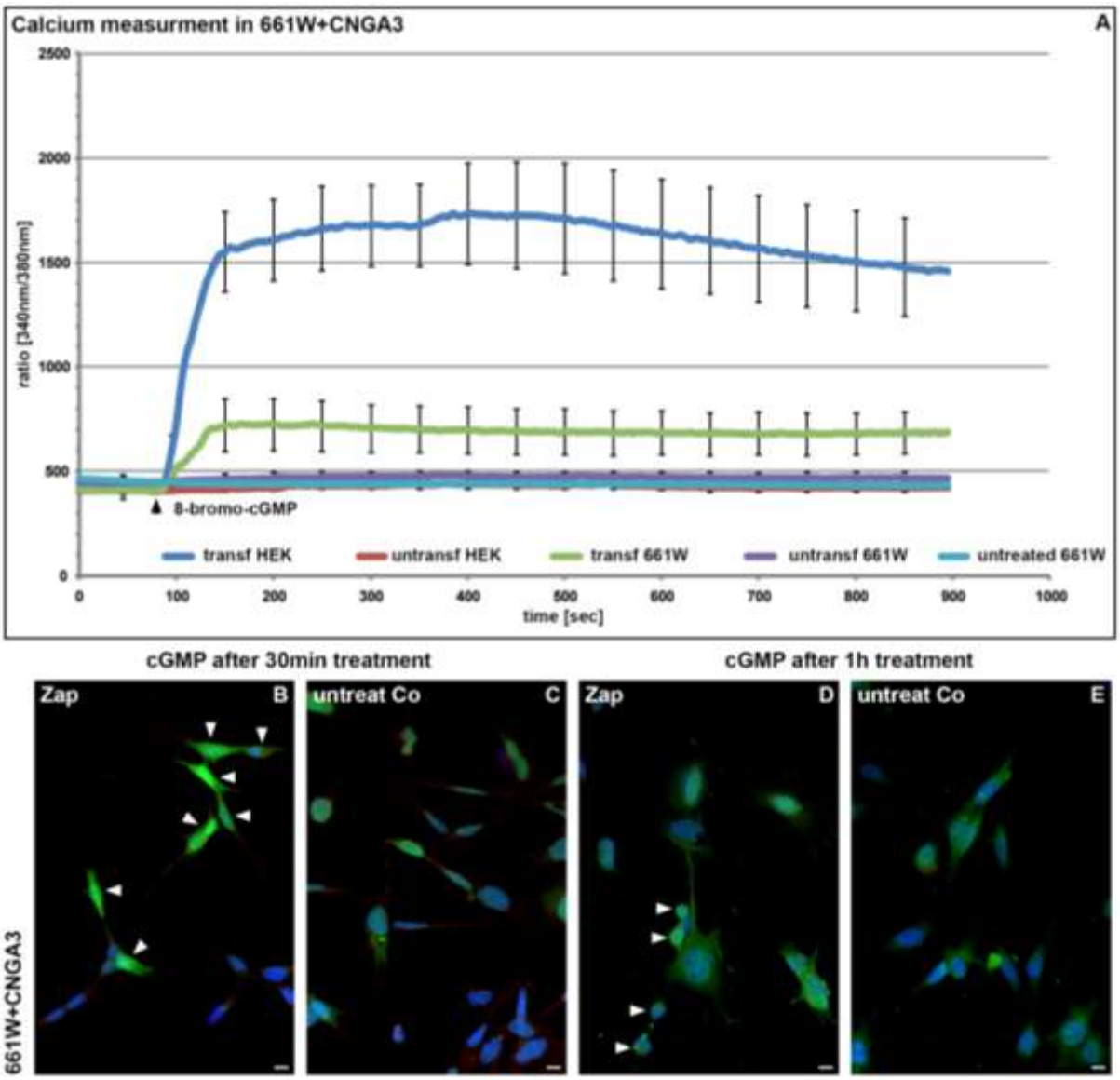

Figure 16: Ca^{2+} and cGMP in 661W after CNG transfection: A) Ca^{2+} measurement of CNGA3 transfected HEK293 and 661W cells showed Ca^{2+} influx after cGMP addition. B-D) cGMP labeling (green) after 30min or 1h of zaprinast treatment of *Cnga3* transfected 661W cells. B) After 30min of 100µm zaprinast, some 661W cells showed cGMP accumulation (arrowheads), while others did not. C) Untreated control cells showed only weak cGMP staining. D) In transfected 661W cells, the cGMP staining was faint after 1h of zaprinast treatment, but some cells showed a rounded morphology (arrowheads), which may indicate beginning of cell death; E) untreated control showed weak staining of cGMP; Scale bar= 10µM; blue staining=nuclear marker DAPI; green staining=cGMP;

5 Discussion

In this thesis, several rodent models of retinal degeneration were used to study expression of the pro-survival transcription factor CREB and its inhibitor ICER in photoreceptors. Because ICER expression was found in cone photoreceptors, we were interested to see whether ICER had a role in primary and/or secondary cone degeneration. While studying cone degeneration in rat and mice retinas, where rods outnumber cones, another interesting project was born. The murine 661W photoreceptor cells were tested as a cone-degeneration model, to analyze cell death mechanism there and to screen for putative neuroprotective substances.

5.1 CREB and ICER

5.1.1 CREB and pCREB expression in C3H-rd1

CREB-1 was found to be significantly higher expressed in wt, than in *rd1* retinas, as shown with microarray experiments (Paquet-Durand *et al.* 2006). Additionally, the pCREB level was quantified with western blot and found to be decreased as well (Paquet-Durand *et al.* 2006). Wahlin and colleagues (2000) showed in *C57BL/6J*$^{+/+}$ mice retinal organotypic explants, that after FGF2, BDNF and CNTF treatment, the pCREB levels were increased and the degeneration delayed, implying a protective effect of active CREB on retinal degeneration (Wahlin *et al.* 2000). Other studies confirmed the increase of pCREB in *rd1* retinal explants treated with CNTF and BDNF or with IGF-I and observed a slower progression of degeneration as well (Azadi *et al.* 2007; Arroba *et al.* 2009).

My western blot results differed from what was found before, since my result showed no significant decrease for CREB and pCREB in *C3H-rd1* retinas, although a slight numerical reduction was seen (Fig.6 K and L). This may be explained with the fact that in *C3H-rd1* mice the pCREB level was found to be regulated in a rhythmic manner, with a peak of pCREB 2h after the light was turned on (Dinet *et al.* 2007).. Since this was not controlled in my study, it may have led to a higher variation of CREB expression and pCREB levels. Another explanation for my results could be the use of different antibodies.

With the pCREB antibodies used in the studies mentioned above, Müller, amacrine, bipolar and ganglion cells were labeled, but no photoreceptors. Nevertheless, with both pCREB antibodies used, positively labeled cells in the ONL were observed. Nuclear pCREB staining was found in rod and cone photoreceptors of RP dog models and in human retinas with AMD as well (Beltran *et al.* 2009). Additionally, a homolog of CREB, CREB-A was found to be expressed in all photoreceptors before cell differentiation in Drosophila (Anderson *et al.* 2005). Furthermore, pCREB was found in the developing eye of mice and in a CREB knockout mouse, severe eye defects and retinal malformation were observed (Dworkin *et al.* 2009). In this study, the authors suggest, that CREB is activated in immature progenitor cells, inactive in mature progenitor cells and gets activated again when the mature progenitors differentiate and integrate.

pCREB immunostaining on *C3H-rd1* and *C3H-wt* retinas at P0, P1, P4, P7, P8, P9, P11, P13, P14, P16 and P30 was performed. In *C3H-rd1* retinas, all stages showed ONL-pCREB staining, while in *C3H-wt* pCREB in the ONL was observed only from P0 to P8. After P8, pCREB staining was very rarely detectable in *C3H-wt* ONL (data not shown). This may indicate that around P8 pCREB dependent regulation of transcription changes from developmental towards pro-survival functions. In the avian retina such a change was shown for the adenosine mediated activation of the A2a receptor, which was either inducing cell death at embryonic stage E6 or was protective against cell death at E8 (Socodato *et al.* 2011). Dependent on the developmental stage, the same activated receptor led to opposite downstream events. This interesting finding may be explained with a decreased or increased CREB phosphorylation, regulating the receptor dependent signaling.

In conclusion, CREB was found to be expressed or activated in the retina of different species and is mainly present in the inner retina. Nevertheless, in photoreceptor development of different species, as well as in photoreceptor degeneration models, activated CREB was found in photoreceptors, suggesting a role for CREB in the development and disease of photoreceptors.

5.1.2 ICER expression in C3H-rd1

Opposite to the pro-survival effects of pCREB, ICER was inducing cell death in various neuronal cell cultures (Bieganska *et al.* 2012, Jaworski *et al.* 2003, Mioduszewska *et al.* 2008, Klejman and Kaczmarek 2006). This fits with the observation that ICER is inhibiting CREB and CREM dependent transcription. It competes with CREB and CREM transcription factors for the same DNA-binding site (CRE-sequence), without bearing the potential to activate the transcription of genes. Interestingly, ICER contains a CRE-sequence as well and its transcription is therefore CREB dependent. With immunolabeling, we showed for the first time expression of ICER in *C3H-rd1* retinas. The expression pattern in the inner retina is comparable to pCREB, with most ganglion cells and most cells of the INL showing ICER expression in *C3H-rd1* and in *C3H-wt* retinas at P11 and at P30 (Fig.7 E-H). In the ONL, co-labeling with the cone-marker glycogen phosphorylase revealed ICER expression in cone photoreceptors only (Fig.7). I never found a glycogen phosphorylase stained cell, which was not showing ICER expression and *vice versa*. Since ICER transcription can be CREB dependent, I did immunolabeling for pCREB and glycogen phosphorylase to assess if cone photoreceptors show activated CREB (data not shown). However, I found no co-labeling of glycogen phosphorylase and pCREB, which could be interpreted as follows: I) the pCREB amount is too low for detection with this method, II) or pCREB induces ICER expression at different time points as we looked at, III) or ICER expression in cone photoreceptors is independent of CREB.

Interestingly, we observed strong ICER labeled cone photoreceptors in *C3H-rd1* retinas at P30, since at this age cone degeneration had already started (Carter-Dawson *et al.* 1978). This suggests a potential involvement of ICER. We performed ICER immunostaining with retinas of two other RP models, the S334ter and P23H rats, and found ICER expression in cone photoreceptors at five time-points during which prominent degeneration occurs.

5.1.3 ICER expression in other photoreceptor degeneration models

ICER was not only expressed in *C3H-rd1* retinas, but also in the *S334ter* and *P23H* rat retina (Fig. 8 A-H). The expression pattern of ICER was similar in rat retinas compared with mouse retinas, but fewer cells were stained in the ganglion cell layer and INL cells (compare Fig.7 F and H with Fig.8 F and H). However, in the mutants

retinas, ICER was upregulated, especially in the older ages when secondary cone degeneration was progressing (compare wt and mutant retinas in Fig.8 A-H). ICER was expressed in cone photoreceptors of three different models of RP and clearly, an upregulation in the later stages was observed. Hence, ICER could have a role in secondary cone degeneration or might be involved in cone degeneration in general. Therefore, we repeated ICER immunolabeling in retinas of the primary cone-degeneration model *cpfl1*. In this model, a mutation induces cone degeneration, while the rod photoreceptors stay intact. As in *C3H-rd1* retinas, ICER expression was located in ganglion cells, inner retina and in all cone photoreceptors (Fig.8 I-L). Differences of ICER intensity were not visible by eye. Nevertheless, we wanted to measure the ICER intensity in cone photoreceptors and compare mutants and wt, to see if there are any significant changes when cone photoreceptors are degenerating.

5.1.4 ICER quantification in four distinct degeneration models

Quantitative protein expression measurements are usually done with western blot or quantitative mass spectrometry, but we needed to quantify the ICER expression of single cells, since our interest was the expression in cone photoreceptors. This cellular resolution was impossible to achieve within the retina with the above-mentioned methods, because we had no possibility to isolate cone photoreceptors only. Additionally, many retinas would be needed to obtain enough tissue to perform western blot quantifications. Therefore, we measured the ICER intensity of fluorescent immunolabeled pictures and compared mutants and wt intensities (Fig.9 A; Hamilton 2009).

In summary, ICER intensity analyzes revealed a significant upregulation of ICER in mutant retinas, compared to wt expression. This upregulation took place in two earlier stages, P14 *cpfl1* (Fig.9 E), and P12 *S334ter* cones (Fig.9 C) and in *C3H-rd1, P23H* and *S334ter* cones at P30 (Fig.9 B, D, C). In both mouse mutants, the upregulation was found at time points with prominent cone degeneration (Carter-Dawson *et al.* 1978; Trifunović *et al.* 2010). Remarkably, ICER was upregulated in both primary (*cpfl1*) and in secondary cone degeneration (*C3H-rd1*). In both rat mutants, the cone degeneration would begin after the analyzed time points (Machida *et al.* 2000; Li *et al.* 2010), but the progressing rod degeneration is likely to increase cell stress in cones. In *S334ter,* the cones lose their outer segments as early as at P12 (Li *et al.* 2010),

furthermore, the cone photoreceptors are rearranged towards a ring shaped distribution, which may be increasing cone cell stress as well (Lee *et al.* 2011). Nevertheless, the cone photoreceptors were either degenerating or their morphology was not normal, when ICER was found to be upregulated. This may suggest a role of ICER in cone protection against the cell stress or ICER was upregulated because of higher cell stress in cone photoreceptors leading finally to cone degeneration. From studies in neural cells, much is known of stress induced ICER expression and often it had negative effects on cell survival (Borlikova and Endo 2009). Still, for retinal cells, the role of ICER expression remains elusive and further investigations will be needed.

5.1.5 pCREB and ICER expression in retinal culture explants treated with zaprinast

With an *in vitro* experiment, we tested the expression of pCREB and ICER while inducing rod degeneration with the specific PDE6 inhibitor zaprinast. The treatment of retinal explant cultures with zaprinast mimics the rod degeneration in *C3H-rd1* (Sahaboglu *et al*. 2010). It was shown that zaprinast is not able to discriminate between the rod and cone PDE6 (Zhang *et al*. 2005). Therefore, we should induce cell death in both types of photoreceptors. Surprisingly, the cone number remained stable after zaprinast treatment, while the ONL got thinner (unpublished data). This implies that zaprinast induced predominantly rod cell death in this experimental paradigm. Maybe cones need a higher concentration of zaprinast or a longer duration of treatment, before they undergo cell death as well.

For this study, it is important to consider that zaprinast specifically induced rod degeneration in retinal cultures. Moreover, in this rod degeneration we measured a significant reduction of pCREB, while ICER expression was unchanged. In line with the *in vivo* models, this implies a role of ICER that is restricted to cone photoreceptors.

5.2 661W cells

5.2.1 661W cells are cone-like

To improve our understanding of cone degeneration a cone photoreceptor-culture system would be helpful, because the mouse and rat retina is rod-dominated and therefore cone cell death difficult to investigate. In order to get a photoreceptor cell line, cell cultures were made from murine retinoblastoma and finally the immortalized cell line 661W was obtained (Al-Ubaidi *et al.* 1992). This cell line resembles the spindle like morphology of neuronal cells, and expresses several photoreceptor specific proteins (Roque *et al.* 1999). More precisely, Tan and colleagues showed that the 661W cells are cone-like as judged by their expression of photoreceptor-specific genes (Tan *et al.* 2004).

We tried to induce further differentiation toward the cone cell fate by culturing 661W cells in the R16 medium used for retinal cultures (Caffé *et al.* 2001b), which we supplemented with serum, but neither protein expression nor the spindle-like morphology was changed. The only difference we observed was an impairment of cell growth (data not shown). A similar differentiation approach was done by applying growth factors to the medium, which were secreted by retinal pigment epithelial cells (Sheedlo *et al.* 2007). 661W cells were grown in media with fibroblast growth factor (FGF-2), nerve growth factor (NGF), epidermal growth factor (EGF) or RPE cell conditioned medium. Cells supplemented with FGF-2 exhibited a thinner cell body, longer and more complex processes and slightly increased growth. However, NGF and RPE conditioned media induced cell cycle arrest and finally cell death. Therefore, FGF-2, R16 medium, or distinct growth factors, were not able to induce a more cone-like morphology and gene expression than already present in native 661W cells. FGF-2 did not induce an increased cone differentiation but was shown to be neuroprotective against oxidative stress (O'Driscoll *et al.* 2007). Since this, could potentially interfere with the screening for neuroprotective substances, we maintained the cells in regular DMEM/RPMI medium without any additional supplements.

Our marker study confirmed the results of Tan and colleagues (2004) and proposed a cone-like phenotype for 661W cells. In summary, we found eight cone-specific proteins expressed in 661W cells. Additionally, we found expression of rod PDE6 and calmodulin. For our purposes, rod PDE6 expression was not problematic, because the PDE6 inhibitor used was not discriminating between rod and cone PDE6.

Immunostaining with the anti-calmodulin antibody in the murine retina showed bipolar and amacrine cell staining (data not shown). Since, calmodulin is a common Ca^{2+}-/calmodulin-dependent signaling cascade protein and expressed in many cell types it was not interfering with the intended experiments.

As a summary of the retinal marker expression study in 661W, we concluded that these cells are more cone-like than rod-like and resemble photoreceptor cells more than any other retinal cell type.

5.2.2 Induction of cell death in 661W cells

To use the 661W cells as model system for cone-degeneration, we had to induce cell death. Additionally, we wanted to induce a kind of cell death that resembles cone degeneration in the *cpfl1* mouse model. Since *cpfl1*-cones suffer from a PDE6 mutation (Chang *et al.* 2009), we wanted to inhibit PDE6 pharmacologically to induce a 661W cell degeneration comparable with *cpfl1* cone degeneration. With this cell culture model, we then wanted to test putative cone neuroprotective substances for therapeutic capacity. Eventually, this cell culture model was to be used for a high-throughput screening system, with which many compounds could be tested in a short time and at different concentrations. After identification of a protective substance its effects would be validated, first in a complex *in vitro* system like the organotypic retinal culture system (e.g. to find the best working concentration for the retina), and finally in an *in vivo* animal model like *cpfl1* mice.

Comparison of cell death assays

To find the most reliable assay, cell death was induced with H_2O_2. We chose H_2O_2 because it is toxic for nearly every cell culture and there are publications available, which induced cell death in 661W with H_2O_2 (Mandal *et al.* 2009). For the cell death assessment in the retina or in organotypic retinal cultures, we used the TUNEL method and for an estimation of oxidative stress, we performed avidin staining (Sahaboglu *et al.* 2010; Kaur *et al.* 2011). Therefore, we performed both methods to analyze 661W cell death as well. Unfortunately, both methods produced a very strong staining (Fig.7; TUNEL after H_2O_2) and did not show a difference between treated and untreated cells (data not shown). Consequently, we needed to find an alternative cell death detection method that would work reliably in 661W cell cultures. Propidiumiodide (PI) is not membrane-permeable and can be used as a cell death marker in living cell cultures (Fig.14 D-F). PI also allows measuring the absolute cell number after cell fixation and

permeabilization. Although PI is easy to use, we needed a method that additionally to the amount of dead cells resulted in the number of live cells. Here, we used the Live/Dead assay that worked well after H_2O_2 treatment (Fig.14 A-C). As a third method, we chose the AlamarBlue assay (Ahmed *et al.* 1994), which is well suited for high throughput screenings and in contrast to the other tests allows for a continuous monitoring of cell viability over an extended period of time. A disadvantage of the AlamarBlue test was a relatively low detection of cell death after H_2O_2 treatment compared with the other two cell death assays (Fig.14 C, F and H). Finally, I decided to measure cell death using Live/Dead staining because it was easy to apply and analyze, and gave the absolute numbers of both dead and live cells.

Comparison of cell death mechanisms in 661W and *cpfl1*

The 661W cells were shown to be light sensitive and susceptible to light-induced cell death (Krishnamoorthy *et al.* 1999). Unfortunately, this does not mean that all proteins of the phototransduction cascade are expressed. For example, both murine opsins are expressed in 661W cells, but not the chromophore (Kanan *et al.* 2007). Therefore, we tested whether key proteins relevant for *cpfl1* cone cell-death were expressed in 661W, so as to allow for a study of cell death mechanisms that would be as close to the "real" cone situation as possible (Trifunovic *et al.* 2010). We were interested if the cone PDE6 was expressed in 661W cells and with an antibody against the inhibitory subunit of the cone PDE6, a cytoplasmic immunostaining (Fig.12; cone PDE6h) was obtained. We assumed that the other subunits of the cone PDE6 are expressed in 661W cells, as well. Furthermore, we found expression of the rod PDE6 (Fig.11 E-H, Tab.5, pictures not shown). With immunolabeling, the second messenger cGMP was found at low levels in the cytoplasm of 661W cells (Fig.12; cGMP after zap). Additionally, the cGMP dependent PKG1 and PKG2 were endogenously expressed in 661W cells (Fig.12; PKG1 after zap), this was very important, because we wanted to see whether activation of PKG could induce cell death. Indeed, when using the unselective PKG activator 8-pCPT-PET-cGMP, we found a significant increase in cell death (Fig.15 A). This result was in line with findings, showing that PKG activation causes photoreceptor cell death in *rd1* and *rd2* (Paquet-Durand *et al.* 2009) and *cpfl1* mice (Trifunovic *et al.* 2010). Finally, we used zaprinast to inhibit the PDE6 in 661W. We used zaprinast because it shows a strong selectivity for PDE6 over PDE5 and does not discriminate between cone and rod PDE6 (Zhang *et al.* 2005). Furthermore, zaprinast treatment in *C3H-wt* organotypic retinal cultures was able to induce photoreceptor cell death comparable with rod degeneration in *C3H-rd1* mice

(Sahaboglu *et al.* 2010). We tried the same and much higher concentrations than were used in the retinal culture paradigm. However, even very high zaprinast concentrations did not induce cell death in 661W cells (Fig.15, B). Similarly, the unspecific PDE inhibitor IBMX did not cause 661W cell death (Lolley *et al.* 1977) (data not shown). In addition, treatment with the membrane permeable cGMP analogue 8-Br-cGMP (Zimmerman *et al.* 1985) did not reduce 661W viability. This was surprising since high cGMP is known to cause cell death either via opening of the CNG channels or activation of PKG (Paquet-Durand *et al.* 2009; Paquet-Durand *et al.* 2011). A literature search revealed that, one subunit of the CNG channels was not expressed in native 661W cells and that CNG channels are likely not functional (Fitzgerald *et al.* 2008). However, transfection of the *Cnga3* subunit into 661W cells rendered the CNG channel functional as shown by Ca^{2+} imaging after 8-Br-cGMP addition (Fig.16A). Interestingly after *Cnga3* transfection, 661W cells seemed to show an increased zaprinast-induced cGMP accumulation (Fig.16 B and C). Since photoreceptor Ca^{2+} and cGMP levels are interlinked by the CNG channel – Ca^{2+} - guanylyl cyclase – cGMP feedback loop (Olshevskaya *et al.* 2002) it is conceivable that functional expression of CNG channels altered 661W Ca^{2+} and cGMP homeostasis.

After 1h zaprinast treatment a number of cells with higher cGMP levels and rounded shapes were seen (Fig.16 D and E), indicating that these cells were dying (Kroemer *et al.* 2009). Therefore, zaprinast may induce cell death in the 661W cell line, when the CNG channel is functional. This in turn would mean that 661W cells are able to degenerate in ways similar to *cpfl1* cones after treatment with PKG activator or PDE inhibitors. The latter was only effective after transfection of the *Cnga3* subunit and functional CNG channels. Taken together, it is in principle possible to use 661W cells to screen for putative cone neuroprotection substances.

6 Conclusion and outlook

The transcriptional repressor ICER was shown to be expressed in mouse and rat retinas in GCL, INL and, most remarkable for us, in all cone photoreceptors. Additionally, we found an upregulation of ICER expression in four models for primary and secondary cone degeneration, before/while cone cell death took place, suggesting a role of ICER in the mechanism of cone degeneration. For further investigations of the cone degeneration mechanism, the 661W murine photoreceptor cells could be beneficial. We showed that these cells were able to degenerate in a similar way as the cones of the murine cone degeneration-model *cpfl1*.

6.1 ICER

For the first time retinal expression of the transcription factor ICER was shown. Furthermore, ICER was intensely expressed in cone photoreceptors, while no expression in rods was found. We analyzed the ICER expression in different rodent photoreceptor models and obtained more ICER expression at stages where the cone photoreceptors are degenerating or displaying signs of cell stress before their degeneration. We investigated primary and secondary cone degeneration models and in both mechanism of cell death, ICER expression was found to be significantly increased. This may imply a general role of ICER in cone degeneration.

Further experiments should focus on the function of ICER expression in cone photoreceptors. Inhibition or gain of function would be very interesting to clarify the role of ICER in cone degeneration or differentiation. Up to date, ICER knockout or overexpression mouse models are available and the retinas of them could be examined for signs of cone death or protection, respectively (Kojima *et al.* 2008; Han *et al.* 2011). Another important matter would be to find the cause of ICER activation. Since ICER activation was shown to be cAMP-dependent, an activation of ICER, not only by cGMP-dependent PKG, but also by the cAMP dependent protein kinase A (PKA) should be investigated. For rod photoreceptor degeneration, activation of the PKA was not observed (data not shown). Nevertheless, activation of PKG was shown in *rd1* rods and in *cpfl1* cones (Paquet-Durand *et al.* 2009). For cone degeneration, PKA activation needs to be examined, maybe by using retinal explant cultures treated with pharmacological inhibitors or activators.

6.2 661W cells

Cone degeneration is challenging to investigate in commonly used rodent degeneration models, since cone photoreceptors represent only 3% of all photoreceptors there. Therefore, the immortalized, murine, cone photoreceptor-like cell line 661W was promising to use for studying cone degeneration in a homogeneous cell culture model. We mimicked *cpfl1* cone degeneration in 661W cells, by inhibiting the PDE6, after transfection of the CNG channel subunit *Cnga3*, to restore channel functionality. In native cells, PKG activation also led to cell death, therefore either *Cnga3* transfected or native 661W cells could undergo *cpfl1*-like degeneration and would be useful in a cell based screening assay. It would be very interesting to induce cell death by PKG activation plus adding antioxidants, calpain or PARP inhibitors to see if they protect the cells against cell death. Moreover, a 661W cell line stably expressing the CNGA3 subunit would be beneficial for using them to inhibit the PDE6 and mimicking the *cpfl1* cone photoreceptors.

We believe this thesis opens new insights in the mechanisms of cone degeneration, which may involve an upregulation of the transcriptional repressor ICER. Additionally, we revealed a useful novel cell based cone-degeneration model, for further investigations of cone death mechanisms and screening of neuroprotective substances.

7 Summary

In hereditary eye diseases of the Retinitis pigmentosa (RP) type, rod photoreceptors degenerate in a mutation-dependent fashion, followed by mutation independent cone cell death. Until today, no adequate treatment is available, but efforts are made to gain more knowledge about the mechanism of photoreceptor degeneration. Various animal models are available, showing mutations and symptoms comparable to human patients. In this study three models for RP (*rd1* mouse, *S334ter* rat, and *P23H* rat) and a cone degeneration model, the *cpfl1* mouse were investigated, asking whether a CRE-mediated transcription repressor, the inducible cAMP early repressor (ICER) was expressed. ICER is known to be involved in cell death in many neuronal and non-neural cells (Borlikova and Endo 2009). With immunostaining, ICER expression was observed in GCL, INL and in cone photoreceptors of all mutants and corresponding wt retinas. However, during cone degeneration or cone cell stress ICER expression was significantly upregulated in all mutant retinas. This finding suggests a role of ICER in cone degeneration and needs to be further investigated.

Human vision is strongly depending on cone photoreceptors, mediating high spatial resolution and color perception. However, cone degeneration is taking place in many eye diseases such as age-related-macula-degeneration (AMD), diabetic retinopathy, achromatopsia, cone-rod-dystrophies and Retinitis pigmentosa. At present, no satisfactory treatment options are available for these diseases and the investigation of cone degeneration models is challenging, because rod photoreceptors outnumber cones by far. Investigations of the mechanism of cone cell death and the search for a neuroprotective compound requires a reliable, high-throughput cell based model system, which we wanted to establish using the murine-photoreceptor cell line 661W (Al-Ubaidi et al. 1992). First, a retinal marker study was performed, to characterize the cells and to learn whether this cone-like cells are suitable for our purpose. Thereafter, the cone degeneration of *cpfl1* cones was mimicked in 661W cells by either inhibition of cone PDE6, after transfection of the *Cnga3* subunit of the CNG channel, or activation of PKG. These results were promising and we showed that the 661W cells may be used for further investigations of cone degeneration mechanisms and the search for neuroprotective substances.

8 Acknowledgements

This thesis was done in the Centre for Ophthalmology, Institute for Ophthalmic Research, Tübingen (Head until 2011 Prof. Dr. Eberhart Zrenner, Head Prof. Dr. Marius Ueffing) and at the Graduate school of cellular and molecular mechanisms, Tübingen, where I attended the PhD-program. This thesis would not have been possible without the finance of the Tistou and Charlotte Kerstan Foundation and the support of Prof. Dr. Eberhart Zrenner. I owe sincere and earnest thankfulness to my supervisors Dr. Stefan Kustermann and Dr. François Paquet-Durand, for their guidance and lively discussions. I would also like to thank the members of Thesis Advisory Board Prof. Dr. Eberhart Zrenner, Prof. Dr. Bernd Wissinger and Dr. Marita Feldkämper for advising and supporting my thesis.

I would like to express my gratitude to Prof. Dr. Eberhart Zrenner and Prof. Dr. Bernd Wissinger for reviewing my dissertation.

I am truly indebted and thankful to Ayse Şahaboğlu, who gave me slices of retinal cultures treated with zaprinast, to Peggy Reuter for providing me with the *Cnga3* plasmid and explained me how to test CNG channel functionality and to Wadood Haq for doing the calcium measurement experiments with me and helping me analyzing the results. The 661W cell line was obtained from Prof. Dr. Muayyad Al-Ubaidi, Department of Cell Biology, University of Oklahoma, USA.

I am obliged to many of my colleagues who supported me, namely Dr. Dragana Trifunović, Dr.med Blanca Arango-González, Ayse Şahaboğlu, Jasvir Kaur, (Dr.) Tao Wei, Katja Dengler, Sandra Bernhard-Kurz, Gordon Eske, and Silvia Bolz. Thank you for the great time, I will miss you a lot.

I would like to thank my family, which supported me a lot and always was interested in my research. Thank you, Nathalie for leaving your flat to let me write there and I would like to thank my friends Tanja, Stephan and especially Hartwig for being patient with me and always cheering me up, when something went wrong. The same is true for many friends, thanks a lot.

Stine Mencl

9 Reference list

Ahmed S. A., Gogal R. M., Jr. and Walsh J. E. (1994) A new rapid and simple non-radioactive assay to monitor and determine the proliferation of lymphocytes: an alternative to [3H]thymidine incorporation assay. *J. Immunol. Methods* **170,** 211-224.

Ahuja P., Caffé A. R., Ahuja S., Ekstrom P. and van Veen. T. (2005) Decreased glutathione transferase levels in rd1/rd1 mouse retina: replenishment protects photoreceptors in retinal explants. *Neuroscience* **131,** 935-943.

Al-Ubaidi M. R., Font R. L., Quiambao A. B., Keener M. J., Liou G. I., Overbeek P. A. and Baehr W. (1992) Bilateral retinal and brain tumors in transgenic mice expressing simian virus 40 large T antigen under control of the human interphotoreceptor retinoid-binding protein promoter. *J. Cell Biol.* **119,** 1681-1687.

Aloe L. (2011) Rita Levi-Montalcini and the discovery of NGF, the first nerve cell growth factor. *Arch. Ital. Biol.* **149,** 175-181.

Altimimi H. F. and Schnetkamp P. P. (2007) Na+/Ca2+-K+ exchangers (NCKX): functional properties and physiological roles. *Channels (Austin.)* **1,** 62-69.

Andersen J. K. (2004) Oxidative stress in neurodegeneration: cause or consequence? *Nat. Med.* **10 Suppl,** S18-S25.

Anderson J., Bhandari R. and Kumar J. P. (2005) A genetic screen identifies putative targets and binding partners of CREB-binding protein in the developing Drosophila eye. *Genetics* **171,** 1655-1672.

Arroba A. I., Wallace D., Mackey A., de la Rosa E. J. and Cotter T. G. (2009) IGF-I maintains calpastatin expression and attenuates apoptosis in several models of photoreceptor cell death. *Eur. J. Neurosci.*

Azadi S., Johnson L. E., Paquet-Durand F., Perez M. T., Zhang Y., Ekstrom P. A. and van Veen. T. (2007) CNTF+BDNF treatment and neuroprotective pathways in the rd1 mouse retina. *Brain Res.* **1129,** 116-129.

Azuma M., Sakamoto-Mizutani K., Nakajima T., Kanaami-Daibo S., Tamada Y. and Shearer T. R. (2004) Involvement of calpain isoforms in retinal degeneration in WBN/Kob rats. *Comp Med.* **54,** 533-542.

Bainbridge J. W. and Ali R. R. (2008) Success in sight: The eyes have it! Ocular gene therapy trials for LCA look promising. *Gene Ther.* **15,** 1191-1192.

Barabas P., Cutler P. C. and Krizaj D. (2010) Do calcium channel blockers rescue dying photoreceptors in the Pde6b (rd1) mouse? *Adv. Exp. Med. Biol.* **664,** 491-499.

Baumgartner W. A. (2000) Etiology, pathogenesis, and experimental treatment of retinitis pigmentosa. *Med. Hypotheses* **54,** 814-824.

Bazan N. G. (2008) Neurotrophins induce neuroprotective signaling in the retinal pigment epithelial cell by activating the synthesis of the anti-inflammatory and anti-apoptotic neuroprotectin D1. *Adv. Exp. Med. Biol.* **613,** 39-44.

Beltran W. A., Allore H. G., Johnson E., Towle V., Tao W., Acland G., Aguirre G. D. and Zeiss C. J. (2009) The CREB1/ATF1 pathway is activated in photoreceptor degeneration and protection. *Invest Ophthalmol. Vis. Sci.* **50,** 5355-63.

Bermingham-McDonogh O. and Reh T. A. (2011) Regulated reprogramming in the regeneration of sensory receptor cells. *Neuron* **71,** 389-405.

Berson E. L., Rosner B., Sandberg M. A., Hayes K. C., Nicholson B. W., Weigel-DiFranco C. and Willett W. (1993) A randomized trial of vitamin A and vitamin E supplementation for retinitis pigmentosa. *Arch. Ophthalmol.* **111,** 761-772.

Besch D., Sachs H., Szurman P., Gülicher D., Wilke R., Reinert S., Zrenner E., Bartz-Schmidt K. U. and Gekeler F. (2008) Extraocular surgery for implantation of an active subretinal visual prosthesis with external connections: feasibility and outcome in seven patients. *Br. J. Ophthalmol.* **92,** 1361-1368.

Bieganska K., Figiel I., Gierej D., Kaczmarek L. and Klejman A. (2012) Silencing of ICERs (Inducible cAMP Early Repressors) results in partial protection of neurons from programmed cell death. *Neurobiol. Dis.* **45,** 701-710.

Blanks J. C. and Johnson L. V. (1984) Specific binding of peanut lectin to a class of retinal photoreceptor cells. A species comparison. *Invest Ophthalmol. Vis. Sci.* **25,** 546-557.

Bloomfield S. A. and Volgyi B. (2009) The diverse functional roles and regulation of neuronal gap junctions in the retina. *Nat. Rev. Neurosci.* **10,** 495-506.

Boldt K., Mans D. A., Won J., van R. J., Vogt A., Kinkl N., Letteboer S. J., Hicks W. L., Hurd R. E., Naggert J. K., Texier Y., den Hollander A. I., Koenekoop R. K., Bennett J., Cremers F. P., Gloeckner C. J., Nishina P. M., Roepman R. and Ueffing M. (2011) Disruption of intraflagellar protein transport in photoreceptor cilia causes Leber congenital amaurosis in humans and mice. *J. Clin. Invest* **121,** 2169-2180.

Borlikova G. and Endo S. (2009) Inducible cAMP early repressor (ICER) and brain functions. *Mol. Neurobiol.* **40,** 73-86.

Bowes C., Li T., Danciger M., Baxter L. C., Applebury M. L. and Farber D. B. (1990) Retinal degeneration in the rd mouse is caused by a defect in the beta subunit of rod cGMP-phosphodiesterase. *Nature* **347,** 677-680.

Bowes C., Li T., Frankel W. N., Danciger M., Coffin J. M., Applebury M. L. and Farber D. B. (1993) Localization of a retroviral element within the rd gene coding for the beta subunit of cGMP phosphodiesterase. *Proc. Natl. Acad. Sci. U. S. A* **90,** 2955-2959.

Brückner R. (1951) [Slit-lamp microscopy and ophthalmoscopy in rat and mouse]. *Doc. Ophthalmol.* **5-6,** 452-554.

Bush R. A., Kononen L., Machida S. and Sieving P. A. (2000) The effect of calcium channel blocker diltiazem on photoreceptor degeneration in the rhodopsin Pro213His rat. *Invest Ophthalmol. Vis. Sci.* **41,** 2697-2701.

Caffé A. R., Ahuja P., Holmqvist B., Azadi S., Forsell J., Holmqvist I., Soderpalm A. K. and van Veen. T. (2001a) Mouse retina explants after long-term culture in serum free medium. *J. Chem. Neuroanat.* **22,** 263-273.

Caffé A. R., Soderpalm A. K., Holmqvist I. and van Veen. T. (2001b) A combination of CNTF and BDNF rescues rd photoreceptors but changes rod differentiation in the presence of RPE in retinal explants. *Invest Ophthalmol. Vis. Sci.* **42,** 275-282.

Canals S., Casarejos M. J., de B. S., Rodriguez-Martin E. and Mena M. A. (2003) Nitric oxide triggers the toxicity due to glutathione depletion in midbrain cultures through 12-lipoxygenase. *J. Biol. Chem.* **278,** 21542-21549.

Canzoniero L. M., Adornetto A., Secondo A., Magi S., Dell'aversano C., Scorziello A., Amoroso S. and Di R. G. (2006) Involvement of the nitric oxide/protein kinase G pathway in polychlorinated biphenyl-induced cell death in SH-SY 5Y neuroblastoma cells. *J. Neurosci. Res.* **84,** 692-697.

Carmody R. J., McGowan A. J. and Cotter T. G. (1999) Reactive oxygen species as mediators of photoreceptor apoptosis in vitro. *Exp. Cell Res.* **248,** 520-530.

Carter-Dawson L. D. and LaVail M. M. (1979) Rods and cones in the mouse retina. I. Structural analysis using light and electron microscopy. *J. Comp Neurol.* **188,** 245-262.

Carter-Dawson L. D., LaVail M. M. and Sidman R. L. (1978) Differential effect of the rd mutation on rods and cones in the mouse retina. *Invest Ophthalmol. Vis. Sci.* **17,** 489-498.

Chakravarthy U., Wong T. Y., Fletcher A., Piault E., Evans C., Zlateva G., Buggage R., Pleil A. and Mitchell P. (2010) Clinical risk factors for age-related macular degeneration: a systematic review and meta-analysis. *BMC. Ophthalmol.* **10,** 31.

Chang B., Grau T., Dangel S., Hurd R., Jurklies B., Sener E. C., Andreasson S., Dollfus H., Baumann B., Bolz S., Artemyev N., Kohl S., Heckenlively J. and Wissinger B. (2009) A homologous genetic basis of the murine cpfl1 mutant and human achromatopsia linked to mutations in the PDE6C gene. *Proc. Natl. Acad. Sci. U. S. A* **106,** 19581-19586.

Chang B., Hawes N. L., Hurd R. E., Davisson M. T., Nusinowitz S. and Heckenlively J. R. (2002) Retinal degeneration mutants in the mouse. *Vision Res.* **42,** 517-525.

Chang J. H., Vuppalanchi D., van N. E., Trepel J. B., Schanen N. C. and Twiss J. L. (2006) PC12 cells regulate inducible cyclic AMP (cAMP) element repressor expression to differentially control cAMP

response element-dependent transcription in response to nerve growth factor and cAMP. *J. Neurochem.* **99,** 1517-1530.

Cideciyan A. V., Aleman T. S., Boye S. L., Schwartz S. B., Kaushal S., Roman A. J., Pang J. J., Sumaroka A., Windsor E. A., Wilson J. M., Flotte T. R., Fishman G. A., Heon E., Stone E. M., Byrne B. J., Jacobson S. G. and Hauswirth W. W. (2008) Human gene therapy for RPE65 isomerase deficiency activates the retinoid cycle of vision but with slow rod kinetics. *Proc. Natl. Acad. Sci. U. S. A* **105,** 15112-15117.

Deguchi A., Thompson W. J. and Weinstein I. B. (2004) Activation of protein kinase G is sufficient to induce apoptosis and inhibit cell migration in colon cancer cells. *Cancer Res.* **64,** 3966-3973.

den Hollander A. I., Roepman R., Koenekoop R. K. and Cremers F. P. (2008) Leber congenital amaurosis: genes, proteins and disease mechanisms. *Prog. Retin. Eye Res.* **27,** 391-419.

Dinet V., Ansari N., Torres-Farfan C. and Korf H. W. (2007) Clock gene expression in the retina of melatonin-proficient (C3H) and melatonin-deficient (C57BL) mice. *J. Pineal Res.* **42,** 83-91.

Ding B., Abe J., Wei H., Xu H., Che W., Aizawa T., Liu W., Molina C. A., Sadoshima J., Blaxall B. C., Berk B. C. and Yan C. (2005) A positive feedback loop of phosphodiesterase 3 (PDE3) and inducible cAMP early repressor (ICER) leads to cardiomyocyte apoptosis. *Proc. Natl. Acad. Sci. U. S. A.* **102,** 14771-14776.

Doonan F., Donovan M. and Cotter T. G. (2005) Activation of multiple pathways during photoreceptor apoptosis in the rd mouse. *Invest Ophthalmol. Vis. Sci.* **46,** 3530-3538.

Dryja T. P., McGee T. L., Hahn L. B., Cowley G. S., Olsson J. E., Reichel E., Sandberg M. A. and Berson E. L. (1990a) Mutations within the rhodopsin gene in patients with autosomal dominant retinitis pigmentosa. *N. Engl. J. Med.* **323,** 1302-1307.

Dryja T. P., McGee T. L., Reichel E., Hahn L. B., Cowley G. S., Yandell D. W., Sandberg M. A. and Berson E. L. (1990b) A point mutation of the rhodopsin gene in one form of retinitis pigmentosa. *Nature* **343,** 364-366.

Dunn T. B. (1954) The importance of differences in morphology in inbred strains. *J. Natl. Cancer Inst.* **15,** 573-591.

Dworkin S., Malaterre J., Hollande F., Darcy P. K., Ramsay R. G. and Mantamadiotis T. (2009) cAMP response element binding protein is required for mouse neural progenitor cell survival and expansion. *Stem Cells* **27,** 1347-1357.

Fain G. L., Matthews H. R., Cornwall M. C. and Koutalos Y. (2001) Adaptation in vertebrate photoreceptors. *Physiol Rev.* **81,** 117-151.

Farber D. B., Brown B. M. and Lllley R. N. (1979) Cyclic nucleotide dependent protein kinase and the phosphorylation of endogenous proteins of retinal rod outer segments. *Biochemistry* **18,** 370-378.

Farber D. B. and Lolley R. N. (1974) Cyclic guanosine monophosphate: elevation in degenerating photoreceptor cells of the C3H mouse retina. *Science* **186,** 449-451.

Farber D. B. and Lolley R. N. (1976) Enzymic basis for cyclic GMP accumulation in degenerative photoreceptor cells of mouse retina. *J. Cyclic. Nucleotide. Res.* **2,** 139-148.

Feigenspan A., Janssen-Bienhold U., Hormuzdi S., Monyer H., Degen J., Sohl G., Willecke K., Ammermuller J. and Weiler R. (2004) Expression of connexin36 in cone pedicles and OFF-cone bipolar cells of the mouse retina. *J. Neurosci.* **24,** 3325-3334.

Feil S., Zimmermann P., Knorn A., Brummer S., Schlossmann J., Hofmann F. and Feil R. (2005) Distribution of cGMP-dependent protein kinase type I and its isoforms in the mouse brain and retina. *Neuroscience* **135,** 863-868.

Fitzgerald J. B., Malykhina A. P., Al-Ubaidi M. R. and Ding X. Q. (2008) Functional expression of cone cyclic nucleotide-gated channel in cone photoreceptor-derived 661W cells. *Adv. Exp. Med. Biol.* **613,** 327-334.

Folco E. J. and Koren G. (1997) Degradation of the inducible cAMP early repressor (ICER) by the ubiquitin-proteasome pathway. *Biochem. J.* **328 (Pt 1),** 37-43.

Fox D. A., Poblenz A. T. and He L. (1999) Calcium overload triggers rod photoreceptor apoptotic cell death in chemical-induced and inherited retinal degenerations. *Ann. N. Y. Acad. Sci.* **893,** 282-285.

Franco R. and Cidlowski J. A. (2009) Apoptosis and glutathione: beyond an antioxidant. *Cell Death. Differ.* **16,** 1303-1314.

Frasson M., Sahel J. A., Fabre M., Simonutti M., Dreyfus H. and Picaud S. (1999) Retinitis pigmentosa: rod photoreceptor rescue by a calcium-channel blocker in the rd mouse. *Nat. Med.* **5,** 1183-1187.

Fu Y. and Yau K. W. (2007) Phototransduction in mouse rods and cones. *Pflugers Arch.* **454,** 805-819.

Gamm D. M., Barthel L. K., Raymond P. A. and Uhler M. D. (2000) Localization of cGMP-dependent protein kinase isoforms in mouse eye. *Invest Ophthalmol. Vis. Sci.* **41,** 2766-2773.

Gorbatyuk M. S., Knox T., LaVail M. M., Gorbatyuk O. S., Noorwez S. M., Hauswirth W. W., Lin J. H., Muzyczka N. and Lewin A. S. (2010) Restoration of visual function in P23H rhodopsin transgenic rats by gene delivery of BiP/Grp78. *Proc. Natl. Acad. Sci. U. S. A* **107,** 5961-5966.

Griciuc A., Aron L., Piccoli G. and Ueffing M. (2010) Clearance of Rhodopsin(P23H) aggregates requires the ERAD effector VCP. *Biochim. Biophys. Acta* **1803,** 424-434.

Grynkiewicz G., Poenie M. and Tsien R. Y. (1985) A new generation of Ca2+ indicators with greatly improved fluorescence properties. *J. Biol. Chem.* **260,** 3440-3450.

Gutscher M., Pauleau A. L., Marty L., Brach T., Wabnitz G. H., Samstag Y., Meyer A. J. and Dick T. P. (2008) Real-time imaging of the intracellular glutathione redox potential. *Nat. Methods* **5,** 553-559.

Hackam A. S. (2008) Regulation of neurotrophin expression and activity in the retina. *Adv. Exp. Med. Biol.* **613,** 343-349.

Hackam A. S., Strom R., Liu D., Qian J., Wang C., Otteson D., Gunatilaka T., Farkas R. H., Chowers I., Kageyama M., Leveillard T., Sahel J. A., Campochiaro P. A., Parmigiani G. and Zack D. J. (2004) Identification of gene expression changes associated with the progression of retinal degeneration in the rd1 mouse. *Invest Ophthalmol. Vis. Sci.* **45,** 2929-2942.

Hageman G. S., Gehrs K., Johnson L. V. and Anderson D. (2008) Age-Related Macular Degeneration (AMD). *In: Kolb H, Fernandez E, Nelson R, editors. Webvision: The Organization of the Retina and Visual System [Internet]. Salt Lake City (UT): University of Utah Health Sciences Center;* http://webvision.med.utah.edu/. (information retrieved February 27, 2012)

Hamel C. P. (2007) Cone rod dystrophies. *Orphanet. J. Rare. Dis.* **2,** 7.

Hamilton N. (2009) Quantification and its Applications in Fluorescent Microscopy Imaging. *Traffic.* **10,** 951-961.

Han W., Takamatsu Y., Kasai S., Endo S., Shirao T., Kojima N. and Ikeda K. (2011) Reduced locomotor sensitization induced by methamphetamine and altered gene expression in ICER overexpressing mice. *Nihon Shinkei Seishin Yakurigaku Zasshi* **31,** 79-80.

Harada T., Harada C., Kohsaka S., Wada E., Yoshida K., Ohno S., Mamada H., Tanaka K., Parada L. F. and Wada K. (2002) Microglia-Muller glia cell interactions control neurotrophic factor production during light-induced retinal degeneration. *J. Neurosci.* **22,** 9228-9236.

Hartong D. T., Berson E. L. and Dryja T. P. (2006) Retinitis pigmentosa. *Lancet.* **368,** 1795-1809.

Haverkamp S. and Wässle H. (2000) Immunocytochemical analysis of the mouse retina. *J. Comp Neurol.* **424,** 1-23.

Haverkamp S., Wässle H., Duebel J., Kuner T., Augustine G. J., Feng G. and Euler T. (2005) The primordial, blue-cone color system of the mouse retina. *J. Neurosci.* **25,** 5438-5445.

Hou Y., Wong E., Martin J., Schoenlein P. V., Dostmann W. R. and Browning D. D. (2006) A role for cyclic-GMP dependent protein kinase in anoikis. *Cell Signal.* **18,** 882-888.

Hu Y., Lund I. V., Gravielle M. C., Farb D. H., Brooks-Kayal A. R. and Russek S. J. (2008) Surface expression of GABAA receptors is transcriptionally controlled by the interplay of cAMP-response element-binding protein and its binding partner inducible cAMP early repressor. *J. Biol. Chem.* **283,** 9328-9340.

Insinna C. and Besharse J. C. (2008) Intraflagellar transport and the sensory outer segment of vertebrate photoreceptors. *Dev. Dyn.* **237,** 1982-1992.

Jaworski J., Mioduszewska B., Sanchez-Capelo A., Figiel I., Habas A., Gozdz A., Proszynski T., Hetman M., Mallet J. and Kaczmarek L. (2003) Inducible cAMP early repressor, an endogenous antagonist of cAMP responsive element-binding protein, evokes neuronal apoptosis in vitro. *J. Neurosci.* **23,** 4519-4526.

Kanan Y., Moiseyev G., Agarwal N., Ma J. X. and Al-Ubaidi M. R. (2007) Light induces programmed cell death by activating multiple independent proteases in a cone photoreceptor cell line. *Invest Ophthalmol. Vis. Sci.* **48,** 40-51.

Kandel E. R., Schwartz J.H. and Jessel T.M. (2000) Principles of Neural Science, McGraw-Hill Medical. New York, ISBN 0-8385-7701-6

Karli P. (1952) [Retinae without visual cells; morphological, physiological and physiopathological research in rodents]. *Arch. Anat. Histol. Embryol.* **35,** 1-76.

Karolczak M., Korf H. W. and Stehle J. H. (2005) The rhythm and blues of gene expression in the rodent pineal gland. *Endocrine.* **27,** 89-100.

Kaur J., Mencl S., Sahaboglu A., Farinelli P., van Veen. T., Zrenner E., Ekstrom P., Paquet-Durand F. and Arango-Gonzalez B. (2011) Calpain and PARP activation during photoreceptor cell death in P23H and S334ter rhodopsin mutant rats. *PLoS. ONE.* **6,** e22181.

Keeler C. E. (1924) The Inheritance of a Retinal Abnormality in White Mice. *Proc. Natl. Acad. Sci. U. S. A.* **10,** 329-333.

Kell C. A., Dehghani F., Wicht H., Molina C. A., Korf H. W. and Stehle J. H. (2004) Distribution of transcription factor inducible cyclicAMP early repressor (ICER) in rodent brain and pituitary. *J. Comp Neurol.* **478,** 379-394.

Kim H. S. and Park C. K. (2005) Retinal ganglion cell death is delayed by activation of retinal intrinsic cell survival program. *Brain Res.* **1057,** 17-28.

Kimura K., Wakamatsu A., Suzuki Y., Ota T., Nishikawa T., Yamashita R., Yamamoto J., Sekine M., Tsuritani K., Wakaguri H., Ishii S., Sugiyama T., Saito K., Isono Y., Irie R., Kushida N., Yoneyama T., Otsuka R., Kanda K., Yokoi T., Kondo H., Wagatsuma M., Murakawa K., Ishida S., Ishibashi T., Takahashi-Fujii A., Tanase T., Nagai K., Kikuchi H., Nakai K., Isogai T. and Sugano S. (2006) Diversification of transcriptional modulation: large-scale identification and characterization of putative alternative promoters of human genes. *Genome Res.* **16,** 55-65.

Klein R., Peto T., Bird A. and Vannewkirk M. R. (2004) The epidemiology of age-related macular degeneration. *Am. J. Ophthalmol.* **137,** 486-495.

Klejman A. and Kaczmarek L. (2006) Inducible cAMP early repressor (ICER) isoforms and neuronal apoptosis in cortical in vitro culture. *Acta Neurobiol. Exp. (Wars.)* **66,** 267-272.

Koeppen K., Reuter P., Kohl S., Baumann B., Ladewig T. and Wissinger B. (2008) Functional analysis of human CNGA3 mutations associated with colour blindness suggests impaired surface expression of channel mutants A3(R427C) and A3(R563C). *Eur. J. Neurosci.* **27,** 2391-2401.

Kojima N., Borlikova G., Sakamoto T., Yamada K., Ikeda T., Itohara S., Niki H. and Endo S. (2008) Inducible cAMP early repressor acts as a negative regulator for kindling epileptogenesis and long-term fear memory. *J. Neurosci.* **28,** 6459-6472.

Komeima K., Rogers B. S. and Campochiaro P. A. (2007) Antioxidants slow photoreceptor cell death in mouse models of retinitis pigmentosa. *J. Cell Physiol* **213,** 809-815.

Krishnakumar R. and Kraus W. L. (2010) The PARP side of the nucleus: molecular actions, physiological outcomes, and clinical targets. *Mol. Cell* **39,** 8-24.

Krishnamoorthy R. R., Crawford M. J., Chaturvedi M. M., Jain S. K., Aggarwal B. B., Al-Ubaidi M. R. and Agarwal N. (1999) Photo-oxidative stress down-modulates the activity of nuclear factor-kappaB via involvement of caspase-1, leading to apoptosis of photoreceptor cells. *J. Biol. Chem.* **274,** 3734-3743.

Kroemer G., Galluzzi L., Vandenabeele P., Abrams J., Alnemri E. S., Baehrecke E. H., Blagosklonny M. V., El-Deiry W. S., Golstein P., Green D. R., Hengartner M., Knight R. A., Kumar S., Lipton S. A., Malorni W., Nunez G., Peter M. E., Tschopp J., Yuan J., Piacentini M., Zhivotovsky B. and Melino G. (2009) Classification of cell death: recommendations of the Nomenclature Committee on Cell Death 2009. *Cell Death. Differ.* **16,** 3-11.

LaVail M. M., Yasumura D., Matthes M.T., Lau-Villacorta C., Unoki K., Sung C. H. and Steinberg R. H. (2009) Protection of mouse photoreceptors by survival factors in retinal degenerations. *Invest. Ophthalmol. Vis. Sci*. **309,** 592-602.

Lee B., Cao R., Choi Y. S., Cho H. Y., Rhee A. D., Hah C. K., Hoyt K. R. and Obrietan K. (2009) The CREB/CRE transcriptional pathway: protection against oxidative stress-mediated neuronal cell death. *J. Neurochem.* **108,** 1251-1265.

Lee E. J., Ji Y., Zhu C. L. and Grzywacz N. M. (2011) Role of Muller cells in cone mosaic rearrangement in a rat model of retinitis pigmentosa. *Glia* **59,** 1107-1117.

Lee E. S. and Flannery J. G. (2007) Transport of truncated rhodopsin and its effects on rod function and degeneration. *Invest Ophthalmol. Vis. Sci.* **48,** 2868-2876.

Lem J., Flannery J. G., Li T., Applebury M. L., Farber D. B. and Simon M. I. (1992) Retinal degeneration is rescued in transgenic rd mice by expression of the cGMP phosphodiesterase beta subunit. *Proc. Natl. Acad. Sci. U. S. A* **89,** 4422-4426.

Levi-Montalcini R., Meyer H. and Hamburger V. (1954) In vitro experiments on the effects of mouse sarcomas 180 and 37 on the spinal and symphathetic ganglia of the chick embryo. *Cancer Res.* **14,** 49-57.

Li Y., Tao W., Luo L., Huang D., Kauper K., Stabila P., LaVail M. M., Laties A. M. and Wen R. (2010) CNTF induces regeneration of cone outer segments in a rat model of retinal degeneration. *PLoS. ONE.* **5,** e9495.

Liu C. M., Li Y., Peng M., Laties A. M. and Wen R. (1999) Activation of Caspase-3 in the Retina of Transgenic Rats with the Rhodopsin Mutation S334ter during Photoreceptor Degeneration. *J. Neurosci.* **19,** 4778-4785.

Liu M. M., Tuo J. and Chan C. C. (2011) Republished review: Gene therapy for ocular diseases. *Postgrad. Med. J.* **87,** 487-495.

Liu X., Garriga P. and Khorana H. G. (1996) Structure and function in rhodopsin: correct folding and misfolding in two point mutants in the intradiscal domain of rhodopsin identified in retinitis pigmentosa. *Proc. Natl. Acad. Sci. U. S. A* **93,** 4554-4559.

Liu Y., Kalintchenko N., Sassone-Corsi P. and Aguilera G. (2006) Inhibition of corticotrophin-releasing hormone transcription by inducible cAMP-early repressor in the hypothalamic cell line, 4B. *J. Neuroendocrinol.* **18,** 42-49.

Lolley R. N., Farber D. B., Rayborn M. E. and Hollyfield J. G. (1977) Cyclic GMP accumulation causes degeneration of photoreceptor cells: simulation of an inherited disease. *Science* **196,** 664-666.

Lonze B. E. and Ginty D. D. (2002) Function and regulation of CREB family transcription factors in the nervous system
5. *Neuron* **35,** 605-623.

Lund I. V., Hu Y., Raol Y. H., Benham R. S., Faris R., Russek S. J. and Brooks-Kayal A. R. (2008) BDNF selectively regulates GABAA receptor transcription by activation of the JAK/STAT pathway. *Sci. Signal.* **1,** ra9.

Luo D. G., Xue T. and Yau K. W. (2008) How vision begins: an odyssey. *Proc. Natl. Acad. Sci. U. S. A* **105,** 9855-9862.

Machida S., Kondo M., Jamison J. A., Khan N. W., Kononen L. T., Sugawara T., Bush R. A. and Sieving P. A. (2000) P23H rhodopsin transgenic rat: correlation of retinal function with histopathology. *Invest Ophthalmol. Vis. Sci.* **41,** 3200-3209.

Maguire A. M., Simonelli F., Pierce E. A., Pugh E. N., Jr., Mingozzi F., Bennicelli J., Banfi S., Marshall K. A., Testa F., Surace E. M., Rossi S., Lyubarsky A., Arruda V. R., Konkle B., Stone E., Sun J., Jacobs J., Dell'Osso L., Hertle R., Ma J. X., Redmond T. M., Zhu X., Hauck B., Zelenaia O., Shindler K. S., Maguire M. G., Wright J. F., Volpe N. J., McDonnell J. W., Auricchio A., High K. A. and Bennett J. (2008) Safety and efficacy of gene transfer for Leber's congenital amaurosis. *N. Engl. J. Med.* **358,** 2240-2248.

Mandal M. N., Patlolla J. M., Zheng L., Agbaga M. P., Tran J. T., Wicker L., Kasus-Jacobi A., Elliott M. H., Rao C. V. and Anderson R. E. (2009) Curcumin protects retinal cells from light-and oxidant stress-induced cell death. *Free Radic. Biol. Med.* **46,** 672-679.

Mantamadiotis T., Lemberger T., Bleckmann S. C., Kern H., Kretz O., Martin V. A., Tronche F., Kellendonk C., Gau D., Kapfhammer J., Otto C., Schmid W. and Schutz G. (2002) Disruption of CREB function in brain leads to neurodegeneration. *Nat. Genet.* **31,** 47-54.

Mayr B. and Montminy M. (2001) Transcriptional regulation by the phosphorylation-dependent factor CREB. *Nat. Rev. Mol. Cell Biol.* **2,** 599-609.

Mayr B. M., Canettieri G. and Montminy M. R. (2001) Distinct effects of cAMP and mitogenic signals on CREB-binding protein recruitment impart specificity to target gene activation via CREB. *Proc. Natl. Acad. Sci. U. S. A* **98,** 10936-10941.

McLaughlin M. E., Sandberg M. A., Berson E. L. and Dryja T. P. (1993) Recessive mutations in the gene encoding the beta-subunit of rod phosphodiesterase in patients with retinitis pigmentosa. *Nat. Genet.* **4,** 130-134.

Michaelides M., Hunt D. M. and Moore A. T. (2004) The cone dysfunction syndromes. *Br. J. Ophthalmol.* **88,** 291-297.

Mioduszewska B., Jaworski J. and Kaczmarek L. (2003) Inducible cAMP early repressor (ICER) in the nervous system--a transcriptional regulator of neuronal plasticity and programmed cell death. *J. Neurochem.* **87,** 1313-1320.

Mioduszewska B., Jaworski J., Szklarczyk A. W., Klejman A. and Kaczmarek L. (2008) Inducible cAMP early repressor (ICER)-evoked delayed neuronal death in the organotypic hippocampal culture. *J. Neurosci. Res.* **86,** 61-70.

Miranda M., Arnal E., Ahuja S., Alvarez-Nölting R., Lopez-Pedrajas R., Ekstrom P., Bosch-Morell F., van Veen. T. and Romero F. J. (2010) Antioxidants rescue photoreceptors in rd1 mice: Relationship with thiol metabolism. *Free Radic. Biol. Med.* **48,** 216-222.

Mizukoshi S., Nakazawa M., Sato K., Ozaki T., Metoki T. and Ishiguro S. (2010) Activation of mitochondrial calpain and release of apoptosis-inducing factor from mitochondria in RCS rat retinal degeneration. *Exp. Eye Res.* **91,** 353-361.

Molina C. A., Foulkes N. S., Lalli E. and Sassone-Corsi P. (1993b) Inducibility and negative autoregulation of CREM: an alternative promoter directs the expression of ICER, an early response repressor. *Cell* **75,** 875-886.

Monaco L. and Sassone-Corsi P. (1997) Cross-talk in signal transduction: Ras-dependent induction of cAMP-responsive transcriptional repressor ICER by nerve growth factor. *Oncogene* **15,** 2493-2500.

Nakazawa M. (2011) Effects of calcium ion, calpains, and calcium channel blockers on retinitis pigmentosa. *J. Ophthalmol.* **2011,** 292040.

Nihira M., Anderson K., Gorin F. A. and Burns M. S. (1995) Primate rod and cone photoreceptors may differ in glucose accessibility. *Invest Ophthalmol. Vis. Sci.* **36,** 1259-1270.

O'Driscoll C., Wallace D. and Cotter T. G. (2007) bFGF promotes photoreceptor cell survival in vitro by PKA-mediated inactivation of glycogen synthase kinase 3beta and CREB-dependent Bcl-2 up-regulation. *J. Neurochem.* **103,** 860-870.

Ohtsubo H., Ichiki T., Miyazaki R., Inanaga K., Imayama I., Hashiguchi Y., Sadoshima J. and Sunagawa K. (2007) Inducible cAMP early repressor inhibits growth of vascular smooth muscle cell. *Arterioscler. Thromb. Vasc. Biol.* **27,** 1549-1555.

Oka T., Tamada Y., Nakajima E., Shearer T. R. and Azuma M. (2006) Presence of calpain-induced proteolysis in retinal degeneration and dysfunction in a rat model of acute ocular hypertension. *J. Neurosci. Res.* **83,** 1342-1351.

Okoye G., Zimmer J., Sung J., Gehlbach P., Deering T., Nambu H., Hackett S., Melia M., Esumi N., Zack D. J. and Campochiaro P. A. (2003) Increased expression of brain-derived neurotrophic factor preserves retinal function and slows cell death from rhodopsin mutation or oxidative damage. *J. Neurosci.* **23,** 4164-4172.

Olshevskaya E. V., Ermilov A. N. and Dizhoor A. M. (2002) Factors that affect regulation of cGMP synthesis in vertebrate photoreceptors and their genetic link to human retinal degeneration. *Mol. Cell Biochem.* **230,** 139-147.

Paquet-Durand F., Azadi S., Hauck S. M., Ueffing M., van Veen T. and Ekstrom P. (2006) Calpain is activated in degenerating photoreceptors in the rd1 mouse. *J. Neurochem.* **96,** 802-814.

Paquet-Durand F., Beck S., Michalakis S., Goldmann T., Huber G., Muhlfriedel R., Trifunovic D., Fischer M. D., Fahl E., Duetsch G., Becirovic E., Wolfrum U., van Veen. T., Biel M., Tanimoto N. and Seeliger M. W. (2011) A key role for cyclic nucleotide gated (CNG) channels in cGMP-related retinitis pigmentosa. *Hum. Mol. Genet.* **20,** 941-947.

Paquet-Durand F., Hauck S. M., van Veen T., Ueffing M. and Ekstrom P. (2009) PKG activity causes photoreceptor cell death in two retinitis pigmentosa models. *J. Neurochem.* **108,** 796-810.

Paquet-Durand F., Johnson L. and Ekstrom P. (2007a) Calpain activity in retinal degeneration. *J. Neurosci. Res.* **85,** 693-702.

Paquet-Durand F., Sanges D., McCall J., Silva J., van Veen T., Marigo V. and Ekstrom P. (2010) Photoreceptor rescue and toxicity induced by different calpain inhibitors. *J. Neurochem.* **115,** 930-940.

Paquet-Durand F., Silva J., Talukdar T., Johnson L. E., Azadi S., van Veen T., Ueffing M., Hauck S. M. and Ekstrom P. A. (2007b) Excessive activation of poly(ADP-ribose) polymerase contributes to inherited photoreceptor degeneration in the retinal degeneration 1 mouse. *J. Neurosci.* **27,** 10311-10319.

Pasantes-Morales H., Quiroz H. and Quesada O. (2002) Treatment with taurine, diltiazem, and vitamin E retards the progressive visual field reduction in retinitis pigmentosa: a 3-year follow-up study. *Metab Brain Dis.* **17,** 183-197.

Pawlyk B. S., Li T., Scimeca M. S., Sandberg M. A. and Berson E. L. (2002) Absence of photoreceptor rescue with D-cis-diltiazem in the rd mouse. *Invest Ophthalmol. Vis. Sci.* **43,** 1912-1915.

Pearce-Kelling S. E., Aleman T. S., Nickle A., Laties A. M., Aguirre G. D., Jacobson S. G. and Acland G. M. (2001) Calcium channel blocker D-cis-diltiazem does not slow retinal degeneration in the PDE6B mutant rcd1 canine model of retinitis pigmentosa. *Mol. Vis.* **7:42-7.,** 42-47.

Peichl L. (2005) Diversity of mammalian photoreceptor properties: adaptations to habitat and lifestyle? *Anat. Rec. A Discov. Mol. Cell Evol. Biol.* **287,** 1001-1012.

Pfeiffer B., Buse E., Meyermann R. and Hamprecht B. (1995) Immunocytochemical localization of glycogen phosphorylase in primary sensory ganglia of the peripheral nervous system of the rat. *Histochem. Cell Biol.* **103,** 69-74.

Pfeiffer-Guglielmi B., Francke M., Reichenbach A., Fleckenstein B., Jung G. and Hamprecht B. (2005) Glycogen phosphorylase isozyme pattern in mammalian retinal Muller (glial) cells and in astrocytes of retina and optic nerve. *Glia* **49,** 84-95.

Pittler S. J. and Baehr W. (1991) Identification of a nonsense mutation in the rod photoreceptor cGMP phosphodiesterase beta-subunit gene of the rd mouse. *Proc. Natl. Acad. Sci. U. S. A* **88,** 8322-8326.

Pittler S. J., Keeler C. E., Sidman R. L. and Baehr W. (1993) PCR analysis of DNA from 70-year-old sections of rodless retina demonstrates identity with the mouse rd defect. *Proc. Natl. Acad. Sci. U. S. A* **90,** 9616-9619.

Read D. S., McCall M. A. and Gregg R. G. (2002) Absence of voltage-dependent calcium channels delays photoreceptor degeneration in rd mice. *Exp. Eye Res.* **75,** 415-420.

Rich K. A., Zhan Y. and Blanks J. C. (1997) Migration and Synaptogenesis of Cone Photoreceptors in the Developing Mouse Retina. *J. Comp. Neurol.* **388,** 47-63.

Roque R. S., Rosales A. A., Jingjing L., Agarwal N. and Al-Ubaidi M. R. (1999) Retina-derived microglial cells induce photoreceptor cell death in vitro. *Brain Res.* **836,** 110-119.

Sahaboglu A., Tanimoto N., Kaur J., Sancho-Pelluz J., Huber G., Fahl E., Arango-Gonzalez B., Zrenner E., Ekstrom P., Lowenheim H., Seeliger M. and Paquet-Durand F. (2010) PARP1 gene knock-out increases resistance to retinal degeneration without affecting retinal function. *PLoS. ONE.* **5,** e15495.

Sakamoto K., Karelina K. and Obrietan K. (2011) CREB: a multifaceted regulator of neuronal plasticity and protection. *J. Neurochem.* **116,** 1-9.

Sancho-Pelluz J., Arango-Gonzalez B., Kustermann S., Romero F. J., van Veen T., Zrenner E., Ekstrom P. and Paquet-Durand F. (2008) Photoreceptor cell death mechanisms in inherited retinal degeneration. *Mol. Neurobiol.* **38,** 253-269.

Sanes J. R. and Zipursky S. L. (2010) Design principles of insect and vertebrate visual systems. *Neuron* **66,** 15-36.

Sanges D., Comitato A., Tammaro R. and Marigo V. (2006) Apoptosis in retinal degeneration involves cross-talk between apoptosis-inducing factor (AIF) and caspase-12 and is blocked by calpain inhibitors. *Proc. Natl. Acad. Sci. U. S. A.* **103,** 17366-17371.

Sanyal S. and Bal A. K. (1973) Comparative light and electron microscopic study of retinal histogenesis in normal and rd mutant mice. *Z. Anat. Entwicklungsgesch.* **142,** 219-238.

Sanz M. M., Johnson L. E., Ahuja S., Ekstrom P. A., Romero J. and van Veen. T. (2007) Significant photoreceptor rescue by treatment with a combination of antioxidants in an animal model for retinal degeneration. *Neuroscience* **145,** 1120-1129.

Sedmak T., Sehn E. and Wolfrum U. (2009) Immunoelectron microscopy of vesicle transport to the primary cilium of photoreceptor cells. *Methods Cell Biol.* **94,** 259-272.

Sharma A. K. and Rohrer B. (2007) Sustained elevation of intracellular cGMP causes oxidative stress triggering calpain-mediated apoptosis in photoreceptor degeneration. *Curr. Eye Res.* **32,** 259-269.

Sheedlo H. J., Bartosh T. J., Wang Z., Srinivasan B., Brun-Zinkernagel A. M. and Roque R. S. (2007) RPE-derived factors modulate photoreceptor differentiation: a possible role in the retinal stem cell niche. *In Vitro Cell Dev. Biol. Anim* **43,** 361-370.

Sidman R. L. and Green M. C. (1965) Retinal Degeneration in the mouse: Location of the *rd* Lokus in Linkage Group XVII. *J. Hered.* **56,** 23-29.

Sieving P. A., Caruso R. C., Tao W., Coleman H. R., Thompson D. J., Fullmer K. R. and Bush R. A. (2006) Ciliary neurotrophic factor (CNTF) for human retinal degeneration: phase I trial of CNTF delivered by encapsulated cell intraocular implants. *Proc. Natl. Acad. Sci. U. S. A* **103,** 3896-3901.

Simonelli F., Maguire A. M., Testa F., Pierce E. A., Mingozzi F., Bennicelli J. L., Rossi S., Marshall K., Banfi S., Surace E. M., Sun J., Redmond T. M., Zhu X., Shindler K. S., Ying G. S., Ziviello C., Acerra C., Wright J. F., McDonnell J. W., High K. A., Bennett J. and Auricchio A. (2010) Gene therapy for Leber's congenital amaurosis is safe and effective through 1.5 years after vector administration. *Mol. Ther.* **18,** 643-650.

Singh M. S. and MacLaren R. E. (2011) Stem cells as a therapeutic tool for the blind: biology and future prospects. *Proc. Biol. Sci.* **278,** 3009-3016.

Socodato R., Brito R., Calaza K. C. and Paes-de-Carvalho R. (2011) Developmental regulation of neuronal survival by adenosine in the in vitro and in vivo avian retina depends on a shift of signaling pathways leading to CREB phosphorylation or dephosphorylation. *J. Neurochem.* **116,** 227-239.

Standish M. (1887) A Case of Retinitis Pigmentosa treated Electrically. *Trans. Am. Ophthalmol. Soc.* **4,** 553-558.

Stehle J. H., Foulkes N. S., Molina C. A., Simonneaux V., Pevet P. and Sassone-Corsi P. (1993) Adrenergic signals direct rhythmic expression of transcriptional repressor CREM in the pineal gland. *Nature* **365,** 314-320.

Stone E. M. (2007) Leber congenital amaurosis - a model for efficient genetic testing of heterogeneous disorders: LXIV Edward Jackson Memorial Lecture. *Am. J. Ophthalmol.* **144,** 791-811.

Sung C. H. and Chuang J. Z. (2010) The cell biology of vision. *J. Cell Biol.* **190,** 953-963.

Sung C. H., Schneider B. G., Agarwal N., Papermaster D. S. and Nathans J. (1991) Functional heterogeneity of mutant rhodopsins responsible for autosomal dominant retinitis pigmentosa. *Proc. Natl. Acad. Sci. U. S. A* **88,** 8840-8844.

Takano Y., Ohguro H., Dezawa M., Ishikawa H., Yamazaki H., Ohguro I., Mamiya K., Metoki T., Ishikawa F. and Nakazawa M. (2004) Study of drug effects of calcium channel blockers on retinal degeneration of rd mouse. *Biochem. Biophys. Res. Commun.* **313,** 1015-1022.

Tan E., Ding X. Q., Saadi A., Agarwal N., Naash M. I. and Al-Ubaidi M. R. (2004) Expression of cone-photoreceptor-specific antigens in a cell line derived from retinal tumors in transgenic mice. *Invest Ophthalmol. Vis. Sci.* **45,** 764-768.

Tezel G. (2006) Oxidative stress in glaucomatous neurodegeneration: mechanisms and consequences. *Prog. Retin. Eye Res.* **25,** 490-513.

Thiadens A. A., den Hollander A. I., Roosing S., Nabuurs S. B., Zekveld-Vroon R. C., Collin R. W., De B. E., Koenekoop R. K., van Schooneveld M. J., Strom T. M., van Lith-Verhoeven J. J., Lotery A. J., van Moll-Ramirez N., Leroy B. P., van den Born L. I., Hoyng C. B., Cremers F. P. and Klaver C. C. (2009) Homozygosity mapping reveals PDE6C mutations in patients with early-onset cone photoreceptor disorders. *Am. J. Hum. Genet.* **85,** 240-247.

Tinti C., Conti B., Cubells J. F., Kim K. S., Baker H. and Joh T. H. (1996) Inducible cAMP early repressor can modulate tyrosine hydroxylase gene expression after stimulation of cAMP synthesis. *J. Biol. Chem.* **271,** 25375-25381.

Tosi J., Davis R. J., Wang N. K., Naumann M., Lin C. S. and Tsang S. H. (2010) shRNA knockdown of guanylate cyclase 2e or cyclic nucleotide gated channel alpha 1 increases photoreceptor survival in a cGMP phosphodiesterase mouse model of retinitis pigmentosa. *J. Cell Mol. Med.* **15,** 1778-1787.

Trankner D., Jagle H., Kohl S., Apfelstedt-Sylla E., Sharpe L. T., Kaupp U. B., Zrenner E., Seifert R. and Wissinger B. (2004) Molecular basis of an inherited form of incomplete achromatopsia. *J. Neurosci.* **24,** 138-147.

Trifunovic D., Dengler K., Michalakis S., Zrenner E., Wissinger B. and Paquet-Durand F. (2010) cGMP-dependent cone photoreceptor degeneration in the cpfl1 mouse retina. *J. Comp Neurol.* **518,** 3604-3617.

Trifunovic D., Sahaboglu A., Kaur J., Mencl S., Zrenner E., Ueffing M., Arango-Gonzalez B. and Paquet-Durand F. (2012) Neuroprotective Stategies for the Treatment of Inherited Photoreceptor Degeneration. *Current Molecular Medicine (accepted).*

Trumpler J., Dedek K., Schubert T., de Sevilla Muller L. P., Seeliger M., Humphries P., Biel M. and Weiler R. (2008) Rod and cone contributions to horizontal cell light responses in the mouse retina. *J. Neurosci.* **28,** 6818-6825.

Usui S., Komeima K., Lee S. Y., Jo Y. J., Ueno S., Rogers B. S., Wu Z., Shen J., Lu L., Oveson B. C., Rabinovitch P. S. and Campochiaro P. A. (2009a) Increased expression of catalase and superoxide dismutase 2 reduces cone cell death in retinitis pigmentosa. *Mol. Ther.* **17,** 778-786.

Usui S., Oveson B. C., Lee S. Y., Jo Y. J., Yoshida T., Miki A., Miki K., Iwase T., Lu L. and Campochiaro P. A. (2009b) NADPH oxidase plays a central role in cone cell death in retinitis pigmentosa. *J. Neurochem.* **110,** 1028-1037.

Vallazza-Deschamps G., Cia D., Gong J., Jellali A., Duboc A., Forster V., Sahel J. A., Tessier L. H. and Picaud S. (2005) Excessive activation of cyclic nucleotide-gated channels contributes to neuronal degeneration of photoreceptors. *Eur. J. Neurosci.* **22,** 1013-1022.

Wahlin K. J., Campochiaro P. A., Zack D. J. and Adler R. (2000) Neurotrophic factors cause activation of intracellular signaling pathways in Muller cells and other cells of the inner retina, but not photoreceptors. *Invest Ophthalmol. Vis. Sci.* **41,** 927-936.

Wang X., Ward C. J., Harris P. C. and Torres V. E. (2010) Cyclic nucleotide signaling in polycystic kidney disease. *Kidney Int.* **77,** 129-140.

Wen R., Song Y., Cheng T., Matthes M. T., Yasumura D., LaVail M. M. and Steinberg R. H. (1995) Injury-induced upregulation of bFGF and CNTF mRNAS in the rat retina. *J. Neurosci.* **15,** 7377-7385.

Wenzel A., Grimm C., Samardzija M. and Reme C. E. (2005) Molecular mechanisms of light-induced photoreceptor apoptosis and neuroprotection for retinal degeneration. *Prog. Retin. Eye Res.* **24,** 275-306.

Wright A. F., Chakarova C. F., Abd El-Aziz M. M. and Bhattacharya S. S. (2010) Photoreceptor degeneration: genetic and mechanistic dissection of a complex trait. *Nat. Rev. Genet.* **11,** 273-284.

Yau K. W. and Hardie R. C. (2009) Phototransduction motifs and variations. *Cell* **139,** 246-264.

Yu D. Y., Cringle S., Valter K., Walsh N., Lee D. and Stone J. (2004) Photoreceptor death, trophic factor expression, retinal oxygen status, and photoreceptor function in the P23H rat. *Invest Ophthalmol. Vis. Sci.* **45,** 2013-2019.

Zhang X., Feng Q. and Cote R. H. (2005) Efficacy and selectivity of phosphodiesterase-targeted drugs in inhibiting photoreceptor phosphodiesterase (PDE6) in retinal photoreceptors. *Invest Ophthalmol. Vis. Sci.* **46,** 3060-3066.

Zimmerman A. L., Yamanaka G., Eckstein F., Baylor D. A. and Stryer L. (1985) Interaction of hydrolysis-resistant analogs of cyclic GMP with the phosphodiesterase and light-sensitive channel of retinal rod outer segments. *Proc. Natl. Acad. Sci. U. S. A* **82,** 8813-8817.

Zrenner E. (2002) Will retinal implants restore vision? *Science* **295,** 1022-5.